Jour. Sci. Hiroshima Univ., Ser. C, Vol. 9, No. 3, 435–493 (1992)

Origin of the Early Mesozoic Granitic Rocks in the Hida Terrane, Japan, and Its Implication for Evolution of the Continental Crust

By

Shinobu TANAKA

(Received, May 29, 1992)

Abstract: The early Mesozoic granitic rocks show Rb-Sr ages of 173 to 211 Ma and are intruded into three belts, Hida Gneiss Belt, Unazuki Belt and Hida Marginal Belt, being divided into Triassic ones and Jurassic ones. The granitic rocks exhibit spatial variation in chemical compositions of constituent minerals, whole-rock geochemistry and Sr and Nd isotopic data. Especially, based on Sr and Nd isotopic compositions of the granites, the Hida Terrane (Hida Gneiss Belt and Unazuki Belt) can be divided roughly into two zones, Outer Plutonic Zone (lower initial $^{87}Sr/^{86}Sr$ ratios: 0.7045 to 0.7065 and higher initial ε Nd values: +3.1 to -4.2) and Inner Plutonic Zone (higher initial $^{87}Sr/^{86}Sr$ ratios: 0.7054 to 0.7105 and lower initial ε Nd values: +1.6 to -9.3). Gabbroic rocks indicate the same spatial variation in isotopic characteristics of the granitic rocks.

The negative initial ε Nd values (-3.3 and -4.2) from Triassic Hayatsukigawa mass suggest that its formation was incorporated by significant amounts of older continental crust. The mass is characterized by low K_2O/Na_2O ratios, Rb and MgO contents and high Sr and Ba contents. The granites belong to the I-type and magnetite-series granitic rocks, which is the same in the Jurassic granitic rocks. The geochemical data indicate that the magma source of the Hayatsukigawa mass rocks is a granulite facies igneous lower crust. The main partial melting in the lower crust may be induced by adiabatic decompression resulting from the rapid uplifting occurred in the Outer Plutonic Zone.

The geochemical criteria imply that the Jurassic granites was generated in a destructive plate margin. From the isotopic data and geochemical characteristics, the granitic rocks in the Outer Plutonic Zone may have been derived from Phanerozoic basic igneous rocks (e.g. basaltic composition) with island-arc or continental margin character. The granitic rocks in the Inner Plutonic Zone can be divided into two groups, Group I and Group II on the basis of their isotopic compositions. The source material of the Group I is inferred to have been enriched in ^{87}Sr than that of the granites in the Outer Plutonic Zone. The Group II rocks with higher initial $^{87}Sr/^{86}Sr$ ratios and lower ε Nd values appear to have primarily been derived from older (Proterozoic) crustal sources.

Considering the isotopic and geochemical informations of the early Mesozoic granitic rocks and Hida metamorphic rocks, the Inner Plutoni Zone of the Hida Terrane would have been an island arc or a microcontinent which collided with the eastern edge of the Sino-Korean craton during the early Paleozoic.

Contents

I. INTRODUCTION

As granitoids are one of the main components of continental crust, the problem of their genesis is linked to that of the origin and evolution of the continental crust. The geochemistry of radiogenic isotopes, Sr, Pb and Nd, in granitic rocks has been found to provide strong constraints on their genesis, because magmatic differentiation processes and partial melting of magma sources do not result in isotopic fractionation of Sr, Pb and Nd. Especially, Nd isotopes have been found to be used as extremely powerful tracer (e.g. Allègre and Ben Othman, 1980; DePaolo, 1981c; MuCulloch and Chappell, 1982). Their usefulness is due to the following two geochemical properties; they are not mobile, and large geochemical fractionation of the parent/daughter Sm/Nd ratio is difficult. In addition to the consideration of petrogenetic problems, therefore, is also given a new way to understand the fundamental features of deeper part of continental crust through the Nd and Sr isotopic characteristics of granitic rocks (Farmer and DePaolo, 1983).

Pithcher's (1983) comprehensive study on granitic rocks in Phanerozoic mobile belts has represented a close connection between granite type and tectonic environment. In order to understand origin of granitoids, hence, it is absolutely necessary to clarify their tectonic setting, as well as their petrological and geochemical characteristics. The impetus for such study, therefore, comes from the previously reported spatial variations in chemical compositions of constituent minerals, major and minor elements of whole rocks and Sr, Nd, Pb and O isotopic data from the granitic batholiths at destructive plate margins or active continental margins.

As concerns radiogenic isotope variations, Kistler and Peterman's (1973) data for the rocks of California batholiths indicated a systematic variation (southeastward increase) of initial $^{87}Sr/^{86}Sr$ ratios. They explained such as areal distribution of initial $^{87}Sr/^{86}Sr$ ratios, that range from 0.7032 to 0.7094, in term of a variation of source region implying upper mantle and lower crust.

In their study on plutonic and volcanic rocks of Central Andes, McNutt et al. (1975) ascribed the systematic variation (eastward increase) in mean initial strontium isotopic ratio, which is from 0.7022 to 0.7077, to such a subduction process of a slab that induced melts of variable composition.

Farmer and DePaolo (1983) made a Nd-Sr isotopic study of the Mesozoic and Tertiary granites from the western United States. Their EG (eugeocline) granites vary spatially in initial $^{143}Nd/^{144}Nd$ (ε Nd) and initial $^{87}Sr/^{86}Sr$ ratios; ε Nd = +8 and initial $^{87}Sr/^{86}Sr$ = 0.7032 to −6 and 0.707 from west to east. They concluded that such a Nd-Sr isotopic variation reflects an increase in proportion of continentally derived sedimentary rocks assimilated by magma from a light REE-depleted, island arc-like mantle. However, Hart (1985) pointed out that the isotopic composition of the EG granites of Farmer and DePaolo (1983) may reflect the isotopic signatures of an evolved mantle source.

It can be said from the above cited data that, in general, the initial $^{87}Sr/^{86}Sr$ ratios for the granitic rocks of the continental margins increase towards the inner side of the continent, while initial $^{143}Nd/^{144}Nd$ ratios (ε Nd) decrease, although there is no agreement over the explanation of such the systematic isotopic variations. Nohda et al. (1988) clarified that the volcanics in the continental margins also show a more enriched isotopic signature of Nd and Sr with increasing distance from the trench, suggesting that such an isotopic profile should be explained with reference to the mantle structure.

The Hida Terrane, which was a part of the eastern margin of the Asian continent before the opening of the Japan Sea, was intruded by granitic rocks of large volume during early Mesozoic (Triassic to Jurassic) age. However, the early Mesozoic granites (so called Funatsu Granitic Rocks) had been explained by Nozawa (1979) that their petrographic character is quite uniform throughout the Hida Terrane but they consist mainly of two types: the earlier intrusives (Shimonomoto type) and later intrusives (Funatsu type). His opinion has been accepted by many geologists (cf. Kano, 1990), although the precise petrographic observation of these granitic rocks had not been performed.

Recently, geological, petrographical, geochemical and geochronological, studies of the early Mesozoic granitic rocks have been performed in details by some authors. According to their results, the granitic rocks have not uniform petrographic characteristics but are composed of masses which various petrographic characteristics and of some different intrusion ages (e.g. Tanaka and Maruyama, 1985a. b; Ohtsubo et al., 1985; Tanaka and Ohtsubo, 1987; Kano, 1990). Moreover, Sr and Nd isotopic investigations (Tanaka and Kagami, 1987a; 1989; Arakawa, 1988) have revealed that in the Hida Terrane there is a clear systematic isotopic variation, which appears to be comparable with that for the continental margin granitoids of some other terranes. Therefore, the geological, petrological and radiogenic isotope studies of the early Mesozoic granitic rocks in the Hida Terrane are considered to give very important information on the genesis of granitic batholiths at the Phanerozoic active continental margins.

On the basis of the Sm-Nd isotopic characteristics of several Phanerozoic continental margin magmatic belts, Liew and McCulloch (1985) suggested that many continental blocks had obtained their present-day size during the mid-Proterozoic ages and that the continental accretion processes related to Phanerozoic arc-type magmatism may have induced little overgrowth of Precambrian continents. If their assumption was available, Phanerozoic continental margin magmatic belts should be generally reworked Precambrian continental crust. Sm-Nd and Rb-Sr isotopic studies of the Hida

Terrane may show to what extent this terrane contains collided Precambrian continents, what kinds of continental crust amalgamated in this terrane and so shed more light on the growth and evolution of its continental crust.

In this study, the author presents the detailed geological, mineralogical, geochemical and Nd-Sr isotopic characteristics of the early Mesozoic granitic masses in the Hida Terrane, discussing their petrogenesis, and makes inferences regarding the age and provenance of the Hida Terrane, sheding light on the growth and evolution of continental crust.

Acknowledgements

The author wishes to his sincere thanks to Professor Ikuo Hara of Hiroshima University for his helpful advices during the course of this study and critical reading and correcting of the manuscript. Special thanks are due to Professor Hiroji Honma, Dr. Hiroo Kagami and graduate students of Institute for Study of the Earth's Interior, Okayama University for their helpful suggestions on isotope analysis. Thanks are extended to Dr. Takashi Kano of Yamaguchi University, Dr. Morihisa Suzuki of Hiroshima University and Dr. Tsuneo Inazuki for their useful information on the geology of Hida Terrane and helpful suggestions, and to Mr. Tomohide Ohtsubo of Tokyo Civil Consultant Co., who provided his unpublished geological and geochemical data on the Utsubo mass. The author is grateful to Professors Hiroshi Kano and Takahiko Maruyama of Akita University and Dr. Tohru Sakiyama for their valuable advice and encouragement. Thanks also go to Professor Shigeru Iizumi of Shimane University and Professor Hisato Hayashi of Akita University for their help on the execution of XRF analyses. Samples from the Unazuki district provided by Mr. Yasuo Katoh are also appreciated. The author gratefully acknowledge the following individual who contributed in many ways to this study: Mr. Asao Minani and Dr. Yasutaka Hayasaka of Hiroshima University for EPMA analyses of minerals; Dr. Teruyoshi Imaoka of Yamaguchi University and Dr. Kozo Inoue of Hiroshima University for chemical analyses of whole rocks; the late Mr. Hideo Takahashi and Mr. Akito Magai of Hiroshima University for preparing thin sections and Mr. Tamikazu Saeki of the Dainichidaira-sansou for his kind assistance during the field survey. Financial support was received from the Grantin Aid for Scientific Research from the Ministry of Education of Japan (No. 58340053).

II. GEOLOGICAL SETTING

The Hida Terrane, which is situated at the northernmost zone of the geotectonic framework of Southwest Japan, is the geological area which consists of rocks of the oldest age found in Japanese Islands. It is divided into two geological units, Hida Gneiss Belt placed in northern side and Unazuki Belt placed in southern side, following Hiroi (1981). The Hida Marginal Belt develops just on the southern outside of the Unazuki Belt (Fig. 1).

The Hida Gneiss Belt is mostly composed by the Hida gneisses and the early Mesozoic granitic rocks. The Hida gneisses consist of biotite gneiss, hornblende gneiss, amphibolite, crystalline limestone, calc-silicate gneiss and felsic gneiss accompanied with minor plutonic rocks. The original rocks have been assumed as follows: Biotite gneiss and felsic gneiss are mudstone, sandy mudstone, sandstone and felsic lava or tuff, amphibolite and hornblende gneiss are intermediate to basic lava or tuff and intermediate to basic tuffaceous sandstone, crystalline limestone and calc-silicate gneiss are limestone, dolomitic limestone and calcareous muddy sandstone (Sohma and Akiyama, 1984). The Hida metapelites are higher in CaO, FeO and MgO, while lower in Al-excess as compared to pelites of other areas in Japan, indicating that the metapelites were probably derived from those intermingled with basic volcanic materials and graywake sandstone (Suzuki, 1975). The minor plutonic rocks are composed of coarse-grained granitic rocks which are named older migmatitic granitoids. They are classified into three types: gray granite, Inishi-type rocks (diopside-bearing quartz-feldspathic rocks) and trondhjemitic rocks (Kano, 1981).

The Hida gneisses are divided into three areal groups, based on minor and major structures, lithological features and distribution, eastern area, central area and western area (Kano, 1981; Sohma and Akiyama, 1984). In the eastern area, Katakai-gawa and Hayatsuki-gawa districts, hornblende gneiss and crystalline limestone are predominant. The lineations and fold axes run generally in north - south trend with gentle plunge. In the central area, Wada-gawa and Kamioka districts, hornblende gneiss and calc-silicate gneiss are predominant. They are severely migmatized and the Inishi-type rocks are commonly found in this area. Tight ~ isoclinal folds are characteristically recognized. The structural trend, lineations and fold axes, is roughly in north and south trend. In the western area, Kubusu-gawa district, rhythmic alternation consisting of fine-grained biotite gneiss, hornblende gneiss and clinopyroxene gneiss is predominant. Migmatite structure is characterized by the simple development of veinlets of gray granite. The foldform is of gentle ~ open type. The lineations and fold axes run generally in north or northeast trend.

Andalusite, sillimanite and cordierite together with garnet are the common constituent minerals of the pelitic gneiss in the most part of the Hida Gneiss Belt (e.g. Fujiyoshi, 1973; Asami and Adachi, 1976; Asami, 1979), showing low pressure condition of metamorphism. On the basis of the detailed analyses of mineral equilibria and the estimation of P-T conditions, recently the Hida Gneiss Belt has been divided into two parts, Inner region and Outer region, (Suzuki et al.,

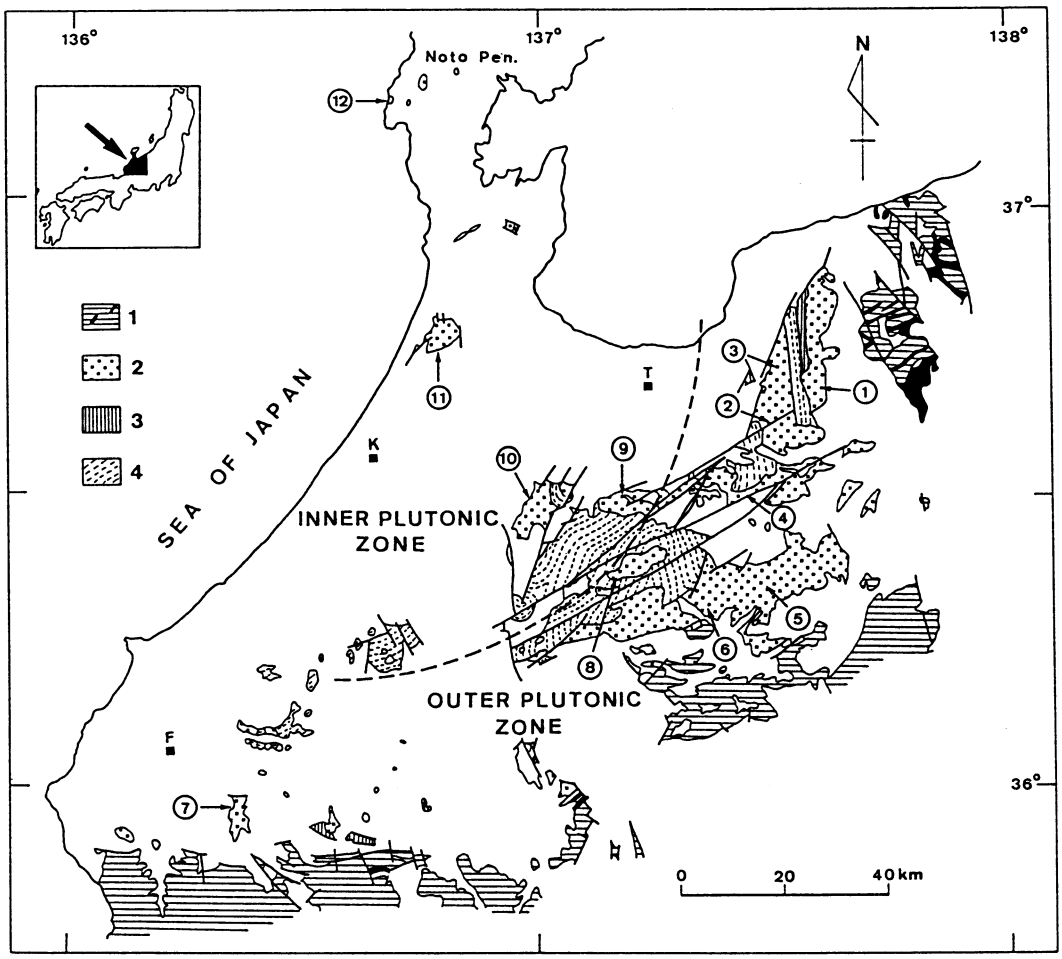

Fig. 1. Geological sketch map of the Hida Terrane and distribution of the granitic masses (modified from Nozawa, 1977). 1, Rocks of the Hida Marginal Belt and Mino Terrane; 2, Early Mesozoic igneous rocks; 3, Unazuki schists and their equivalents in the Unazuki Belt; 4, Hida gneisses. The numbers circled are 1 = Kekachidake mass; 2 = Okumayama mass; 3 = Hayatsukigawa mass; 4 = Wadagawa mass; 5 = Shimonomoto mass; 6 = Funatsu mass; 7 = Asuwagawa mass; 8 = Utsubo mass; 9 = Yatsuo mass; 10 = Shogawa mass; 11 = Hodatsusan mass; 12 = Togi area. T, Toyama; K, Kanazawa; F, Fukui.

1989). Rocks of the Outer region, situated between the Inner region and the Unazuki Belt, are more intensely metamorphosed than those of the Inner one.

Isotopic ages of the Hida gneisses are concentrated around about 180 Ma (mainly K-Ar and Rb-Sr ages of biotite) showing subordinate clusters between 210 and 240 Ma (K-Ar ages of amphibole, U-Th-Pb ages of zircon and sphene and Rb-Sr whole-rock age), at about 340 Ma(K-Ar ages of amphibole and biotite) and at about 410 Ma (Rb-Sr and Sm-Nd whole-rock ages) (Fig. 2). The mineral ages around 210-220 Ma may be derived from the processes of cooling from a metamorphic event at ca. 240 Ma. The Jurassic age (150-190 Ma) obtained on biotite, hornblende and muscovite is probably due to the influence of local reheating such as granite intrusions. The Jurassic granites which show ages between 182 and 201 Ma (Rb-Sr whole-rock ages) havebeen extensively found throughout the Hida Gneiss Belt. Their contact phenomena have been studied in several areas (Inazuki, 1980, 1982; Yamamoto, 1983; Okui, 1985).

According to many isotopic studies, the original rocks of Hida gneisses might have been derived from Precambrian rocks. However, there are only two reliable isotopic ages which indicate Precambrian age, $^{207}Pb/^{206}Pb$ age of 1493 Ma on detrital zircon (Ishizaka and Yamaguchi, 1969) and 746 Ma on sphene-zircon mixture (Shibata et al., 1970) both from the Amo gneiss in the western area. Although Sato et al. (1967) reported the Precambrian age (1200 Ma) for the gray granite, a recent Rb-Sr isotopic study (Shibata et al., 1989) indicated that the emplacement age of the gray granite must be about 500 Ma.

The Unazuki Belt is mainly composed by the Unazuki schists, their equivalents and the early Mesozoic granitic rocks. The Unazuki schists are mainly exposed in the Unazuki and Katakai-gawa districts. The original rocks of the Unazuki schists are fine-grained bedded limestones, ferruginous pelitic rocks, quartzo-feldspathic rocks derived from acidic volcanics (leptite),

alternation of basic and pelitic-psammitic rocks and conglomeratic rocks (Ishioka and Suwa, 1954, 1956; Suwa, 1966b, 1979; Hiroi, 1978). Fossil bryozoa and foraminifera occur in the bedded limestones (Hiroi et al., 1978), suggesting that the original rocks are of late Carboniferous age. The Unazuki schists were regionally metamorphosed in the facies series of kyanite-sillimanite type (Hiroi, 1983), and are over-thrust by the Hida gneisses from the west (Hiroi, 1981). Hara (1982) said that the over-thrusting of the Hida gneisses onto the Upper Palaeozoic rocks might have been contemporaneous with the uplifting of the medium-pressure metamorphic rocks. The Unazuki schists are thermally remetamorphosed by the early Mesozoic granites, and the temperature and pressure of the contact metamorphism have been estimated petrologically to be about 700℃ and 3-4 kbar, respectively (Hiroi, 1980).

The rocks, which have been considered to be equivalent to the Unazuki schists in regard to age, lithology and biofacies of original rocks and age and type of the regional metamorphism, have been found in the Fukuji area (Igo, 1961; Niko et al., 1984), Sokawa and Makido area (Shibata et al., 1980; Sohma, 1986), Itoshiro area (Konishi, 1954), Arashimadake area (Asami, 1979) and Asuwagawa area (Hattori, 1984).

Isotopic ages for the Unazuki schists as determined by Rb-Sr and K-Ar methods can be divided into two groups, group of about 180 Ma and group of about 230 Ma (Fig. 2). The group of about 180 Ma corresponds to the contact metamorphism by the Jurassic granitic rocks, while the group of about 230 Ma to the regional metamorphism of the medium-pressure type.

The Hida Marginal Belt is a narrow serpentinite melange zone and is situated between the Hida Terrane and the Mino Terrane. This Belt is made up of non ~ weakly-metamorphosed Ordovician to Permian shallow marine sedimentary rocks, glaucophane schists, garnet amphibolites and metagabbros, which are tectonically squeezed and in serpentinites, and of accretionary complex of middle to late Paleozoic ages (Komatsu and Suwa, 1986). The exposed areas of the serpentinite melange zone are, from north to south and southwest, the Omi, Asahidake, Shiroumadake, Yarigatake, Gamata, Fukuji, Hongo, Takayama, Naradani and Ise districts. The early Mesozoic granites are intruded into Paleozoic formations in the Hongo and Takayama districts (Nozawa et al., 1979) and into serpentinites and greenstones in Gamata area (Sohma et al., 1985).

Glaucophanitic metamorphic rocks of the Hida Marginal Belt yield mica and hornblende, which show Rb-Sr and K-Ar ages of 315-362 Ma (Omi district), 311-323 Ma (Shiroumadake district) and about 415 Ma (Ise district). Amphibolite and metagabbro give hornblende which shows K-Ar ages of about 336 Ma (Omi district) and about 370 Ma (Shiroumadake district), (Shibata and Nozawa,

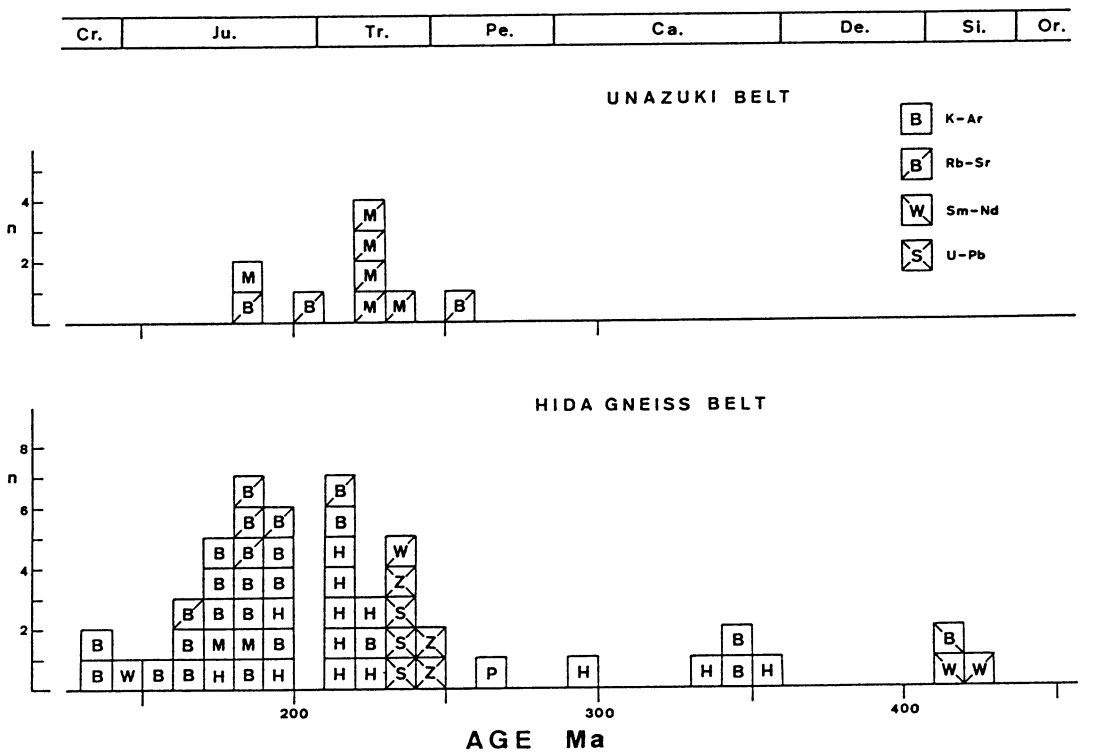

Fig. 2. Histograms showing the variation of isotopic ages for the Hida metamorphic rocks. B = biotite; H = hornblende; P = plagioclase; M = muscovite; K = k-feldspar; S = sphene; Z = zircon; W = whole-rocks. Data are of Kuno (1960), Ohmoto (1964), Kawano and Ueda (1966), Shibata and Nozawa (1966; 1978), Hayase and Ishizaka (1968), Ishizaka and Yamaguchi (1969), Shibata et al. (1970; 1979; 1984), MMAJ (1973), Arakawa (1984), Tanaka and Adachi (1987) and Asano et al. (1988).

1968; Shibata et al., 1970; 1979; 1984; Shibata and Ito, 1978). The Sangun crystalline schists, which are of glaucophanitic type and sporadically distributed in the Inner Zone of Southwest Japan, are divided into three terranes, Chizu Terrane (180 Ma), Suo Terrane (220 Ma) and Sangun-Renge Belt (300 Ma) (Hayasaka et al., 1987; Shibata and Nishimura, 1989). On the basis of radiometric ages and geological signatures, the Sangun-Renge Belt is correlated to the Hida Marginal Belt (Nishimura, 1989).

Hiroi (1981) speculated that the Hida gneisses were the basement of the late Paleozoic sedimentation of the original rocks of the Unazuki schists which are of continental shelf type. However, the non-metamorphic rocks in the Hida Marginal Belt are comparable with the original rocks of the Unazuki schists with reference to lithology and age. Thus, Hara (1981) suggested that the sedimentary basin for the original rocks of the Unazuki schists developed through both the region of Hida gneisses and the Hida Marginal Belt. Recently, Yamada et al. (1989) said that the Unazuki schists are a component of the Hida Marginal Belt. The basement problem appears to be still unsolved one.

The Mino Terrane, which is widely distributed to the south of the Hida Marginal Belt, is mostly composed of Jurassic accretionary complexes containing Carboniferous to Jurassic sedimentary rocks such as chert, siliceous shale, mudstone, and greenstone. The early Mesozoic granites are not known to be developed in the Mino Terrane. Hirooka et al. (1983) presumed that the sedimentary complex of the Mino Terrane was formed in the equatorial region and subsequently transported to the north, and these collided with the Hida Terrane probably during early to middle Cretaceous age.

The Kuruma Group of early to middle Jurrasic age and the Tetori Group of late Jurassic to Cretaceous age, both, which are made up of conglomerate derived mainly from the early Mesozoic granitic rocks, sandstone and shale deposited subaerially in shallow sea environments, unconformably overlie the rock formations of the Hida Belt, the Unazuki Belt and the Hida Marginal Belt.

The early Mesozoic granitic rocks show Rb-Sr ages of 173 to 211 Ma, and are intruded into the Hida Gneiss Belt, Unazuki Belt and Hida Marginal Belt, being divided into Triassic ones and Jurassic ones. Based on Sr and Nd isotopic compositions of the granites, the Hida Terrane can be divided roughly into two zones, Outer Plutonic Zone (zone of lower initial $^{87}Sr/^{86}Sr$ ratios and higher initial εNd values) and Inner Plutonic Zone (zone of higher initial $^{87}Sr/^{86}Sr$ ratios and lower initial εNd values) (Fig. 1). The Outer Plutonic Zone includes the Hida Marginal Belt. The boundary between the two zones is roughly comparable with that between the Inner region and the Outer region proposed by Suzuki et al. (1989) with reference to P-T conditions of metamorphism.

In the Outer Plutonic Zone there are Triassic Hayatsukigawa mass (quartz monzodiorite and granodiorite and Rb-Sr feldspar age of 210.9 Ma), Jurassic Kekachidake mass and Funatsu mass (adamellite and granodiorite and Rb-Sr whole-rock ages of 196.1 Ma and 184.1 Ma respectively), Jurassic Okumayama mass (tonalite and Rb-Sr biotite age of 182.6 Ma), Jurassic Shimonomoto mass (gabbro,diorite, quartz diorite, granodiorite and adamellite and Rb-Sr whole-rock age of 201.2 Ma), Jurassic Utsubo mass (tonalite, granodiorite and adamellite and Rb-Sr whole-rock age of 182.5 Ma), and probably Jurassic Wadagawa mass (quartz diorite and adamellite) and Asuwagawa mass (quartz diorite).

In the Inner Plutonic Zone occur three large masses, Jurassic Yatsuo mass (tonalite, granodiorite and adamellite and Rb-Sr feldspar age of 173.4 Ma), probably Jurassic Shogawa mass (gabbro-quartz diorite core and adamellite mantle with Rb-Sr biotite age of 193.9 Ma), Jurassic Hodatsusan mass (tonalite core, granodiorite mantle and adamellite rim with Rb-Sr biotite age of 174.6 Ma) and several small masses in the vicinity of the Togi area.

III. DESCRIPTION

A. GRANITIC MASSES IN THE OUTER PLUTONIC ZONE

1. Kekachidake Mass (Fig. 3)

The mass occurs in the Tsurugidake ~ Kekachiyama area of northern Japan Alps and is principally composed of coarse-grained biotite adamellite and granodiorite. It is intruded into the Hida gneisses and Unazuki schists in the northern part of this area, while it is contact with the Tsurugidake Granite (Tanaka and Kagami, 1987b), one of the Late Cretaceous - Early Paleogene Granites, in the southern part of this area. Although rocks in the Kekachidake mass are commonly massive, a foliation defined by alignment of potassium feldspar crystals and biotite flakes is found in some places and has north - south trend. Medium-grained biotite adamellite is exposed in the upper reaches of the Kama-dani. Basic inclusions with blurred margins have also been found in a few localities. The adamellite and granodiorite facies consist of quartz, potassium feldspar, plagioclase and biotite with accessory minerals.

Potassium feldspar is generally the coarsest-grained mineral (up to 2 × 5 cm) in the rocks and euhedral to subhedral crystals with a pinkish tint, containing inclusions of plagioclase, biotite and opaque oxides. It is strongly perthitic and show well developed microcline-lattice structure. Twinned crystals of potassium feldspar are common. Plagioclase occurs as euhedral to subhedral crystals, showing chemical zoning of An_{36} to An_{17}. Oscillatory zoning is well developed. Its cores tend to be sericitized and contain minor epidote. In a few thin sections, plagioclase twin lamellae are bent, and quartz grains show undulatory extinction. Biotite (2.7-4.7 % in volume) is mainly subhedral crystals with average grain size of 1 × 0.5 mm; the Z color is greenish to dark brown. The biotite is high in Al_2O_3 (14.9-16.1 wt%) and MnO (0.8-1.6 wt%) and

low in TiO_2 (2.9-3.5 wt%). In the vicinity of the Tsurugidake Granite, the decussate texture of biotite grains is well found. The texture is not found in the other part of the mass, showing that it is ascribed to the thermal effect of the Tsurugidake Granite. Accessory minerals include apatite, allanite, sphene (up to 0.1 % in volume), opaque oxides (0.2-0.7 % in volume) and scarce zircon. Opaque oxides are ubiquitous, and nearly composed of magnetite. The basic inclusions are mainly composed of plagioclase (An_{30} to An_{24}) and biotite (mg-value=0.57) with subordinate amount of hornblende, magnetite and apatite. The hornblende grains (mg-value=0.57-0.59) are very small in size and commonly included in plagioclase crystals. The magnetic susceptibility is generally high, ranging from 270 to 800 × 10^{-6} emu/g, showing that the mass is of the magnetites-series granitoids (Ishihara, 1977).

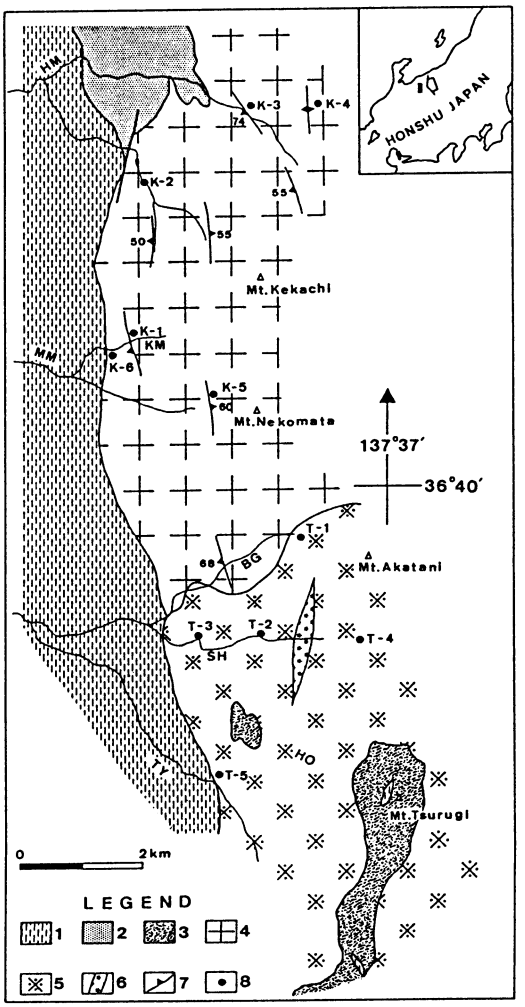

Fig. 3. Diagram showing geological map of the Kekachidake mass district and locations of samples for isotopic study. 1, Hida gneisses 2, Unazuki schists; 3, Gabbroic rocks; 4, Kekachidake mass rocks; 5, Tsurugidake Granite; 6, Granite porphyry; 7, foliation; 8, sample locality; HM, Higashimata-dani; MM, Minanimata-dani;KM, Kama-dani; BG, Bunagura-dani; SH, Shirahagi-gawa; TY, Tateyama-gawa; HO, Hayatsuki-one.

2. Okumayama Mass (Fig. 4)

The mass is exposed in the area of about 10 km to southwest of the Kekachidake mass and consists of medium-grained hornblende-biotite tonalite. Its lithofacies is nearly uniform and it shows a foliation. The foliation is defined by parallel arrangement of hornblende crystals, biotite flakes and lenticular basic inclusions. In general, it has a northwest - southeast trend with northward dip (Fig. 5). The mass intrudes into the Hida gneisses with sharp contact, and is overlain by the Tateyama volcanic rocks of the Quaternary age in its southern part. Basic inclusions are found in swarms along the Sengoku River which develop in width of 1~2 m and inlength of ca. 20 m.

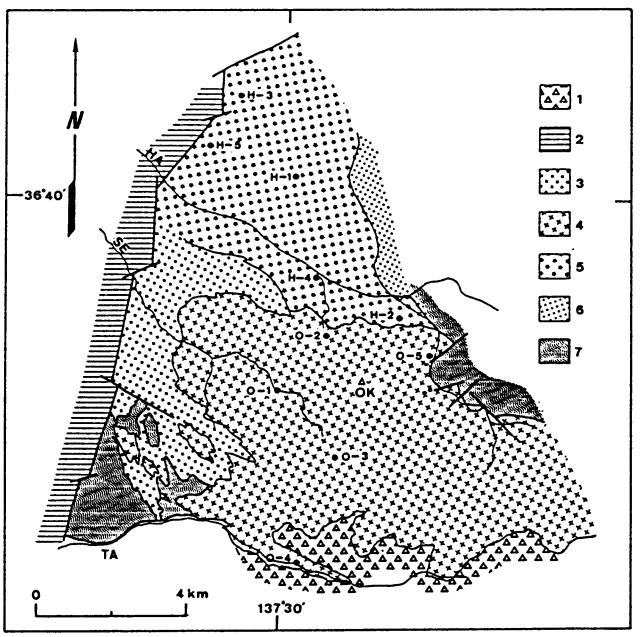

Fig. 4. Diagram showing geological map of the Okumayama mass and Hayatsukigawa mass district and locations of samples for isotopic study. 1, Tateyama volcanic rocks; 2, Tetori Group; 3, Aplitic granite; 4, Okumayama mass rocks; 5, Hayatsukigawa mass rocks; 6, Augen gneissos granite; 7, Hida gneisses; HA, Hayatsuki-gawa; SE, Sengoku-gawa;OK, Okumayama;TA, Tateyama.

Potassium feldspar (3.0-8.0 % in volume) is anhedral, interstitial and very weakly perthitic. It shows also microcline-lattice structure. Plagioclase is broadly zoned in chemical composition (An_{39} to An_{22}) and commonly euhedral crystals with average grain size of 2 × 1.5 mm, which partially contains quartz, biotite and hornblende grains as inclusions. Oscillatory zoning is well developed. Myrmekitic texture is found along rims of plagioclase. Quartz is generally anhedral (up to 5 mm in diameter) with inclusion minerals such as plagioclase, potassium feldspar, biotite and hornblende and shows weakly undulatory extinction. Biotite (4.3-9.1 % in volume) occurs mainly as subhedral plates with average grain size of 1 × 1 mm; the Z color is dark to reddish brown. It is high in TiO_2 (3.2-4.1 wt%) and low in Al_2O_3 (14.2-15.2 wt%). The decussate texture of biotite grains is well found

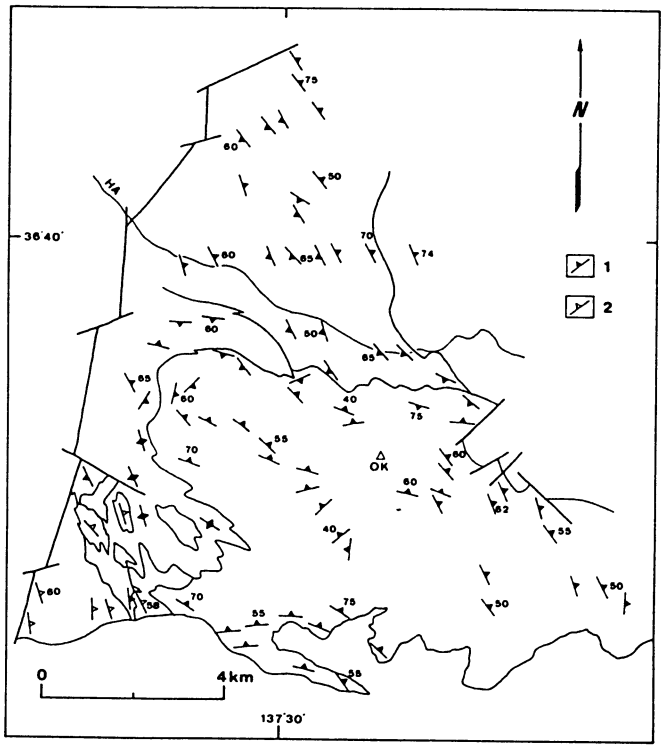

Fig. 5. Structural map of the Okumayama mass and Hayatsukigawa mass district. 1, Foliation of the granitic rocks; 2, Foliation of the gneisses; HA, Hayatsuki-gawa; OK, Okumayama.

in the upper reaches of the Omata River. It is considered to be ascribed to the contact metamorphic effect by the Tsurugidake Granite. Hornblende (1.2-6.5 % in volume) is generally conspicuous euhedral crystals with average grain size of 3 × 1 mm having a bluish green color. Twinned crystals are common. Biotite, magnetite and quartz commonly are included in hornblende. The hornblende has a zonal structure of chemical composition, showing decrease in mg-value (0.66 to 0.53) from core to rim, and is high in SiO_2 (46.2-49.4 wt%) and low in Al_2O_3 (4.5-7.6 wt%). Accessory minerals are apatite, allanite, sphene, opaque oxides (mainly magnetite, 0.2-0.8 % in volume) and zircon. Sphene (about 0.1 % in volume) occurs as euhedral to subhedral crystals (often large, up to 5 mm in length). The basic inclusions are composed mainly of plagioclase (An_{37} to An_{27}), hornblende (mg-value=0.55-0.65) and biotite (TiO_2=2.9-3.6 wt%), with subordinate amount of potassium feldspar, magnetite and apatite. The magnetic susceptibility is strongly high, ranging from 400 to 1075 × 10^{-6} emu/g, showing that the mass is of the magnetite-series granitoids.

3. Hayatsukigawa Mass (Fig. 4)

The mass is exposed on the northern side of the Okumayama mass, and is mainly composed of weakly foliated fine- to medium-grained hornblende biotite quartz monzodiorite and granodiorite. It is relatively uniform in lithofacies and poor in basic inclusions. The foliation defined by alignment of biotite flakes, which show north - south trend, is relatively well developed in the eastern part (Fig. 5). On the whole, it is parallel to that of the Hida gneisses at the eastern part, but cut discordantly across by the Okumayama mass. Thus, the intrusion age of the Hayatsukigawa mass must be older than that of the Okumayama mass. However, the furthermore obvious field evidence for the mutual relation of both masses is still scarce. The Hayatsukigawa mass intrudes into the augen gneissose granite [Katakaigawa granodiorite after Kawano and Nozawa (1968)], whereas it is intruded by the aplitic granite which appears to be in close association with the Okumayama mass.

Potassium feldspar occurs chiefly as subhedral crystals (up to 5 × 5mm) with a pinkish tint and is micro-perthitic with well defined microcline-lattice structure. Twinned crystals are common. It encloses euhedral to subhedral quartz, plagioclase, biotite, hornblende and magnetite grains as inclusions. Plagioclase is euhedral crystals with average grain size of 2 × 1 mm, and zoned in chemical composition from An_{27} to An_{15}. It encloses sphene and opaque oxides as inclusion minerals. The plagioclase cores often are strongly saussurited and its rims are coated by myrmekite. Quartz is generally anhedral crystals with average grain size of 1 × 1 mm, and contains inclusions of hornblende, biotite and magnetite. Undulatory or polygonized grains of quartz are well developed in the eastern part of the mass, in which the foliation is clearly found. Biotite (0.8-1.9 % in volume) is mainly subhedral crystals with average grain size of 0.5 × 0.2 mm; the Z color is dark brown. It is high in Al_2O_3 (14.8-16.1 wt%) and low in TiO_2 (2.1-2.7 wt%) and mg-value (0.34-0.39). Hornblende (0-0.9 % by volume) occurs as euhedral to subhedral crystals with average grain size of 2 × 1 mm and is brownish green in tint. In general, these have irregular boundaries and contains inclusions of biotite and magnetite. The hornblende has a zonal structure characterized by decrease of mg-value (0.49 to 0.34) from core to rim and is high in Na_2O (1.5-2.3 wt%) and K_2O (0.9-1.2 wt%). Apatite, zircon, allanite, sphene, opaque oxides and epidote are accessory minerals. Sphene and opaque oxides occur commonly as contiguous grains. Chlorite partially or completely replaces biotite. The magnetic susceptibility of the mass, ranging from 14 to 648 × 10^{-6} emu/g, is obviously lower than that of the Okumayama mass.

4. Wadagawa Mass (Fig. 6)

The mass is exposed in the area of about 15 km to south of the Okumayama mass and consists mainly of foliated medium-grained hornblende-biotite quartz diorite and weakly foliated fine-grained biotite adamellite, accompanying small bodies of fine-grained hornblende diorite. The quartz diorite has a foliation defined by parallel arrangement of hornblende crystals and basic schlieren, which shows northeast - southwest trend with northward dip (Fig. 6). This rock intrudes into the Hida gneisses with sharp contact and often encloses small blocks of the gneisses. While the adamellite, badly altered, intrudes into the quartz diorite. Quartz monzodiorite facies with

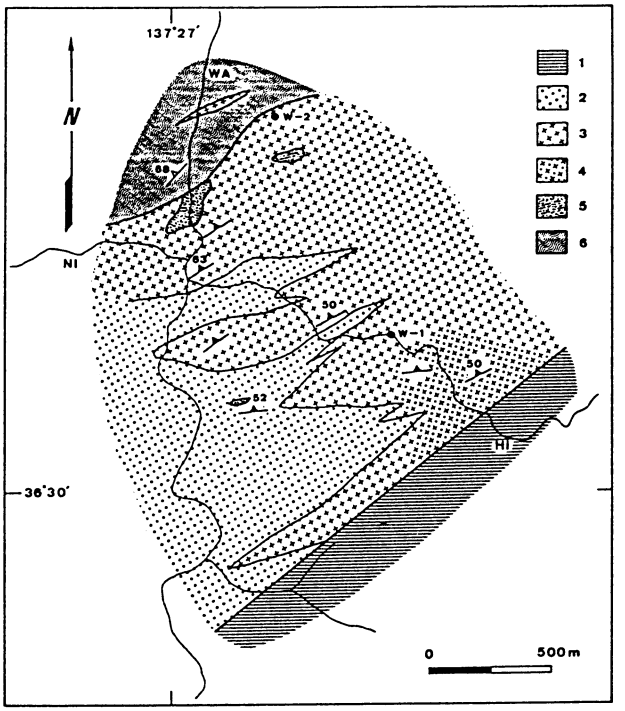

Fig. 6. Diagram showing geological map of the Wada-gawa mass district and locations of samples for this study. 1, Tetori Group; 2, Adamellite 3, Quartz diorite; 4, Quartz monzodiorite; 5, Hornblende diorite; 6, Hida gneisses; WA, Wada-gawa; NI, Nishisakamori-dani; HI, Higashisakamori-dani.

euhedral potassium feldspar crystals (up to 3 × 2 cm) is found in the upper reaches of the Higashisakamori-dani, but the mutual relation of this facies and the quartz diorite is unclear.

The quartz diorite is constant in composition and does not contain any plagioclase with chemical zonation. An-content of the plagioclase is constantly about 24 percent. Biotite (7.9-9.8 % in volume) is mainly subhedral crystals and low in TiO_2 (2.6-3.2 wt%). Hornblende (1.6-5.5 % in volume) is commonly subhedral crystals and has a zonal structure showing decrease in mg-value (0.55 to 0.51) from core to rim. Accessory minerals are apatite, allanite, sphene (0.1-1.0 % in volume), opaque oxides (mainly magnetite, 0.9-1.2 % in volume) and zircon. The granitic rocks of the mass show a wide range of magnetic susceptibility from 75 × 10^{-6} emu/g in quartz monzodiorite to 1117 × 10^{-6} emu/g in quartz diorite.

5. Shimonomoto Mass (Fig. 7)

The mass crops out about 30 km to south of the Okumayama mass and is highly variable in lithofacies, being composed of foliated medium-grained hornblende biotite quartz diorite, granodiorite and adamellite. Based on their field occurrence and petrographical features, the mass divided into three facies as follows: Kanekido Facies, Kuwasaki Facies and Ikenoo Facies (Tanaka and Maruyama, 1985a). The lithofacies variation is generally clear forming a normal zoned pluton. The foliation defined by aligned hornblende crystals, biotite flakes and lenticular basic inclusions makes two-basin structure in the mass. The mass is intruded by the coarse-grained adamellite and aplite of the Funatsu mass in the western part, while it is overlain by the Tetori Group of the late Jurassic - early Cretaceous sediments in the northern part.

The Kanekido Facies consists mainly of quartz diorite and granodiorite accompanied with small rock bodies of diorite which contains gabbroic rocks in small amount (Fig. 8). The gabbroic rocks consist of pyroxene gabbro and pyroxene-hornblende gabbro which encloses a small block (100 × 30 cm) of amphibolite. The dioritic and the gabbroic rocks are intergradational to each other. Basic inclusions are common and are flattened into discus-like shapes oriented along foliation plane.

The pyroxene gabbro in the dioritic masses consists of orthopyroxene and plagioclase with lesser amounts of hornblende, biotite, clinopyroxene and opaque oxides. Plagioclase shows conspicuous zoning from An_{89} to An_{57}, but oscillatory zoning is absent. Orthopyroxene (En_{71-74}, Fs_{23-27}, Wo_3) occurs commonly as euhedral crystals and is faintly pleochroic from colourless to pale pink. Plagioclase and magnetite are included in orthopyroxene. Clinopyroxene (En_{42-46}, Fs_{10-14}, Wo_{42-47}) is subhedral to anhedral, and rarely occurs as zoned crystals. Hornblende (mg-value = 0.68-0.72) occurs generally as rims around clinopyroxene and is pleochroic from pale green to brownish green. Biotite (mg-value = 0.67-0.68) is interstitial to plagioclase and orthopyroxene, and very reddish brown in tint. Opaque oxides (4.1 % in volume) are predominantly magnetite with lesser amount of ilmenite.

The small dioritic masses are usually composed of medium-grained minerals such as brown to green amphibole (16.6-21.9 % in volume), biotite (10.9-12.2 % in volume), plagioclase, interstitial quartz, minor clinopyroxene and opaque minerals. Orthopyroxene and potassium feldspar are usually absent. Plagioclase is broadly zoned (An_{62} to An_{37}) and commonly euhedral, enclosing minute crystals of hornblende and clinopyroxene. Hornblende (mg-value = 0.59-0.60) is euhedral to subhedral and rarely contains relict core of clinopyroxene (En_{39-40}, Fs_{13-14}, Wo_{46-48}). Biotite is entirely decomposed to chlorite, prehnite and epidote. Opaque minerals (sometimes up to 1.1 % in volume) are predominantly magnetite.

Potassium feldspar (0-15.2 % in volume) in the granodiorite is of average grain size of 2 mm in diameter and anhedral interstitial, showing microcline-lattice structure. Plagioclase is strongly zoned (An_{54} to An_{26}) and commonly euhedral with average grain size of 3 × 2 mm, enclosing plagioclase laths, biotite and magnetite grains. Oscillatory zoning is well developed. Quartz is generally anhedral and shows weakly undulatory extinction. Biotite (2.6-10.5 % in volume) occurs as euhedral to subhedral crystals with average grain size of 2 × 1 mm; the Z color is dark to reddish brown. Apatite, plagioclase and quartz are included in biotite. The biotite is high in TiO_2 (4.0-4.3 wt%) and mg-value (0.52). Hornblende (0-21.3 % in volume) occurs commonly as

euhedral prismatic crystals with average grain size of 3 × 1 mm showing dark green color and twining. Magnetite and plagioclase are commonly inclusions in hornblende. The hornblende has a zonal structure which characterized decrease in TiO_2 (2.3 to 1.2 wt%) and in mg-value (0.57 to 0.54) from core to rim. Apatite, allanite, sphene (up to 0.1 % in volume) and opaque oxides (mainly magnetite) are accessory minerals. Most of magnetite grains are euhedral and usually included in hornblende or biotite. Chlorite often replaces biotite. Basic inclusions are essentially composed of plagioclase (An_{58} to An_{56}), chloritized biotite and hornblende (mg-value=0.54-0.56) with accessories such as magnetite and apatite.

The Kuwasaki Facies, comprising medium-grained hornblende-biotite adamellite, intrudes into the Kanekido Facies. The foliation in the former is not so well developed as compared with that in the latter.

Potassium feldspar (23.9-27.2 % in volume) occurs generally as subhedral crystals with average grain size of 3 × 1 mm and pinkish tint and encloses plagioclase and quartz grains. Plagioclase is broadly zoned (An_{41} to An_{27}) and commonly euhedral with average grain size of 3 × 2 mm. It is occasionally coated by myrmekite. Quartz is generally anhedral and shows weakly undulatory extinction. Biotite (3.4-7.0 % in volume) is euhedral to subhedral with average grain size of 2 × 1 mm; the Z color is dark brown. It is high in TiO_2 (3.8-4.6 wt%) and low in Al_2O_3 (13.2-13.6 wt%). Hornblende (3.5-6.0 % in volume) occurs as subhedral to anhedral crystals with irregular boundaries and average grain size of 3 × 2 mm. It is palegreen in tint and rarely contains small clinopyroxene grains in core. The hornblende is low in Al_2O_3 (5.8-6.3 wt%) and TiO_2 (0.9-1.3 wt%). Accessory minerals include apatite, allanite, sphene, zircon and opaque oxides (mostly magnetite). Zircon often occurs within hornblende grains.

The Ikenoo Facies consists of granodiorite and adamellite, and is usually gradational to the Kanekido Facies. In comparison with the latter, the former is coarse-grained and rich in felsic minerals. In the center area of the facies, the foliation is weak to absent and potassium feldspar (up to 10 × 5 mm) with pinkish tint is much more commonly found.

Under the microscope, potassium feldspar (11.1 -24.8 % in volume) is micro-perthitic with microcline-lattice structure and mostly interstitial to plagioclase and quartz crystals. Plagioclase is of average grain size of 4 × 3 mm and strongly zoned (An_{49} to An_{18}). It is euhedral

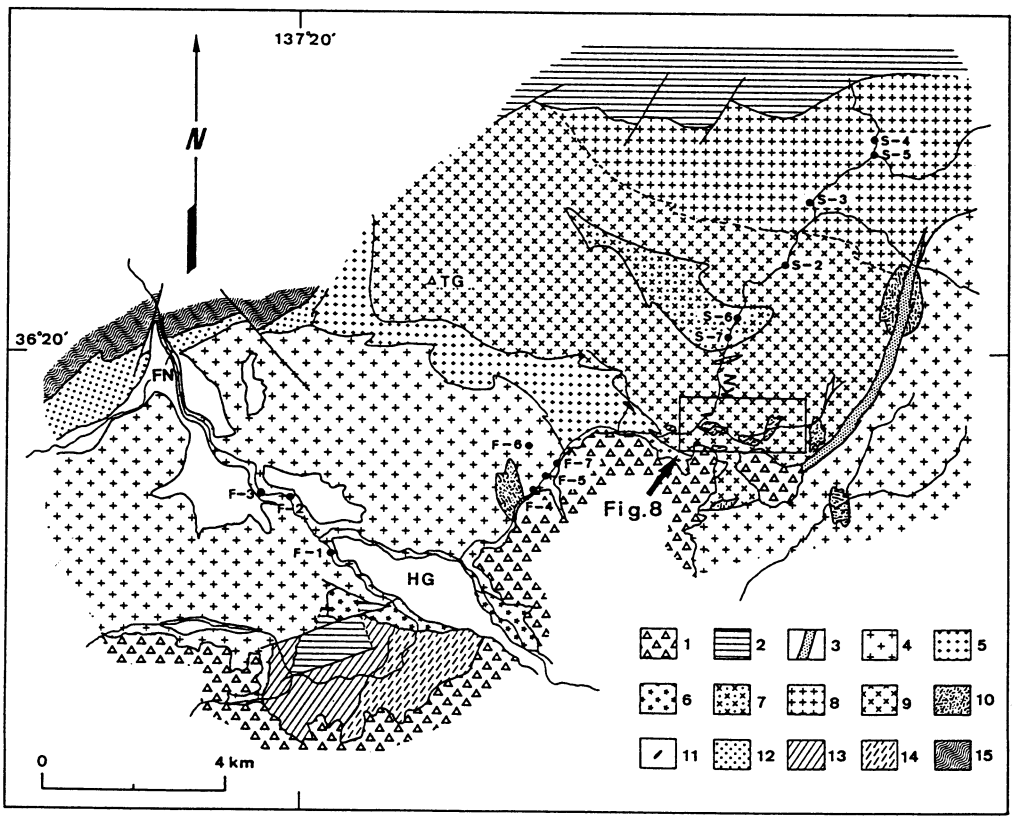

Fig. 7. Diagram showing geological map of the Shimonomoto mass and Funatsu mass district and locations of samples for isotopic study. 1, Oamamiyama Group and Kamitakahara Pyroclastic Flow Deposit; 2, Tetori Group; 3, Aplite; 4, Funatsu mass rocks; 5, Nakasawa Granite; 6, Hongo Granodiorite; 7 to 9, Shimonomoto mass rocks; 7, Kuwasaki Facies; 8, Ikenoo Facies; 9, Kanekido Facies; 10, Dioritic rocks; 11, Gabbroic rocks; 12, Granite mylonite; 13, Moribu Formation; 14, Arakigawa Formation; 15, Hida gneisses; FN, Funatsu; HG, Hongo; TG, Tengai-san; KN, Kanekido-gawa.

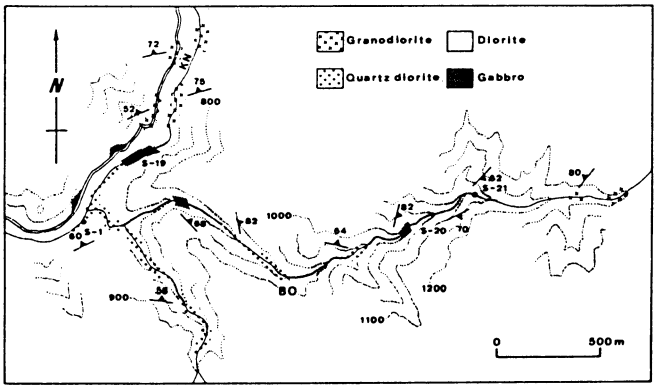

Fig. 8. Diagram showing route map of the Budo-odani district and locations of samples for this study. KN, Kanekido-gawa; BO, Budo-odani.

to subhedral and often saussurited in cores, accompanying myrmekite in rims. Oscillatory zoning is well developed. Quartz is generally anhedral and shows weakly undulatory extinction, containing inclusion minerals such as plagioclase, biotite and hornblende. Biotite (1.6-10.6 % in volume) occurs as euhedral to anhedral crystals with average grain size of 1 × 1 mm; the Z color is dark brown. It is are commonly decomposed to chlorite, prehnite and epidote. The biotite is high in TiO_2 (3.6-3.9 wt%) and low in Al_2O_3 (13.8-14.3 wt%). Hornblende (0-11.5 wt% in volume) occurs as euhedral prismatic crystals (often up to 2 × 1 cm) having bluish green color. Magnetite, biotite and apatite are commonly included in hornblende crystals. The hornblende has a zonal structure, which is characterized by increase in SiO_2 (44.8 to 47.0 wt%) from core to rim, and is high in mg-value (0.54-0.64). Apatite, allanite, sphene, opaque oxides (mainly magnetite, 0-0.4 % in volume) and zircon are accessory minerals. Sphene (up to 0.3 mm in length and 0.1 % in volume) often occurs in hornblende and biotite grains as inclusions.

The rocks of the Shimonomoto mass have magnetic susceptibility ranging from 30 to 550 × 10^{-6} emu/g, except for diorite and gabbro masses, and largely belong to the magnetite-series granitoids.

6. Funatsu Mass (Fig. 7)

The mass is made up of coarse- to medium-grained biotite adamellite and granodiorite characterized by subhedral pink potassium feldspar, which are frequently accompanied by pegmatite and aplite. Quartz diorite commonly occurs as xenolithic masses within the mass. The Funatsu mass intrudes into the Moribu Formation, which is composed of sandstone and shale of early Permian age, as well as the granite mylonite (so called augen gneiss in the Kamioka area) and the Nakasawa Granite which consists of fine-grained hornblende-bearing biotite granodiorite (Tanaka and Maruyama, 1985a). A weak foliation, which is formed by alignment of biotite flakes and lenticular basic inclusions, is locally developed. The foliation forms two-basin structure. Lenticular basic inclusions (up to 100 × 30 cm) consist of massive fine-grained dioritic rocks with phenocrysts of quartz and plagioclase. The Funatsu mass with porphyritic pink potassium feldspar resembles the Kekachidake mass.

Potassium feldspar (up to 2 cm in length) occurs as subhedral crystals and is strongly perthitic with well-developed microcline-lattice structure. Its large crystals show commonly Carlsbad twinning. The feldspar includes poikilitically minerals such as plagioclase, biotite, quartz and opaque oxides in order to decreasing. Plagioclase is euhedral to subhedral occasionally with myrmekitic rims and shows zoning from An_{28} to An_8, commonly enclosing irregular quartz grains and biotite flakes. Quartz occurs as large grains with irregular boundaries or clusters of smaller grains. Biotite (0.3-7.9 % in volume) occurs as large simple grains or clusters of small grains and tends to be chloritized; the Z color is dark brown. The large crystals contain apatite, zircon, quartz and opaque oxides as inclusions. The biotite is high in TiO_2 (3.4-3.7 wt%) and MnO (0.7-1.6 wt%) and low in Al_2O_3 (13.7-14.6 wt%). Hornblende is locally found in trace amount and occurs as anhedral crystals with dark green color. It is closely associated with biotite grains and low in mg-value (0.45). Accessory minerals are apatite (up to 0.2 mm in length), allanite, sphene, zircon and opaque oxides (mainly magnetite). Allanite (up to 1.5 mm in length) is often zoned, typically associated with biotite. Magnetite (up to 1 mm in diameter) is included in biotite and potassium feldspar and associated with ilmenite grains and lamellae in small amount. Basic inclusions are essentially composed of plagioclase (An_{31} to An_{21}),quartz, biotite (TiO_2= 2.9-3.3 wt%) and hornblende (mg-value=0.43-0.48) with apatite and magnetite as accessory minerals. The magnetic susceptibility of the mass, except for the quartz dioritic masses, ranging from 20 to 580 × 10^{-6} emu/g, is the same as that of the Shimonomoto mass.

7. Asuwagawa Mass

The mass occurs along the Asuwa River in the Fukui Prefecture and is mainly composed of weakly foliated fine- to medium-grained hornblende-biotite quartz diorite with small masses of crystallized limestone (Tsukano and Miura, 1959). The lithofacies of the mass is similar to that of the Kanekido Facies of the Shimonomoto mass. The limestone masses are reported to yield fossil such as Brachiopoda (Hattori, 1984). The Asuwagawa mass is unconformably overlain by the Higashiamada conglomerate of the Tetori Group (Maeda, 1961).

Potassium feldspar (3.8-4.3 % in volume) is anhedral and interstitial and shows microcline-lattice structure. Plagioclase (andesine) is mainly euhedral, commonly zoned and tends to be highly sericitized. Biotite (5.7-10.0 % in volume) occurs as subhedral to anhedral crystals and is strongly chloritized. Hornblende is present in nearly the same volume as biotite and has bluish green color. Accessory minerals are zircon, apatite, allanite, sphene, epidote and opaque oxides (mostly magnetite). Sphene (up to 1.4 % in volume) occurs as euhedral crystals, occasionally enclosing abundant magnetite grains.

8. Utsubo Mass (Fig. 9)

The mass is a typical normal zoned pluton and crops out in the area of about 15 km to northwest of the Funatsu mass, discordantly intruding into the Hida gneisses. It is divided into main- and associated-part based upon their modes of distribution (Ohtsubo, 1985). The former consists of concentrically arranged three facies as follows: Otani Facies, Nariteyama Facies and Horadani Facies in order toward the inner side. The latter is Western-part Facies, which may be a separated from the Utsubo mass but not a componential part of this mass (Kano, 1988, personal communication).

The Otani Facies is composed of medium-grained hornblende-biotite tonalite and granodiorite with mafic inclusions of large amount. The inclusions are fine-grained and consist of dark gray rocks of the assemblage plagioclase-hornblende-biotite-(quartz). The Nariteyama Facies varies gradually from medium-grained hornblende-biotite granodiorite in the western-half portion of the zone to coarse-grained biotite adamellite in the eastern-half portion. Both facies clearly intrude into the Otani Facies. The Horadani Facies comprises mainly massive fine-grained biotite adamellite intruding into the Nariteyama Facies. The lithofacies of the Western-part Facies is roughly medium-grained biotite adamellite.

Plagioclase crystals are strongly zoned with calcic core (andesine). Oscillatory zoning is well developed in plagioclase of the Otani and Nariteyama Facies. Myrmekite is particularly abundant in these facies. Biotite occurs typically as euhedral to subhedral crystals and is brown in tint, but it is entirely decomposed to chlorite, prehnite and epidote in the Nariteyama Facies. Hornblende is subhedral and dark green to brownish green in tint. It contains numerous inclusions of long prismatic apatite. Muscovite is present as small grains in plagioclase crystals and as euhedral crystals in the Nariteyama Facies.

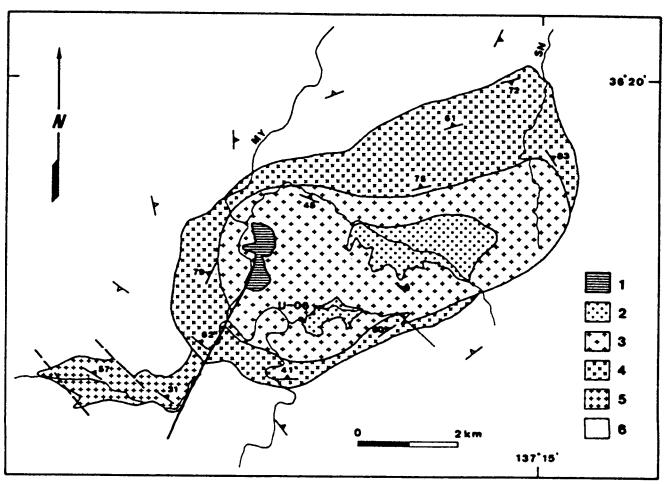

Fig. 9. Diagram showing geological map of the Utsubo mass district and location of a sample for isotopic study (after Ohtsubo 1985). 1, Shioya Formation; 2, Horadani Facies; 3, Nariteyama Facies; 4, Otani Facies; 5, Western-part Facies; 6, Hida gneisses; MY, Miya-kawa; SN, Sonbo-dani.

Zircon, apatite, allanite, sphene, epidote and opaque oxides (mostly magnetite) are accessory minerals. The rocks of the Utsubo mass have the magnetic susceptibility ranging from 0 to 950 × 10^{-6}emu/g and largely belong to the magnetite-series granitoids.

B. GRANITIC MASSES IN THE INNER PLUTONIC ZONE

1. Yatsuo Mass (Fig. 10)

The mass is exposed in the area of 15 km to north of the Utsubo mass and has a shape elongated to the east-west direction. It is a zoned pluton, which consists of the Todamine Facies in the outer zone, the Besougawa Facies in the inner zone and the aplitic granite intruding into the boundary between these two facies (Fig. 10). A foliation defined by parallel arrangement of hornblende crystals and basic schlieren forms a dome-like structure in the mass.

The Todamine Facies is composed of foliated coarse- to medium-grained hornblende biotite-tonalite and contacts with the Hida gneisses in the southern part. The basic schlieren is formed in about 300 m wide along the mass border. Its main constituent is biotite and plagioclase with hornblende and quartz as subordinate constituents. Crystalline limestone occasionally occurs as small bodies frequently associated with skarn (Kano, 1980).

Potassium feldspar (0.7-4.4 % in volume) is anhedral to interstitial and very weakly perthitic. Plagioclase is zoned (An_{48} to An_{31}) and occurs as euhedral to subhedral crystals with average grain size of 2.5 × 2 mm, commonly enclosing biotite and hornblende grains. Oscillatory zoning is poorly developed. Quartz (1-2 mm in diameter) is anhedral and shows strongly undulatory extinction. Sutured boundaries are remarkable for quartz. Biotite (7.4-15.7 % in volume) occurs as anhedral crystals with average grain size of 1 × 0.5 mm; the Z color is brown. The biotite is high in Al_2O_3 (15.2-15.3 wt%) and low in TiO_2 (2.6-4.0 wt%). Hornblende (0-12.3 % by volume) is commonly subhedral with average grain size of 1.5 × 1 mm and has dark green color. Biotite, magnetite and apatite are usually found in hornblende crystals as inclusions. The hornblende has a zonal structure which exhibits decrease in SiO_2 (46.3 to 41.3 %) and in mg-value (0.52 to 0.43) from core to rim. Apatite, zircon, allanite, euhedral sphene, opaque oxides (mainly magnetite) and epidote are accessory minerals. Particularly, sphene (0.2-0.7 % in volume) is conspicuous.

The Besougawa Facies consists of weakly foliated coarse- to medium-grained hornblende biotite granodiorite and biotite adamellite, which encloses a small body of fine-grained hornblende-biotite gneiss and amphibolite in its center part (Fig. 10). The granodiorite changes gradually the Todamine Facies in the western part of the mass, while the adamellite intrudes into the latter in the eastern part of the mass. Thus, it may be said that the adamellite is younger in intrusion age than the granodiorite, although the mutual relation of the former and the latter is unclear.

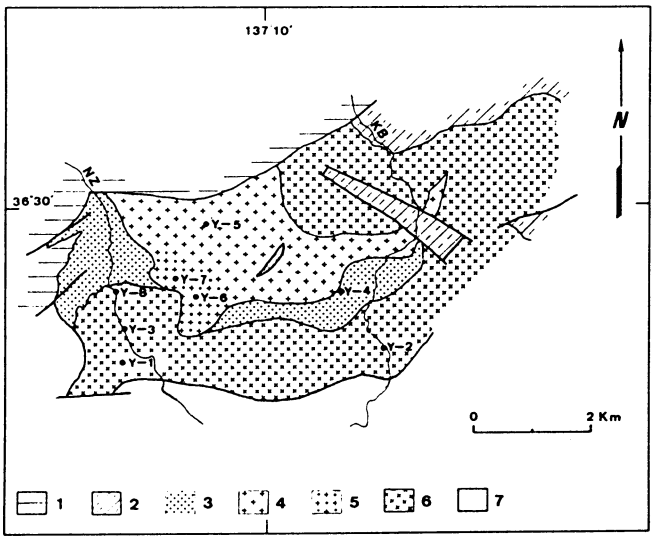

Fig. 10. Diagram showing geological map of the Yatsuo mass district and locations of samples for isotopic study. 1, Hokuriku Group; 2, Tetori Group; 3, Aplitic Granite; 4 and 5, Besougawa Facies (4, Adamellite; 5, Granodiorite); 6, Todamine Facies; 7, Hida gneisses, KB, Kubusu-gawa, NZ, Nozumi-gawa.

The Besougawa Facies is mineralogically characterized by potassium feldspar (up to 20 mm long) with pinkish tint. It (13.8-24.2 % in volume) is commonly subhedral and very weakly perthitic with shows microcline-lattice structure. The large potassium feldspar crystals contain plagioclase, quartz, sphene and magnetite as inclusions. Myrmekite is slightly developed at the contact between potassium feldspar and plagioclase crystals. Plagioclase is weakly zoned (An_{31} to An_{23}) and subhedral to anhedral with average grain size of 3 × 1 mm. It frequently shows bending of albite twin lamellae. Oscillatory zoning is poorly developed or absent. Quartz is anhedral and shows strongly undulatory extinction. Biotite (5.3-8.6 % in volume) occurs as subhedral crystals with average grain size of 1 × 0.3 mm and deformation wedges; the Z color is brown. The biotite is high in Al_2O_3 (15.1-15.3 wt%) and low in TiO_2 (2.4-2.7 wt%). Hornblende is present in minor amount (about 1.0 % in volume) and anhedral. Accessory minerals are apatite, euhedral sphene, zircon, epidote and opaque oxides (chiefly magnetite).

The aplitic granite is fine-grained biotite granodiorite. Plagioclase crystals (oligoclase) have cores fairly replaced by muscovite. Biotite (about 5 % in volume) is decomposed to some extent to chlorite and prehnite, but fresh part with reddish brown color is still remained. Sphene, allanite, zircon and epidote are accessory minerals.

The rocks of the Yatsuo mass have the magnetic susceptibility ranging from 30 to 600 × 10^{-6}emu/g and largely belong to the magnetite-series granitoids.

2. Shogawa Mass (Fig. 11)

The mass is a reversely zoned pluton with long diameter of about 10 km in a northeast-southwest direction and composed of three lithological facies as follows: Omaki Facies, Toga Facies and Nashitani Facies. The Omaki Facies is intruded by the Toga Facies and placed in the center area of the mass. The Toga Facies is most extensive developed in the mass, gradually changing into the Nashitani Facies at the western part.

The Omaki Facies consists mainly of fine- to medium-grained quartz diorite and tonalite, though it is remarkably variable in lithofacies with small bodies of hornblende gabbro and pyroxene gabbro. According to field observation, the hornblende gabbro may be regarded as enclosed rock in the quartz diorite and tonalite. However, the pyroxene gabbro and quartz diorite are intergradational. The Omaki Facies nearly corresponds to the Omaki Diorite after Nozawa et al. (1981).

The pyroxene gabbro is massive and composed of plagioclase (73 % in volume), clinopyroxene (7 %), orthopyroxene (6 %), biotite (5 %), hornblende (4 %), opaque oxides (3 %) and quartz (1 %). Plagioclase shows conspicuous zoning from An_{61} to An_{39} and its twin lamellae are often bent. Oscillatory zoning is absent. Orthopyroxene (En_{59-61}, Fs_{37-39}, Wo_{2-3}) occurs as euhedral crystals and is faintly pleochroic from colourless to pale pink. Clinopyroxene (En_{38-40}, Fs_{14-17}, Wo_{44-47}) is generally subhedral and unzoned. Hornblende (mg-value=0.54-0.59) commonly occurs as rims around clinopyroxene. Biotite (mg-value=0.53-0.57) is closely associated with hornblende and very reddish brown in tint. Opaque oxides are mainly magnetite with lesser amount of ilmenite.

The hornblende gabbro is foliated and consists essentially of hornblende (54 % in volume) and plagioclase (40 %), with accessory epidote, chlorite, muscovite and opaque oxides. Zoning in plagioclase is not remarkable (An_{91-83}), but rim of An_{51} is rarely found. Hornblende is bluish brown in color and contains elongate needles of exsolved rutile. It has a zonal structure, which is characterized by increase in SiO_2 (41.8 to 43.7 wt%) from core to rim and is high in mg-value (0.58-0.63) and in Al_2O_3 (12.4-13.9 wt%). Opaque oxides are magnetite, pyrite and ilmenite.

The medium-grained quartz diorite has a foliation defined by parallel arrangement of hornblende crystals which shows north - south trend (Fig. 11). Plagioclase is broadly zoned (An_{52} to An_{33}) and occurs as euhedral to subhedral crystals with average grain size of 2 × 1 mm, partially enclosing hornblende and biotite grains. Oscillatory zoning is absent. Biotite (11.9-13.8 % in volume) occurs as subhedral crystals with average grain size of 1 × 1.5 mm; the Z color is greenish brown. The biotite is high in Al_2O_3 (15.2-15.6 wt%) and low in TiO_2 (2.8-3.6 wt%). Hornblende (14.4-21.6 % in volume) is subhedral crystals with average grain size of 1 × 1.5 mm and dark green in color, frequently enclosing rounded and corroded quartz grains (sieve structure) in large amount. The hornblende with sieve structure is higher in mg-value (0.57-0.60) and in SiO_2 (47.0-48.0 wt%) than that without it. Apatite,

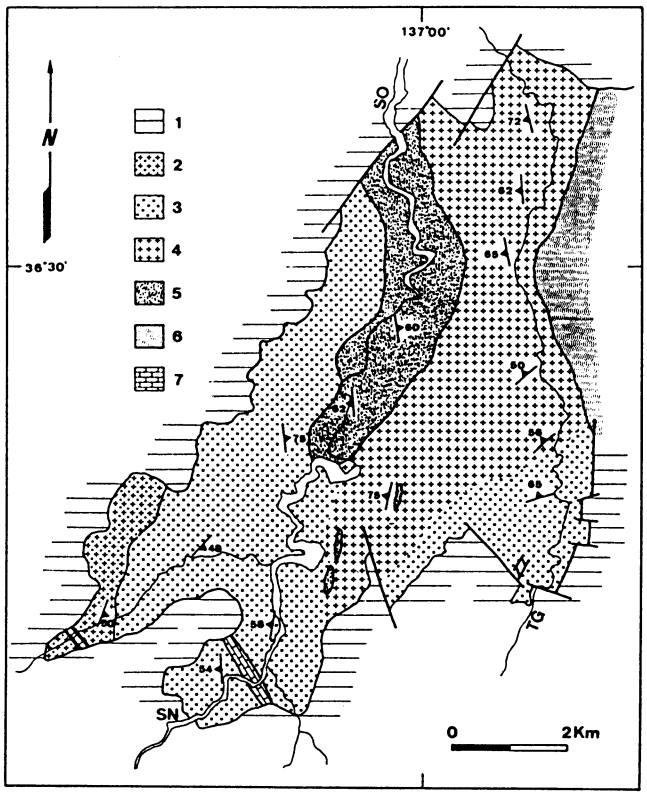

Fig. 11. Geological map of the Shogawa mass district 1, Hokuriku Group; 2, Nashitani Facies; 3 and 4, Toga Facies (3, Fine-grained rocks; 4, Medium-grained rocks); 5, Omaki Facies; 6, Hida gneisses; 7, Crystalline limestone; SO, Shogawa; TG, Toga-gawa; SN, Shimonashi.

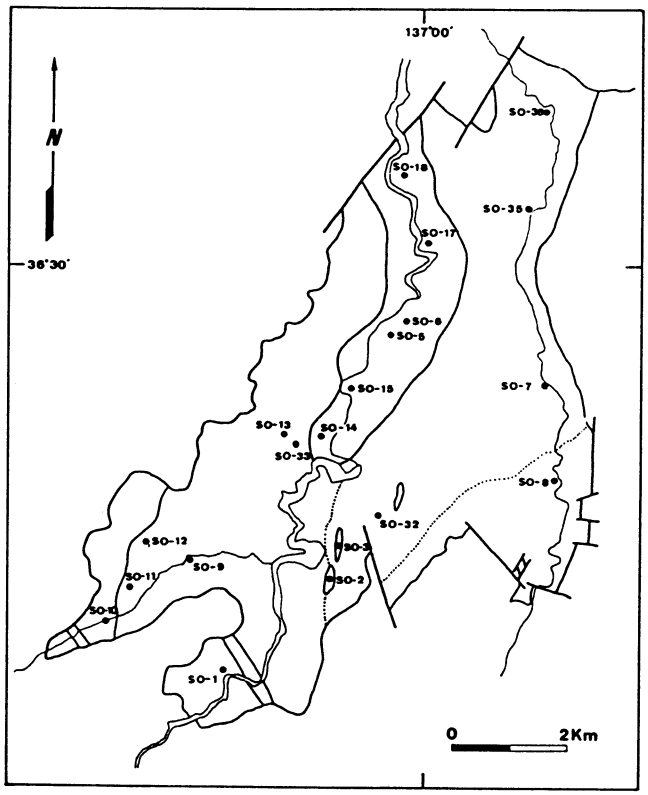

Fig. 12. Diagram showing locations of the Shogawa mass samples.

subhedral sphene (0.7-1.0 % in volume), opaque oxides (mainly magnetite), zircon and epidote are accessory minerals.

The Toga Facies is composed of weakly foliated fine- to medium-grained granodiorite and adamellite which contains scarcely inclusions. These rocks are commonly light to dark gray and homogeneous. The foliation defined only by parallel arrangement of biotite flakes has a north - northeast trend (Fig. 11) which is the same as that in the quartz diorite. The medium-grained rocks are dominant in the eastern part and the fine-grained ones are rich in the western part of the mass. Small bodies of crystalline limestone occur occasionally in the southern part.

Potassium feldspar is subhedral to anhedral with average grain size of 2 × 1 mm, commonly enclosing plagioclase, quartz and biotite grains, and weakly perthitc with microcline-lattice structure. Plagioclase is euhedral to subhedral with average grain sizeof 1 × 1 mm and generally weakly zoned (An_{27} to An_{15}), although a conspicuous zoning from An_{61} to An_{18} is found in the vicinity of the Omaki Facies. It frequently shows bending of albite twin lamellae. Oscillatory zoning is poorly developed. Quartz (1-2 mm in diameter) occurs as subhedral to anhedral crystals and shows strongly undulatory extinction. Sutured boundaries are remarkable for quartz. Biotite (3.8-8.3 % in volume) occurs as euhedral to subhedral crystals with average grain size of 0.2 × 0.6 mm; the Z color is dark brown. The bio titeis high in Al_2O_3 (15.5-16.7 wt%) and low in mg-value (0.29-0.43). Muscovite (up to 1.6 % in volume) commonly occurs as irregular grains within large plagioclase grains; it is low in Al_2O_3 (30.1-30.6 wt%) and Na_2O (0.2 wt%) and high in FeO (6.0-6.1 wt%) and MgO (1.2-1.5 wt%). As compared with the chemical composition of muscovite from the Cretaceous - Paleogene batholiths in southwestern Japan (Czamanske et al. 1981), the muscovite in the Toga Facies is inferred to be a secondary one. Accessory minerals include apatite, allanite, sphene (0-0.2 % in volume), opaque oxides (mainly magnetite), zircon and epidote. Opaque oxides are scarcely found.

The Nashitani Facies, which is characterized by euhedral potassium feldspar with pinkish tint, consists of massive to weakly foliated medium-grained biotite adamellite with small masses of crystalline limestone. Generally, plagioclase twin lamellae are bent and quartz grains show strongly undulatory extinction. Biotite (about 4 % in volume) occurs as euhedral to subhedral crystals with average grain size of 0.2 × 0.5 mm; the Z color is greenish brown. Apatite, euhedral sphene, zircon, allanite, epidote and opaque oxides (mainly magnetite) are accessory minerals.

3. Hodatsusan Mass (Fig. 13)

The mass is a reversely zoned pluton with tonalitic core, granodioritic mantle and granitic

rim and crops out in the area of about 25 km to northeast of the Kanazawa city (Kanayama and Hiroi, 1979). The granitic rocks intrude into both tonalitic rocks and granodioritic rocks which are intergradational to each other. Occasionally small rock bodies of the Hida gneisses and diorite occur in the tonalitic core and granodioritic mantle. The foliation in the tonalitic core and granodioritic mantle, which is defined by alignment of hornblende crystals and biotite flakes, has a north-northeast strike, which is parallel to that of the Shogawa mass.

Potassium feldspar (0.2-7.8 % in volume) is anhedral to interstitial and weakly perthitic with microcline-lattice structure. Quartz is interstitial and commonly shows undulatory extinction. Plagioclase is zoned (An_{41} to An_{22}) and euhedral to subhedral with average grain size of 2 × 1 mm. Oscillatory zoning is absent. Biotite (7.3-10.9 % in volume) is euhedral to subhedral with average grain size of 1 × 0.5 mm; the Z color is greenish brown. The biotite is high in Al_2O_3 (14.9-15.4 wt%) and low in TiO_2 (2.4-3.1 wt%). Hornblende (2.5-14.0 % in volume) occurs commonly as subhedral to anhedral crystals with average grain size of 2 × 1 mm showing dark green color. These grains commonly have irregular boundaries and form clusters with biotite and sphene. The hornblende has a zonal structure, which is characterized by the decrease in SiO_2 (43.3 to 40.8 wt%) and in mg-value (0.44 to 0.37) from core to rim. Apatite, sphene (0-1.3 % in volume), opaque oxides (mainly magnetite) and epidote are accessory minerals.

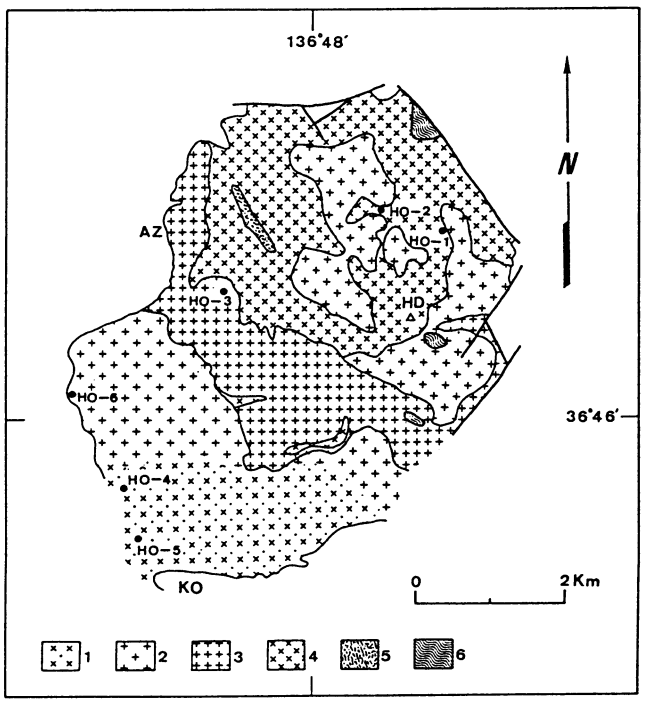

Fig. 13. Diagram showing geological map of the Hodatsusan mass district and locations of samples for isotopic study (simplified from Kanayama and Hiroi, 1979). 1 and 2, Granitic rim (1, Adamellite; 2, Granodiorite); 3, Granodioritic mantle; 4, Tonalitic core; 5, Dioritic rocks; 6, Hida gneisses; AZ, Azuma; HD, Hodatsusan; KO, Kamiota.

The granitic rim is composed of massive coarse-grained granodiorite and adamellite and contains scarcely basic inclusions. Potassium feldspar (up to 2 cm in length) is generally subhedral and weakly perthitic with microcline-lattice structure. It often has myrmekitic rim, including poikilitically plagioclase, hornblende, biotite, quartz and opaque oxides. Plagioclase is zoned (An_{43} to An_{22}), rarely including calcic core (An_{50}). Oscillatory zoning is well developed. Quartz occurs as large grains or interstitial, commonly enclosing hornblende and sphene grains. Biotite (6.1-7.3 % in volume) occurs as euhedral to subhedral crystals with average grain size of 3 × 2 mm; the Z color is greenish brown. The large biotite crystals (up to 5 × 5 mm) contain abundant minerals such as sphene, apatite, opaque oxides and zircon as inclusions. The biotite is high in Al_2O_3 (14.6-15.4 wt%) and low in TiO_2 (2.2-2.7 wt%). Hornblende (1.5-2.9 % in volume) is mainly euhedral with average grain size of 2 × 1 mm and dark green in color. It has a zonal structure which is characterized by decrease in SiO_2 (47.2 to 43.2 wt%) and in mg-value (0.53 to 0.47) from core to rim. Accessory minerals include apatite, allanite, euhedral sphene (0.4-0.9 % in volume), zircon, epidote and opaque oxides (mainly magnetite).

4. Togi area

In the northwestern part of the Noto Peninsula, the Togi area, are sporadically developed several small masses consisting of granitic and metamorphic rocks (Kaseno et al., 1965). Biotite gneiss and medium-grained biotite tonalite crop out along the Shishizu coast.

A foliation defined by alignment of biotite flakes is well developed in the tonalite having a northwest strike. Both potassium feldspar and quartz are anhedral and interstitial. Undulatory extinction of quartz is not conspicuous. Plagioclase is strongly zoned (An_{50} to An_{23}) and euhedral with average grain size of 2 × 1 mm. Oscillatory zoning is well developed. Biotite (about 13 % in volume) is euhedral to subhedral with average grain size of 0.2 × 0.5 mm; the Z color is brown. It is high in Al_2O_3 (15.0-15.2 wt%) and low in TiO_2 (2.9-3.1 wt%) and in mg-value (0.38-0.40). Hornblende is present but in very minor amount. Apatite, allanite, sphene, zircon, epidote and opaque oxides (mainly magnetite) are accessory minerals.

IV. MINERAL CHEMISTRY

Chemical composition of minerals such as pyroxene, biotite, amphibole and plagioclase have been analyzed by X-ray microprobes (JXA-5, JXA-5A and JCMA-733Ⅱ). Operating condition was 15 kv accelerating potential, 18 na sample current and a 5-micron beam diameter. Sr in plagioclase was analyzed using a JCMA-733Ⅱ microprobe with a Ba-Sr synthetic glass standard. Operating condition was

Table 1. Representative plagioclase analyses.

Sample No.	S-20		S-25		S-21		HK-159	
Mass Name[1]	SHI		SHI		SHI			
Rock type	gabbro		gabbro		diorite		gabbro	
	core	rim	core	rim	core	rim	core	rim
SiO_2 (wt%)	45.99	53.75	53.48	55.00	55.40	57.87	45.69	53.26
TiO_2	0.00	0.00	0.00	0.01	0.04	0.02	0.02	0.02
Al_2O_3	33.80	28.76	28.84	28.36	27.83	26.03	33.92	28.99
FeO*	0.30	0.27	0.29	0.25	0.21	0.16	0.06	0.02
MnO	0.00	0.05	0.00	0.02	0.00	0.00	0.00	0.00
MgO	0.01	0.02	0.00	0.01	0.00	0.00	0.01	0.00
CaO	17.59	11.40	11.80	10.68	10.51	8.32	18.09	11.94
Na_2O	1.22	4.62	4.70	5.34	5.17	6.45	1.39	4.91
K_2O	0.05	0.09	0.18	0.20	0.27	0.22	0.04	0.04
Total	98.96	98.96	99.29	99.87	99.43	99.07	99.22	99.18
Si	8.553	9.807	9.751	9.936	10.034	10.449	8.491	9.718
Ti	0.000	0.000	0.000	0.001	0.005	0.002	0.002	0.002
Al	7.409	6.185	6.197	6.038	5.941	5.540	7.430	6.234
Fe	0.047	0.041	0.045	0.038	0.032	0.024	0.009	0.003
Mn	0.000	0.008	0.000	0.002	0.000	0.000	0.000	0.000
Mg	0.001	0.004	0.001	0.004	0.000	0.000	0.002	0.000
Ca	3.506	2.229	2.305	2.067	2.040	1.610	3.603	2.334
Na	0.441	1.636	1.662	1.871	1.814	2.259	0.503	1.736
K	0.011	0.020	0.043	0.046	0.062	0.050	0.009	0.010
An	88.6	57.4	57.5	51.9	52.1	41.1	87.6	57.2
Ab	11.1	42.1	41.4	46.9	46.3	57.6	12.2	42.5
Or	0.3	0.5	1.1	1.2	1.6	1.3	0.2	0.3

Sample No.	SO-14		SO-18		SO-6		MG-1	
Mass Name[1]	SHO		SHO		SHO			
Rock type	gabbro		gabbro		diorite		gabbro	
	core	rim	core	rim	core	rim	core	rim
SiO_2 (wt%)	45.93	54.51	53.53	57.97	57.32	59.80	52.20	60.01
TiO_2	0.00	0.00	0.01	0.00	0.00	0.01	0.05	0.01
Al_2O_3	34.36	28.74	29.10	26.35	26.70	25.18	29.83	24.96
FeO*	0.03	0.05	0.14	0.12	0.09	0.02	0.08	0.18
MnO	0.04	0.01	0.02	0.02	0.00	0.03	0.00	0.00
MgO	0.01	0.00	0.00	0.00	0.00	0.00	0.00	0.00
CaO	18.38	11.29	12.20	8.30	8.92	7.01	12.80	7.25
Na_2O	1.00	5.16	4.13	6.45	6.42	7.46	4.20	7.35
K_2O	0.00	0.05	0.21	0.36	0.14	0.16	0.12	0.21
Total	99.75	99.81	99.34	99.57	99.59	99.67	99.12	99.97
Si	8.479	9.853	9.740	10.420	10.318	10.688	9.538	10.708
Ti	0.000	0.000	0.001	0.000	0.000	0.002	0.006	0.002
Al	7.476	6.125	6.240	5.584	5.663	5.306	6.423	5.249
Fe	0.005	0.008	0.021	0.018	0.013	0.003	0.012	0.027
Mn	0.006	0.001	0.003	0.003	0.000	0.005	0.000	0.000
Mg	0.002	0.000	0.000	0.000	0.000	0.000	0.000	0.000
Ca	3.636	2.187	2.379	1.599	1.720	1.342	2.506	1.386
Na	0.359	1.810	1.458	2.248	2.239	2.585	1.490	2.543
K	0.000	0.011	0.050	0.082	0.033	0.036	0.027	0.047
An	91.0	54.5	61.2	40.7	43.1	33.9	62.3	34.9
Ab	9.0	45.2	37.5	57.2	56.1	65.2	37.0	63.9
Or	0.0	0.3	1.3	2.1	0.8	0.9	0.7	1.2

The structural formulae have been calculated on the basis of 32 oxygen equivalents. FeO* :total Fe as FeO.
[1] Abbreviations as in Table 5.

Table 1. (continued)

Sample No.	F-3		S-2			O-1		
Mass Name[1]	FUN		SHI			OKU		
Rock type	granodiorite		granodiorite			tonalite		
	core	rim	core	1/2way	rim	core	1/2way	rim
SiO_2 (wt%)	60.94	64.24	55.57	56.47	59.53	59.45	59.81	61.62
TiO_2	0.01	0.00	0.00	0.00	0.00			
Al_2O_3	24.12	22.14	27.29	26.92	24.88	24.39	24.25	22.95
FeO*	0.05	0.06	0.17	0.15	0.13	0.13	0.07	0.07
MnO	0.02	0.00	0.00	0.00	0.00			
MgO	0.00	0.00	0.01	0.00	0.00			
CaO	5.99	3.54	9.86	9.30	7.15	6.81	6.24	4.81
Na_2O	8.20	9.63	5.77	5.95	7.29	7.45	7.59	8.69
K_2O	0.22	0.14	0.29	0.33	0.32	0.23	0.18	0.16
SrO			0.08	0.08	0.05	0.07	0.06	0.04
Total	99.54	99.75	99.04	99.20	99.35	98.45	98.20	98.34
Si	10.888	11.363	10.110	10.232	10.697	10.761	10.831	11.106
Ti	0.002	0.000	0.000	0.000	0.000			
Al	5.079	4.617	5.851	5.749	5.269	5.204	5.176	4.876
Fe	0.008	0.009	0.026	0.022	0.020	0.019	0.011	0.010
Mn	0.002	0.000	0.000	0.000	0.000			
Mg	0.000	0.000	0.004	0.001	0.001			
Ca	1.146	0.617	1.922	1.806	1.376	1.321	1.211	0.929
Na	2.840	3.302	2.036	2.091	2.541	2.614	2.665	3.037
K	0.051	0.031	0.068	0.075	0.073	0.052	0.041	0.037
An	28.4	15.6	47.7	45.5	34.5	33.1	30.9	23.2
Ab	70.3	83.6	50.6	52.6	63.7	65.6	68.0	75.9
Or	1.3	0.8	1.7	1.9	1.8	1.3	1.1	0.9

Sample No.	SO-35		HO-3		HO-6		
Mass Name[1]	SHO		HOD		HOD		
Rock type	granodiorite		granodiorite		granodiorite		
	core	rim	core	rim	core	1/2way	rim
SiO_2 (wt%)	60.12	63.34	59.84	61.65	57.13	59.29	61.02
TiO_2	0.00	0.01					
Al_2O_3	24.86	22.95	24.87	23.59	25.87	24.45	23.17
FeO*	0.04	0.23	0.10	0.11	0.15	0.08	0.12
MnO	0.00	0.00					
MgO	0.00	0.00					
CaO	6.54	4.24	7.06	5.46	8.83	7.00	5.32
Na_2O	7.38	9.05	7.09	8.36	6.43	7.46	8.51
K_2O	0.14	0.14	0.30	0.09	0.21	0.27	0.16
SrO					0.15	0.13	0.11
Total	99.09	99.96	99.25	99.26	98.77	98.68	98.41
Si	10.779	11.206	10.736	11.015	10.390	10.732	11.022
Ti	0.000	0.001					
Al	5.253	4.786	5.259	4.967	5.545	5.216	4.933
Fe	0.007	0.034	0.015	0.016	0.023	0.012	0.018
Mn	0.000	0.000					
Mg	0.000	0.000					
Ca	1.256	0.804	1.358	1.045	1.721	1.358	1.030
Na	2.564	3.103	2.467	2.896	2.268	2.620	2.981
K	0.033	0.033	0.068	0.021	0.049	0.062	0.038
An	32.6	20.4	34.9	26.4	42.6	33.6	25.4
Ab	66.5	78.8	63.4	73.1	56.2	64.9	73.6
Or	0.9	0.8	1.7	0.5	1.2	1.5	0.9

The structural formulae have been calculated on the basis of 32 oxygen equivalents. FeO* :total Fe as FeO.
[1] Abbreviations as in Table 5.

15 kv accelerating potential and 45 na sample current, and a 5-micron beam diameter was used. SrO concentrations were reproducible to within ± 200 ppm.

PLAGIOCLASE

Plagioclase is an early crystallizing phase in the early Mesozoic igneous rocks. Chemical composition and structural formulae of selected samples are given in Table 1. Plagioclase in the two-pyroxene gabbro (sample S-20) from the Shimonomoto mass is very calcic and ranges from bytownite (An_{89}) to labradorite (An_{57}). In the two-pyroxene gabbro (sample SO-18) from the Shogawa mass, however, plagioclase ranges from labradorite (An_{61}) to andesine (An_{39}). Plagioclase in the hornblende gabbros, sample HK-159 from the Kamioka mining area and sample SO-14 from the Shogawa mass, is also very calcic and ranges from anorthite (An_{91}) to labradorite (An_{50}), except for that in sample MG-1 (so called meta-gabbro) from the Unazuki area (Katoh, 1989). The sample HK-159, comblayering rock, crops out in the heterogeneous dioritic rocks [so called metabasite after Kano et al. (1989)] and is in close association with the metabasite.

Core compositions of plagioclase from the granitic rocks of the Outer Plutonic Zone range from An_{54} to An_{27}, while those from the Inner Zone range from An_{61} to An_{27}. Rim compositions from the former range from An_{27} to An_8, while those from the latter range from An_{34} to An_{15}. Calcic cores are occasionally present in the plagioclase crystals from acid facies of the Inner Zone masses. The high-calcic cores, An_{61} for the Shogawa mass (sample SO-13 from the Toga Facies) and An_{50} for the Hodatsusan mass (sample HO-4 from the granitic rim), are quite minute component and may be refractory xenocrysts from source region. They may also reflect the mixing of granitic melt and basic magma (liquid + calcic core), which occurred during the early stage of the crystallization history of the former.

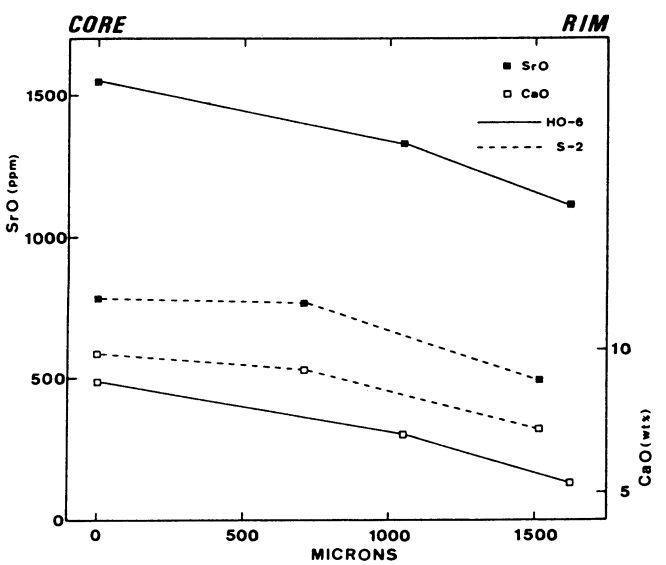

Fig. 14 Microprobe traverse for SrO and CaO in plagioclase feldspars from sample S-2 (Shimonomoto mass) and HO-6 (Hodatsusan mass).

Plagioclases of sample S-2 (46 % plagioclase, 64 wt% SiO_2, 352 ppm Sr) from the Shimonomoto mass, sample O-1 (55 % plagioclase, 65 wt% SiO_2, 373 ppm Sr) from the Okumayama mass in the Outer Plutonic Zone and sample HO-6 (52 % plagioclase, 65 wt% SiO_2, 765ppm Sr) from the Hodatsusan mass in the Inner Plutonic Zone were analysed for Sr and major elements (Table 1). Plagioclase cores of sample HO-6 contains SrO of about twice as much as those of sample S-2 and sample O-1. SrO in plagioclase decreases progressively toward its rim (Fig. 14). Sr was estimated to be much more highly concentrated in plagioclase than in other constituent minerals, based on the modal abundance and SrO concentration of plagioclase. As only the feldspars have values of mineral/liquid Sr partition coefficient (K_{DSr}) greater than unity (Arth, 1976), the remaining Sr may be contained in potassium feldspar.

CLINOPYROXENE

Clinopyroxene is the most abundant constituent of the gabbroic rocks, but is absent in the most acidic rocks. Calcium pyroxenes analyzed in this study are classified as augite and salite (Fig. 15). Chemical composition and structural formulae of selected samples are given in Table 2. Clinopyroxene compositions show a systematic decrease in mg values (Mg/(Fe+Mn+Mg)) from 0.81 to 0.75 in the gabbros (sample S-20 and S-25), and from 0.74 to 72 in the diorite (sample S-21) from the Shimonomoto mass. Whereas clinopyroxenes in the gabbro (sample SO-18) from the Shogawa mass have lower mg values (0.73 to 0.69) than those from the Shimonomoto mass. TiO_2 and Na_2O contents of all these clinopyroxenes are low and comparable with those of clinopyroxene phenocrysts in orogenic basalts and andesites (calc-alkaline and tholeiitic rocks) (e.g. Gill, 1981, Leterrier et al, 1982). The Al_2O_3 content is variable but generally low (1.0-3.5 %). Such values of Al_2O_3 and Na_2O contents are indicative of low-pressure crystallization of clinopyroxene (Herzberg, 1978). Zoned clinopyroxene crystals tend to show increase of Ti, Al and iron content as towards their rims (Table 2).

ORTHOPYROXENE

Orthopyroxene occurs only in the gabbroic rocks. Its compositional data are presented in Table 3. Orthopyroxene compositions (Fig. 15) range from bronzite (sample S-20) to hypersthene (sample SO-18) and are of low-pressure plutonic orthopyroxene (Herzberg, 1978). Al_2O_3 and Na_2O contents are lower in orthopyroxene than in clinopyroxene. Zoned orthopyroxene crystals (sample S-20) show a tendency to become iron-rich towards their rims without change in Ca-content (Table 3). Fig. 15 indicates the relationship between the two pyroxene phases. Temperature for the crystallization of coexisting pyroxene cores in the gabbroic

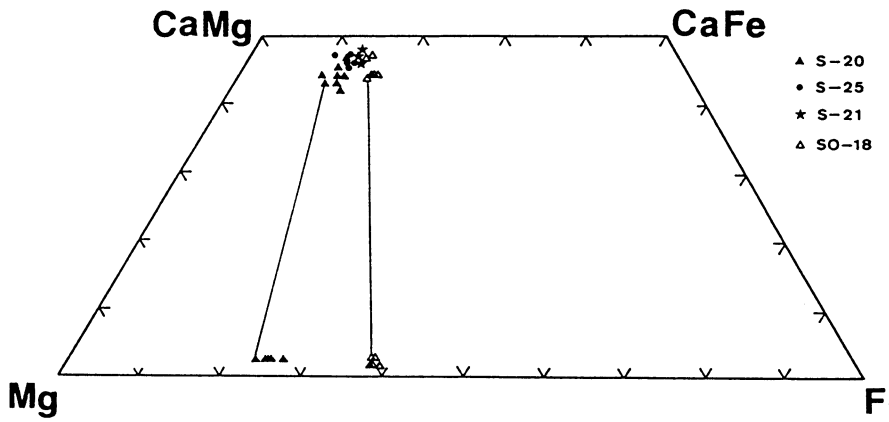

Fig. 15. Molecular composition of Ca-rich and Ca-poor pyroxenes from the gabbroic and dioritic rocks plotted on the pyroxene quadrilateral: Shimonomoto mass samples (S-20, S-21, S-25) and Shogawa mass sample (SO-18). Tie lines connect coexisting pyroxenes in the same rock.

Table 2. Representative clinopyroxene analyses.

Sample No.	S-20		S-25	S-21	SO-18	
Mass Name[1]	SHI		SHI	SHI	SHO	
Rock type	gabbro		gabbro	diorite	gabbro	
	core	rim			core	rim
SiO_2 (wt%)	51.90	51.25	52.71	52.35	52.87	52.21
TiO_2	0.38	0.74	0.25	0.19	0.19	0.27
Al_2O_3	2.37	3.53	1.47	0.98	1.40	1.61
FeO*	6.46	7.31	6.56	8.38	8.77	9.69
MnO	0.18	0.26	0.25	0.31	0.29	0.35
MgO	16.04	14.74	14.99	13.84	13.63	13.72
CaO	21.50	21.27	23.18	22.94	22.10	20.82
Na_2O	0.24	0.31	0.24	0.32	0.40	0.38
K_2O	0.02	0.03	0.02	0.01	0.01	0.01
Total	99.09	99.44	99.67	99.32	99.66	99.06
Si	1.931	1.907	1.958	1.969	1.977	1.968
Ti	0.011	0.021	0.007	0.005	0.005	0.008
Al^{IV}	0.069	0.093	0.042	0.031	0.023	0.032
Al^{VI}	0.035	0.062	0.022	0.013	0.039	0.040
Fe	0.201	0.227	0.204	0.264	0.274	0.306
Mn	0.006	0.008	0.008	0.010	0.009	0.011
Mg	0.889	0.817	0.830	0.776	0.760	0.771
Ca	0.857	0.848	0.923	0.925	0.886	0.841
Na	0.017	0.023	0.018	0.024	0.029	0.028
K	0.001	0.002	0.001	0.000	0.001	0.001
mg	0.811	0.777	0.797	0.739	0.729	0.709
En	45.66	43.18	42.41	39.49	39.58	40.20
Fs	10.32	12.00	10.42	13.44	14.27	15.95
Wo	44.02	44.82	47.16	47.07	46.15	43.85

The structural formulae have been calculated on the basis of 6 oxygen equivalents. FeO* :total Fe as FeO, mg=Mg/(Mg+Mn+Fe). En, Fs, and Wo calculated using Mg, Ca, and total Fe.
[1] Abbreviations as in Table 5.

Table 3. Representative orthopyroxene analyses.

Sample No.	S-20		SO-18	
Mass Name[1]	SHI		SHO	
	core	rim	core	rim
SiO_2 (wt%)	54.67	53.94	52.84	52.75
TiO_2	0.24	0.23	0.11	0.18
Al_2O_3	1.15	1.39	0.80	0.84
FeO*	14.71	18.91	23.34	23.36
MnO	0.40	0.54	0.74	0.71
MgO	26.69	25.40	20.71	21.03
CaO	1.39	1.28	0.83	0.96
Na_2O	0.02	0.02	0.03	0.00
K_2O	0.03	0.00	0.01	0.01
Total	99.30	99.71	99.41	99.85
Si	1.980	1.967	1.992	1.981
Ti	0.007	0.006	0.003	0.005
Al^{IV}	0.020	0.033	0.008	0.019
Al^{VI}	0.029	0.027	0.027	0.018
Fe	0.446	0.516	0.736	0.733
Mn	0.012	0.017	0.024	0.023
Mg	1.441	1.381	1.163	1.177
Ca	0.054	0.050	0.033	0.039
Na	0.001	0.002	0.002	0.000
K	0.002	0.000	0.001	0.001
mg	0.759	0.722	0.605	0.609
En	74.24	70.93	60.20	60.39
Fs	22.98	26.50	38.10	37.67
Wo	2.78	2.57	1.70	2.00

The structural formulae have been calculated on the basis of 6 oxygen equivalents. FeO* :total Fe as FeO, mg=Mg/(Mg+Mn+Fe). En, Fs, and Wo calculated using Mg, Ca, and total Fe.
[1] Abbreviations as in Table 5.

rocks, which was estimated following the method of Wood and Banno (1973), ranges from 950 to 1000℃ for sample S-20 and is 880℃ for sample SO-18.

AMPHIBOLE

Amphibole is commonly found in all masses of the early Mesozoic igneous rocks, except for the Kekachidake mass. Chemical composition and structural formulae of amphiboles in selected samples are given in Table 4. Ferroan-pargasite, ferroan-pargasitic-hornblende, magnesio-hornblende, actinolitic-hornblende and actinolite occur in the gabbroic rocks (Fig. 16). In general, amphibole in the hornblende gabbros (sample HK-159, MG-1 and SO-14) is highly rich in Al, Ti and Na contents. The compositional variation is manifested as zoning which is characterized by decrease of Al, Ti and Na contents from core to rim. Experimental and petrological studies (Kostyuk and Sobolev, 1969; Leake, 1971; Helz, 1973; Gilbert et al., 1982; Robinson et al., 1982) have shown that Al, Ti, Na and K contents all increase with increase of temperature. Therefore, it can be said that amphibole in the hornblende gabbros records temperature variation during its cooling. Actinolite and actinolitic hornblende are thought to have been formed by alteration of clinopyroxene.

In the granitic rocks occur magnesian-hastingsitic-hornblende, ferro-edenitic-hornblende, ferro-edenite, magnesio-hornblende and actinolitic-hornblende occur (Figs. 16, 17). The most alkali enrichment was measured in ferro-edenitic-hornblende from the Hayatsukigawa mass, where (Na+K)=0.86 atoms per 23 oxygens (Table 4). Amphibole in the masses of the Outer Plutonic Zone is mainly magnesio-hornblende, except for that in the Hayatsukigawa mass, whereas that in the Inner Plutonic Zone masses is mainly ferro-edenitic hornblende. Hornblende of the Inner Zone masses is richer in Na+K, Al^{IV} and Al^{VI} than that of the Outer Zone masses (Table 4). The mg value and Si content within individual amphibole crystals tend

Table 4. Representative amphibole analyses.

Sample No.	S-20	S-25	HK-159		MG-1		SO-14	
Mass Name[1]	SHI	SHI					SHO	
			core	rim	core	rim	core	rim
SiO_2 (wt%)	48.96	47.56	42.03	43.95	41.83	47.47	41.83	43.69
TiO_2	1.34	1.54	2.58	2.11	3.63	1.25	2.38	0.98
Al_2O_3	6.71	7.05	13.04	11.67	11.18	6.81	13.80	12.50
FeO*	10.89	12.25	11.33	11.55	14.96	14.62	12.78	12.47
MnO	0.26	0.24	0.23	0.22	0.30	0.31	0.18	0.16
MgO	16.06	15.17	13.61	13.80	10.94	13.41	12.52	12.25
CaO	11.75	11.75	11.73	11.69	12.01	12.20	11.37	11.89
Na_2O	0.89	1.17	2.32	2.08	2.03	1.03	2.12	1.97
K_2O	0.56	0.59	0.28	0.34	0.80	0.74	0.40	0.40
Total	97.42	97.32	97.15	97.41	97.68	97.84	97.38	96.31
Si	7.088	6.965	6.199	6.443	6.275	7.004	6.182	6.496
Ti	0.146	0.170	0.286	0.233	0.410	0.139	0.265	0.109
Al^4	0.912	1.035	1.801	1.557	1.725	0.996	1.818	1.504
Al^6	0.233	0.182	0.466	0.459	0.252	0.188	0.586	0.686
Fe	1.319	1.500	1.389	1.416	1.877	1.804	1.580	1.551
Mn	0.032	0.030	0.029	0.028	0.039	0.039	0.022	0.021
Mg	3.465	3.311	2.992	3.016	2.446	2.949	2.758	2.716
Ca	1.823	1.844	1.854	1.836	1.931	1.928	1.800	1.894
Na	0.248	0.331	0.662	0.592	0.591	0.295	0.606	0.569
K	0.103	0.110	0.053	0.064	0.153	0.138	0.075	0.077
mg	0.719	0.684	0.677	0.676	0.561	0.615	0.632	0.633

Sample No.	SO-18	SO-6		H-1		H-3		F-3
Mass Name[1]	SHO	SHO		HAY		HAY		FUN
		core	rime	core	rim	core	rim	
SiO_2 (wt%)	45.39	45.45	43.13	43.48	42.74	42.88	43.56	46.05
TiO_2	1.20	0.65	0.78	1.49	1.48	1.59	1.30	0.73
Al_2O_3	9.49	8.68	10.49	9.01	8.85	9.03	8.34	7.04
FeO*	16.90	16.09	18.44	18.33	23.01	21.45	22.74	18.90
MnO	0.27	0.42	0.35	0.61	1.14	1.27	1.50	2.34
MgO	11.42	11.18	9.98	10.44	7.09	7.53	7.00	9.69
CaO	11.21	11.94	11.94	11.72	11.44	11.29	10.89	10.32
Na_2O	1.00	1.00	1.29	1.77	1.74	2.07	1.67	1.38
K_2O	0.87	0.85	1.14	0.68	1.07	1.19	1.07	0.67
Total	97.75	96.26	97.54	97.70	98.57	98.29	98.07	97.11
Si	6.766	6.876	6.555	6.607	6.607	6.609	6.746	7.029
Ti	0.135	0.074	0.090	0.170	0.173	0.184	0.152	0.084
Al^4	1.234	1.124	1.445	1.393	1.393	1.391	1.254	0.971
Al^6	0.434	0.425	0.434	0.221	0.220	0.250	0.268	0.295
Fe	2.107	2.036	2.343	2.330	2.975	2.765	2.946	2.412
Mn	0.033	0.054	0.045	0.078	0.150	0.165	0.196	0.303
Mg	2.538	2.522	2.260	2.364	1.635	1.729	1.616	2.204
Ca	1.791	1.935	1.944	1.908	1.895	1.865	1.807	1.688
Na	0.289	0.292	0.380	0.522	0.521	0.620	0.502	0.409
K	0.165	0.165	0.221	0.167	0.212	0.233	0.212	0.130
mg	0.543	0.547	0.486	0.495	0.343	0.371	0.340	0.448

The structural formulae have been calculated on the basis of 23 oxygen equivalents. FeO* :total Fe as FeO, mg=Mg/(Mg+Mn+Fe).
[1] Abbreviations: SHI, Shimonomoto; SHO, Shogawa; HAY, Hayatsukigawa; FUN, Funatsu.

Table 4. (continued)

Sample No.	0-3		0-9		S-2		AM-1	
Mass Name[1]	OKU		OKU		SHI		SHI	
	core	rim	core	rim	core	rim	core	rim
SiO_2 (wt%)	46.60	45.72	46.67	46.86	45.51	45.89	47.56	46.54
TiO_2	1.53	1.40	0.98	1.26	2.25	1.21	1.43	0.77
Al_2O_3	7.54	7.57	6.12	7.23	8.03	8.07	7.06	6.42
FeO*	15.82	15.93	14.94	15.77	15.63	16.74	14.14	16.26
MnO	0.90	0.93	0.77	0.80	0.47	0.45	0.28	0.58
MgO	12.11	12.16	13.47	12.54	12.05	11.52	14.08	12.60
CaO	11.77	11.66	11.85	12.03	11.52	11.78	11.38	11.55
Na_2O	1.19	1.33	0.89	1.11	1.37	1.36	1.47	1.23
K_2O	0.54	0.62	0.46	0.56	0.72	0.76	0.38	0.49
Total	98.00	97.31	97.15	98.17	97.56	97.79	97.80	96.44
Si	6.915	6.858	7.087	6.940	6.789	6.860	6.982	7.027
Ti	0.171	0.158	0.110	0.140	0.253	0.137	0.158	0.087
Al^4	1.085	1.142	0.913	1.060	1.211	1.140	1.018	0.973
Al^6	0.234	0.196	0.160	0.203	0.201	0.282	0.204	0.170
Fe	1.964	1.999	1.858	1.945	1.950	2.092	1.736	2.053
Mn	0.113	0.118	0.097	0.101	0.059	0.057	0.035	0.074
Mg	2.679	2.717	2.985	2.768	2.680	2.568	3.081	2.836
Ca	1.871	1.874	1.887	1.910	1.841	1.887	1.790	1.868
Na	0.343	0.388	0.255	0.319	0.398	0.393	0.419	0.361
K	0.102	0.118	0.088	0.105	0.137	0.144	0.071	0.095
mg	0.563	0.562	0.604	0.574	0.572	0.544	0.635	0.571

Sample No.	Y-3		Y-7		HO-1		HO-3	
Mass Name[1]	YAT		YAT		HOD		HOD	
	core	rim	core	rim	core	rim	core	rim
SiO_2 (wt%)	43.30	41.72	44.80	42.77	43.29	42.64	41.46	40.78
TiO_2	1.56	1.31	1.16	1.13	1.17	1.06	1.37	1.38
Al_2O_3	8.81	10.09	8.17	9.44	9.45	10.21	10.39	10.53
FeO*	19.56	20.22	17.96	19.36	19.26	19.65	21.57	21.63
MnO	0.60	0.54	1.15	1.10	0.52	0.51	0.62	0.60
MgO	9.85	8.88	10.12	9.03	8.86	8.39	7.67	7.41
CaO	11.98	11.74	11.59	11.53	12.10	12.14	11.53	11.65
Na_2O	1.44	1.45	1.46	1.47	1.37	1.30	1.54	1.45
K_2O	1.00	1.27	0.84	1.11	1.05	1.11	1.39	1.45
Total	98.07	97.27	97.26	96.92	97.06	97.01	97.55	96.88
Si	6.599	6.455	6.813	6.603	6.648	6.570	6.439	6.393
Ti	0.179	0.152	0.133	0.131	0.135	0.123	0.160	0.163
Al^4	1.401	1.545	1.187	1.397	1.352	1.430	1.561	1.607
Al^6	0.181	0.295	0.277	0.321	0.359	0.425	0.342	0.340
Fe	2.489	2.616	2.284	2.499	2.473	2.532	2.802	2.836
Mn	0.078	0.071	0.148	0.144	0.068	0.066	0.082	0.080
Mg	2.238	2.048	2.295	2.078	2.029	1.926	1.776	1.731
Ca	1.956	1.946	1.889	1.907	1.991	2.005	1.918	1.958
Na	0.427	0.436	0.430	0.441	0.408	0.388	0.464	0.439
K	0.195	0.251	0.163	0.218	0.205	0.219	0.276	0.289
mg	0.466	0.433	0.486	0.440	0.444	0.426	0.381	0.372

The structural formulae have been calculated on the basis of 23 oxygen equivalents. FeO* :total Fe as FeO, mg=Mg/(Mg+Mn+Fe).
[1] Abbreviations: OKU, Okumayama; SHI, Shimonomoto; YAT, Yatsuo; HOD, Hodatsusan.

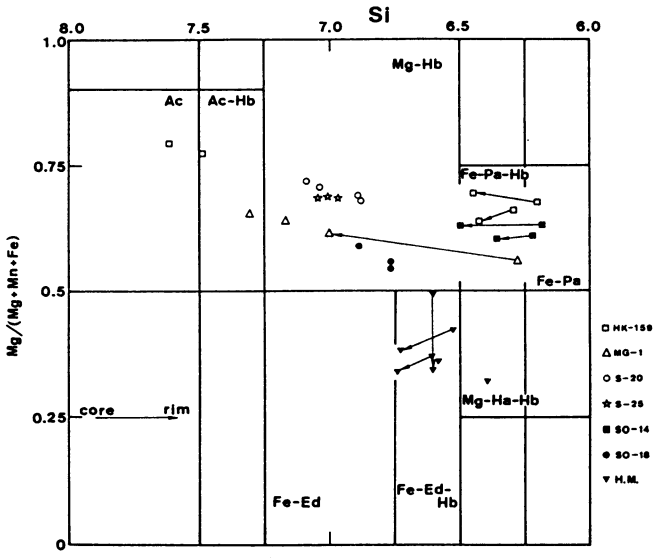

Fig. 16. mg value (Mg/(Mg+Mn+Fe) ratio) vs. Si diagram of amphiboles (O=23) in the gabbroic rocks and the Hayatsukigawa mass rocks. Sample HK-159, MG-1 and SO-14 are hornblende gabbro. Sample S-20, S-25 and SO-18 are pyroxene gabbro. Solid triangles represent the Hayatsukigawa mass samples (H.M.). Ac= actinolite; Ac-Hb=actinolitic-hornblende; Mg-Hb=magnesio-hornblende; Fe-Pa-Hb= ferro-pargastic-hornblende; Fe-Pa=ferro-pargasite; Fe-Ed=ferro-edenite; Fe-Ed-Hb= ferro-edenitic-hornblende; Mg-Ha-Hb= magnesian-hastingsitic-hornblende (after Leake, 1968).

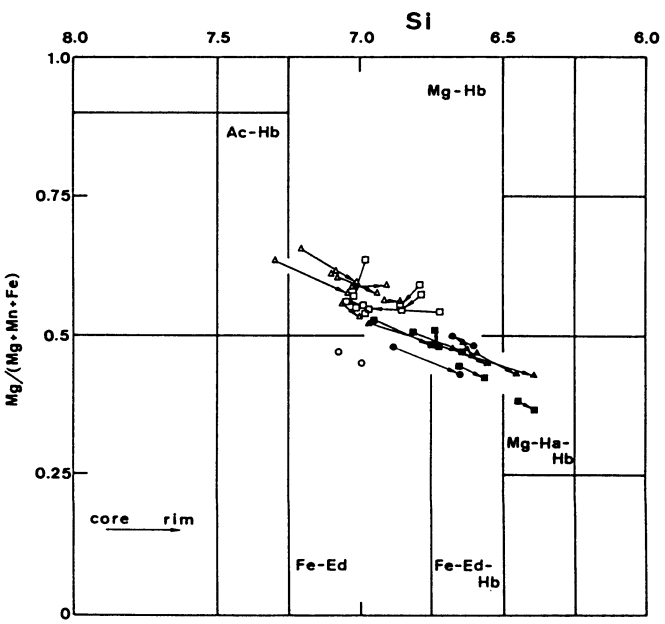

Fig. 17. mg value (Mg/(Mg+Mn+Fe) ratio) vs. Si diagram of amphiboles (O=23) in the Jurassic granitic rocks. Symbols as in Fig. 18. For abbreviations see Fig. 16.

to decrease from core to rim except for those of the Shimonomoto and Hayatsukigawa masses (Figs. 16, 17). This may be explained as an effect of decreasing oxygen fugacity during crystallization, since Si content and mg value increase with increase of oxygen fugacity (Helz, 1973; Popp et al., 1977; Spear, 1981).

BIOTITE

Biotite is commonly found in mafic constituent of many plutonic masses. Its representative chemical and structural data are shown in Table 5. Ti content of biotite varies from 0.24 to 0.53 (22 oxygens) and from mass to mass (Fig. 18). As compared with biotite from the Outer Plutonic Zone granites, except for the Hayatsukigawa mass, biotite from the Inner Plutonic Zone granites in general is poorer in Ti and richer in Al (Al^{IV}) (Fig. 18, Table 5). Ti content is the highest in the Shimonomoto mass adamellite (Ti=0.52). While the Hodatsusan mass adamellite has the lowest Ti content (0.26). It has been so far considered that the composition of biotite is largely dependent on rock composition and mineral assemblage (e.g., Anderson, 1980). As shown in Fig. 19, however, variation in the Al (Al^{IV}) content is scarcely related to that in modal value of hornblende. Czamanske and Wones (1973) have reported that the TiO_2 content of biotite coexisting with ilmenite or sphene for the rocks of the Finnmarka complex increases with increase of temperature of crystallization. Experimental studies by Robert (1976) and Guidotti et al. (1975) have shown that

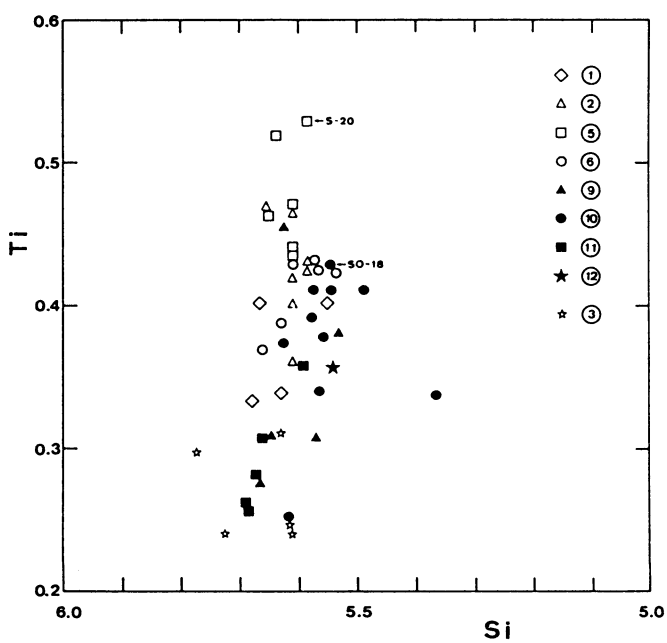

Fig. 18. Ti vs. Si diagram of biotites (O=22) in the early Mesozoic igneous rocks. The numbers circled are 1=Kekachidake mass; 2= Okumayama mass; 3=Hayatsukigawa mass; 5= Shimonomoto mass; 6=Funatsu mass; 9=Yatsuo mass; 10=Shogawa mass; 11=Hodatsusan mass; 12=Togi area.

Table 5. Representative biotite analyses.

Sample No.	S-20	SO-18	SO-6	H-1	H-3	H-9	H-10	K-1
Mass Name[1]	SHI	SHO	SHO	HAY	HAY	HAY	HAY	KEK
SiO_2 (wt%)	37.97	36.77	36.82	36.27	37.55	36.00	37.31	36.07
TiO_2	4.82	3.93	3.61	2.06	2.58	2.12	2.07	3.46
Al_2O_3	14.56	14.96	15.35	16.06	15.34	15.62	15.23	15.09
FeO*	13.77	18.92	19.85	23.05	23.42	22.95	23.44	20.84
MnO	0.10	0.12	0.33	0.83	1.12	0.96	1.15	0.76
MgO	15.71	12.14	10.69	8.22	6.99	8.07	8.01	9.88
CaO	0.03	0.00	0.01	0.18	0.05	0.05	0.04	0.02
Na_2O	0.25	0.05	0.07	0.06	0.04	0.06	0.03	0.07
K_2O	9.09	9.28	9.77	8.88	9.36	9.53	9.58	9.49
Total	96.30	96.17	96.50	95.61	96.45	95.36	96.86	95.68
Si	5.567	5.545	5.574	5.611	5.772	5.616	5.726	5.550
Ti	0.531	0.446	0.411	0.240	0.298	0.248	0.239	0.401
Al^4	2.433	2.455	2.426	2.389	2.228	2.384	2.274	2.450
Al^6	0.084	0.204	0.313	0.540	0.552	0.488	0.481	0.288
Fe	1.689	2.386	2.513	2.983	3.011	2.995	3.009	2.683
Mn	0.013	0.015	0.042	0.109	0.146	0.127	0.149	0.099
Mg	3.435	2.728	2.413	1.897	1.602	1.878	1.832	2.266
Ca	0.004	0.000	0.002	0.030	0.008	0.008	0.007	0.003
Na	0.071	0.014	0.021	0.018	0.011	0.017	0.010	0.022
K	1.701	1.786	1.887	1.753	1.835	1.897	1.875	1.862
mg	0.669	0.532	0.486	0.380	0.337	0.376	0.367	0.449

Sample No.	K-2	K-3	K-5	O-1	O-3	O-5	O-9	S-2
Mass Name[1]	KEK	KEK	KEK	OKU	OKU	OKU	OKU	SHI
SiO_2 (wt%)	37.35	37.24	37.53	36.90	37.36	37.17	36.75	37.28
TiO_2	3.52	2.97	2.92	4.09	4.11	3.74	3.77	4.16
Al_2O_3	15.48	16.13	14.93	14.45	14.17	15.04	14.81	14.32
FeO*	19.24	20.25	18.48	19.78	19.44	19.26	20.36	19.40
MnO	0.97	1.35	1.63	0.45	0.60	0.66	0.63	0.35
MgO	9.88	9.32	11.08	10.89	11.05	11.44	10.57	11.66
CaO	0.03	0.01	0.09	0.06	0.03	0.10	0.10	0.04
Na_2O	0.10	0.11	0.06	0.08	0.07	0.06	0.09	0.12
K_2O	9.26	9.37	9.48	9.34	9.39	9.41	9.43	9.45
Total	95.83	96.75	96.20	96.04	96.22	96.88	96.51	96.78
Si	5.665	5.630	5.678	5.609	5.656	5.584	5.581	5.610
Ti	0.401	0.338	0.333	0.467	0.468	0.423	0.430	0.471
Al^4	2.335	2.370	2.322	2.391	2.344	2.416	2.419	2.390
Al^6	0.434	0.506	0.341	0.198	0.186	0.247	0.232	0.150
Fe	2.442	2.560	2.339	2.514	2.462	2.420	2.586	2.441
Mn	0.125	0.173	0.209	0.057	0.077	0.084	0.081	0.036
Mg	2.234	2.099	2.499	2.467	1.494	2.562	2.391	2.616
Ca	0.004	0.002	0.015	0.009	0.004	0.016	0.016	0.005
Na	0.029	0.031	0.018	0.022	0.026	0.018	0.027	0.034
K	1.791	1.806	1.829	1.812	1.814	1.804	1.826	1.815
mg	0.465	0.434	0.495	0.490	0.496	0.506	0.473	0.514

The structural formulae have been calculated on the basis of 22 oxygen equivalents. FeO* :total Fe as FeO, mg=Mg/(Mg+Mn+Fe).
[1] Abbreviations: KEK, Kekachidake; OKU, Okumayama; SHI, Shimonomoto; FUN, Funatsu; YAT, Yatsuo; SHO, Shogawa; HOD, Hodatsusan; TOK, Togi.

Table 5. (continued)

Sample No.	S-7	AM-1	F-2	F-3	F-9	Y-3	Y-5	Y-7
Mass Name[1]	SHI	SHI	FUN	FUN	FUN	YAT	YAT	YAT
SiO_2 (wt%)	37.22	36.75	36.19	36.95	35.94	35.94	37.43	36.97
TiO_2	4.55	3.78	3.71	3.20	3.64	3.27	2.43	2.67
Al_2O_3	13.40	13.89	13.95	13.87	13.94	15.17	15.13	15.28
FeO*	19.56	20.23	20.83	21.46	21.98	20.52	19.59	19.50
MnO	0.46	0.36	1.23	1.31	1.38	0.38	0.82	0.85
MgO	11.68	11.44	10.41	10.22	9.70	10.46	11.19	10.48
CaO	0.02	0.05	0.03	0.02	0.07	0.00	0.01	0.01
Na_2O	0.09	0.09	0.09	0.03	0.06	0.10	0.08	0.07
K_2O	9.44	9.37	9.43	9.48	9.33	9.76	9.80	9.89
Total	96.42	95.96	95.78	96.54	96.04	95.60	96.48	95.72
Si	5.637	5.609	5.578	5.660	5.565	5.529	5.665	5.648
Ti	0.518	0.434	0.430	0.369	0.424	0.379	0.276	0.307
Al^4	2.363	2.391	2.422	2.340	2.435	2.471	2.335	2.352
Al^6	0.029	0.107	0.112	0.164	0.108	0.279	0.363	0.399
Fe	2.478	2.583	2.686	2.749	2.847	2.640	2.480	2.492
Mn	0.059	0.047	0.161	0.170	0.182	0.049	0.105	0.110
Mg	2.637	2.602	2.391	2.334	2.238	2.399	2.525	2.387
Ca	0.003	0.008	0.005	0.003	0.012	0.000	0.002	0.001
Na	0.027	0.027	0.026	0.010	0.016	0.029	0.024	0.022
K	1.824	1.826	1.854	1.852	1.842	1.915	1.892	1.928
mg	0.510	0.497	0.456	0.444	0.425	0.472	0.494	0.478

Sample No.	SO-2	SO-7	SO-8	SO-35	HO-1	HO-4	HO-6	TK-2
Mass Name[1]	SHO	SHO	SHO	SHO	HOD	HOD	HOD	TOK
SiO_2 (wt%)	37.14	35.28	35.36	36.18	36.79	37.08	37.81	35.91
TiO_2	2.33	3.47	3.52	3.28	2.43	2.26	2.72	3.06
Al_2O_3	16.20	15.74	16.01	16.24	14.88	14.63	15.36	15.07
FeO*	20.58	24.61	25.97	24.16	20.57	19.87	19.75	23.56
MnO	0.36	0.58	0.48	0.51	0.35	0.60	0.44	0.93
MgO	10.17	6.16	6.13	6.92	10.36	11.28	11.47	8.72
CaO	0.01	0.01	0.01	0.01	0.02	0.03	0.01	0.04
Na_2O	0.05	0.06	0.06	0.06	0.09	0.06	0.09	0.10
K_2O	9.80	9.52	9.55	9.74	9.34	9.35	9.47	9.25
Total	96.64	95.43	97.09	97.10	95.01	95.16	97.12	96.64
Si	5.620	5.544	5.488	5.557	5.672	5.689	5.660	5.540
Ti	0.266	0.410	0.411	0.379	0.282	0.261	0.306	0.355
Al^4	2.380	2.456	2.512	2.443	2.328	2.311	2.340	2.460
Al^6	0.508	0.459	0.418	0.496	0.377	0.335	0.370	0.281
Fe	2.604	3.234	3.371	3.103	2.675	2.548	2.472	3.040
Mn	0.046	0.076	0.063	0.067	0.046	0.078	0.055	0.121
Mg	2.294	1.444	1.418	1.584	2.379	2.578	2.558	2.006
Ca	0.001	0.002	0.002	0.002	0.004	0.005	0.002	0.006
Na	0.015	0.017	0.017	0.019	0.028	0.018	0.025	0.031
K	1.892	1.909	1.892	1.909	1.836	1.829	1.809	1.821
mg	0.464	0.304	0.292	0.333	0.466	0.495	0.503	0.388

The structural formulae have been calculated on the basis of 22 oxygen equivalents. FeO* :total Fe as FeO, mg=Mg/(Mg+Mn+Fe).
[1] Abbreviations: KEK, Kekachidake; OKU, Okumayama; SHI, Shimonomoto; FUN, Funatsu; YAT, Yatsuo; SHO, Shogawa; HOD, Hodatsusan; TOK, Togi.

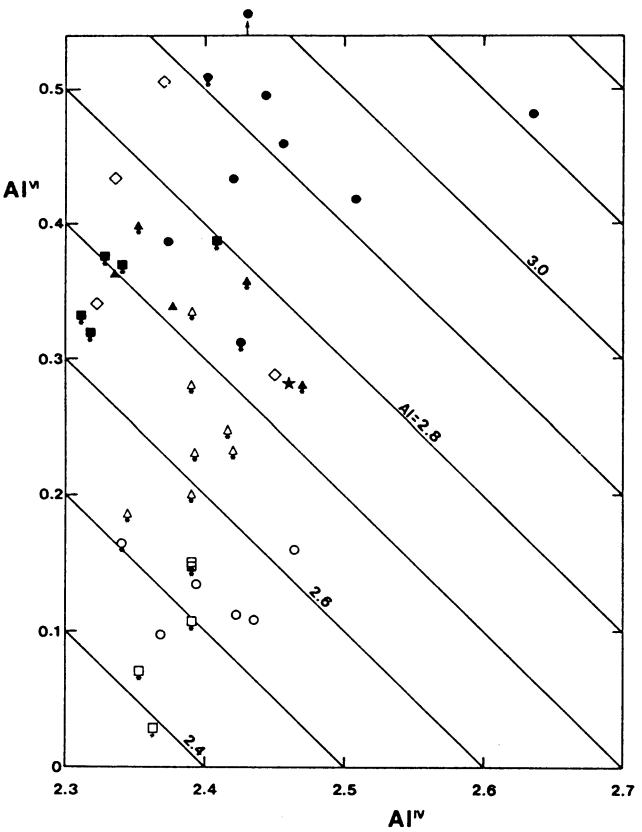

Fig. 19. Al^{VI} vs. Al^{IV} diagram of biotites (O=22) in the Jurassic granitic rocks. For symbols see Fig.18. The symbols with asterisk are the rocks including hornblende.

Table 6. Mineralogical difference between the Jurassic granitic rocks of the Outer Plutonic Zone and those of the Inner Plutonic Zone.

	Outer Plutonic Zone	Inner Plutonic Zone
[Plagioclase]		
An %:	8-54 (avg.: 27)	15-61 (avg.: 35)
[Hornblende]		
pleochroism:	bluish green	dark green
mg-value:	0.53-0.66	0.37-0.53
Si:	6.73-7.30	6.39-6.96
Ca+Na+K:	2.12-2.42	2.32-2.69
[Biotite]		
pleochroism:	dark brown	greenish brown
mg-value:	0.43-0.51	0.29-0.50
Ti:	0.33-0.52	0.26-0.45
Al^{6} :	0.03-0.51 (avg.:0.21)	0.28-0.48 (avg.:0.37)
[Accessory minerals]		
Magnetite:	abundant	moderate-scarce
Allanite:	moderate-scarce	moderate
Epidote:	scarce	abundant
Sphene:	moderate	abundant

the solubility limit of Ti in biotite decreases with decrease of temperature. Anderson (1980) has reported zoned biotite with decrease in Ti content and increase in Al^{VI} content from core to rim, suggesting substitution mechanism of $3Ti=4Al^{VI}$. Thus, the variation in Ti content of biotite between the two plutonic zones can be ascribed to the temperature variation.

The mg value of biotite in the Shogawa mass and that in the Hayatsukigawa mass range from 0.25 for adamellite to 0.49 for diorite and from 0.34 to 0.38, respectively, but for biotite from the other masses, except for gabbroic rocks, that shows as cluster around 0.48 (Table 5).

Mineralogical difference between the granitic rocks of the Inner Plutonic Zone and those of the Outer Plutonic Zone is briefly summarized in Table 6.

V. WHOLE-ROCK GEOCHEMISTRY

Major element analyses (except for Na_2O) were done by X-ray fluorescence of fused discuses, using the method of Kobayashi et al. (1981). Na_2O content was determined by atomic absorption according to the method of Inoue et al. (1985). Rb, Sr, Ba and Zr were determined by X-ray fluorescence of using pressed powder pellets (Tanaka and Ohtsubo, 1987). Y and V were analysed by X-ray fluorescence of fused discuses, following the method of Ichikawa et al. (1987).

The results of major and trace element analyses of the early Mesozoic granites are shown in Table 7. The Kekachidake granite mass displays very restricted range for 71.9 to 73.4 % for SiO_2 content, but clear increase in Rb and Y and decrease in TiO_2, Fe_2O_3, MgO, CaO, P_2O_5, Sr and Zr with increasing SiO_2 content. K_2O content is high at 3.6-4.6 %; Sr content is relatively low at 148-245 ppm; Rb content is rather high at 61-127 ppm.

SiO_2 content of the Okumayama mass is limited with in 63.9-68.4 %, but the variation of TiO_2, Fe_2O_3, MgO, CaO and V versus SiO_2 is coherent. Whereas Al_2O_3, K_2O, Rb and Sr contents are constant being related to variation in modal mafic minerals within the mass. In general the K_2O, P_2O_5, Rb, Sr and Zr contents as measured at a fixed SiO_2 value are lower than those of the Jurassic granites.

Two specimens from the Wadagawa mass show SiO_2 content of about 62 %. Their chemical characteristics are not generally comparable to those of the Okumayama and Shimonomoto masses: Na_2O, P_2O_5 and Zr contents of the Wadagawa mass are appreciably higher than those of these masses.

The Shimonomoto mass displays a broad range of SiO_2 content from 55.5 % in quartz-diorite to 71.4 % in adamellite of the Ikenoo Facies (without the pyroxene gabbros). The Shimonomoto mass has the lowest Na_2O, P_2O_5 and Sr and the highest MgO contents among the Jurassic granites as measured at a fixed SiO_2 value.

The Funatsu mass has higher SiO_2 content, ranging from 70.8 to 77.0 %, and lower Al_2O_3 of 12.3 to 14.7 %. Although its chemical characteristics are roughly comparable with those of the Kekachidake mass, the Al_2O_3, K_2O and Rb contents are lower in it than in the Kekachidake mass at a fixed SiO_2 value.

Two granite specimens from the Asuwagawa mass

Table 7. Major and trace element composition of the granitic rocks.

Sample No.	S-19	S-20	S-21	S-24	HK-159	SO-14	SO-18
Mass Name[1]	SHI	SHI	SHI	SHI		SHO	SHO
SiO_2 (wt%)	49.42	49.13	53.60	55.54	41.39	44.46	51.94
TiO_2	0.94	0.80	0.99	0.74	1.83	1.67	1.10
Al_2O_3	17.87	16.78	17.15	17.74	18.96	19.08	18.45
Fe_2O_3*	10.51	10.83	8.32	8.25	13.98	11.04	9.45
MnO	0.17	0.21	0.15	0.15	0.07	0.09	0.14
MgO	6.32	10.65	6.29	4.42	6.43	7.36	4.05
CaO	9.64	9.19	7.78	6.56	12.41	12.19	8.39
Na_2O	3.22	1.52	3.40	3.61	1.83	2.00	4.12
K_2O	0.24	0.24	1.48	1.20	0.54	0.96	0.65
P_2O_5	0.15	-	-	0.08	0.06	0.04	0.27
Total	98.48	99.30	99.16	98.29	97.50	98.89	98.56
Rb (ppm)	5.0	7.3	-	31.4	23.2	44.2	16.0
Sr	536.2	423.4	-	431.6	613.2	749.5	780.4
Ba	320.3	-	-	229.0	360.5	495.7	582.0
Zr	28.4	-	-	-	9.0	16.6	96.0
Y	19.0	-	-	-	15.5	10.4	15.5
V	257.2	-	-	-	446.7	331.5	178.6

Sample No.	H-1	H-2	H-3	H-4	H-5	H-6	H-7
Mass Name[1]	HAY	HAY	HAY	HAY	HAY	HAY	HAY
SiO_2 (wt%)	68.88	68.93	71.32	72.23	70.21	66.05	68.81
TiO_2	0.20	0.19	0.13	0.11	0.16	0.30	0.21
Al_2O_3	17.31	16.98	15.66	14.66	16.10	17.69	16.78
Fe_2O_3*	1.75	1.59	1.16	1.18	1.47	2.41	1.81
MnO	0.02	0.02	0.02	0.02	0.02	0.04	0.02
MgO	0.28	0.25	0.16	0.12	0.35	0.30	0.27
CaO	2.54	2.32	1.81	1.36	2.08	2.64	2.32
Na_2O	5.35	5.92	4.78	4.60	5.78	5.85	5.26
K_2O	3.10	3.08	3.47	3.95	3.24	3.02	2.90
P_2O_5	0.03	0.02	0.01	0.01	0.02	0.04	0.03
Total	99.46	99.30	98.52	98.24	99.43	98.34	98.41
Rb (ppm)	42.4	63.5	60.6	86.2	68.5	49.8	48.1
Sr	757.5	739.7	501.1	420.8	664.6	798.8	813.9
Ba	1749	1677	1124	1010	1554	1617	1847
Zr	230.7	220.6	161.1	152.0	192.8	283.2	250.1
Y	-	-	-	-	-	-	-
V	-	-	-	-	-	-	-
K_2O/Na_2O	0.58	0.52	0.73	0.86	0.56	0.52	0.55
A/CNK**	1.03	0.98	1.05	1.02	0.96	1.00	1.05
K/Rb	607	403	475	380	393	503	501
Rb/Sr	0.06	0.09	0.12	0.20	0.10	0.06	0.06
M***	0.15	0.15	0.13	0.10	0.21	0.12	0.14

Table 7. (continued)

Sample No.	K-1	K-2	K-3	K-4	K-5	K-6	K-7
Mass Name[1]	KEK	KEK	KEK	KEK	KEK	KEK	KEK
SiO_2 (wt%)	71.87	71.85	73.07	73.41	72.56	72.86	72.89
TiO_2	0.30	0.23	0.18	0.18	0.19	0.17	0.20
Al_2O_3	13.87	15.11	14.38	13.69	14.09	13.86	14.48
Fe_2O_3*	2.21	1.86	1.49	1.43	1.67	1.41	1.74
MnO	0.06	0.07	0.09	0.08	0.09	0.09	0.09
MgO	0.61	0.44	0.39	0.35	0.41	0.14	0.45
CaO	1.44	1.62	1.27	1.04	1.57	1.07	1.54
Na_2O	4.09	4.31	4.29	4.02	4.61	4.18	4.10
K_2O	3.89	3.88	3.97	3.97	3.55	4.56	3.63
P_2O_5	0.07	0.05	0.04	0.03	0.05	0.06	0.05
Total	98.41	99.42	99.17	98.20	98.79	98.40	99.17
Rb (ppm)	60.7	79.2	98.8	112.2	114.5	127.2	103.2
Sr	237.4	245.1	182.2	148.1	198.9	157.2	213.1
Ba	1959.8	1334.2	835.7	930.6	491.9	832.6	597.0
Zr	204.4	175.8	120.0	115.6	118.5	123.4	111.4
Y	13.9	15.0	18.3	19.3	20.1	20.3	-
V	31.3	25.6	26.7	41.0	40.2	32.2	-
K_2O/Na_2O	0.95	0.90	0.93	0.99	0.77	1.09	0.89
A/CNK**	1.02	1.06	1.05	1.07	0.99	1.01	1.07
K/Rb	532	407	334	294	258	296	292
Rb/Sr	0.26	0.32	0.54	0.76	0.58	0.81	0.48
M***	0.23	0.21	0.23	0.21	0.21	0.10	0.22

Sample No.	K-8	O-1	O-2	O-3	O-4	O-5	O-6
Mass Name[1]	KEK	OKU	OKU	OKU	OKU	OKU	OKU
SiO_2 (wt%)	72.44	65.35	65.42	65.52	68.37	66.67	64.80
TiO_2	0.23	0.57	0.58	0.58	0.46	0.52	0.56
Al_2O_3	14.29	16.34	16.11	16.09	15.86	15.92	15.92
Fe_2O_3*	1.86	4.56	4.60	4.66	3.67	4.18	4.71
MnO	0.10	0.09	0.10	0.10	0.10	0.10	0.10
MgO	0.51	1.79	1.81	1.96	1.16	1.56	1.92
CaO	1.50	4.33	4.05	4.13	3.16	3.82	4.17
Na_2O	4.07	4.15	4.14	3.92	4.81	4.22	3.94
K_2O	3.61	1.93	1.86	1.85	2.01	2.20	1.98
P_2O_5	0.05	0.10	0.11	0.11	0.10	0.10	0.11
Total	98.66	99.21	98.78	98.92	99.70	99.29	98.21
Rb (ppm)	99.7	50.2	43.4	45.9	55.3	58.5	51.0
Sr	199.7	373.4	394.0	371.3	332.2	347.3	373.4
Ba	813.0	508.6	651.7	551.1	711.2	669.6	622.0
Zr	115.1	150.3	163.0	139.9	181.0	160.6	146.5
Y	-	18.5	18.4	23.0	26.2	12.9	-
V	-	76.6	96.8	83.4	69.8	64.4	-
K_2O/Na_2O	0.89	0.47	0.45	0.47	0.42	0.52	0.50
A/CNK**	1.07	0.97	1.00	1.01	1.00	0.98	0.98
K/Rb	301	319	356	335	302	312	322
Rb/Sr	0.50	0.13	0.11	0.12	0.17	0.17	0.14
M***	0.23	0.30	0.30	0.32	0.26	0.29	0.31

Table 7. (continued)

Sample No.	O-7	O-8	O-9	O-10	O-11	O-12	O-13
Mass Name[1]	OKU	OKU	OKU	OKU	OKU	OKU	OKU
SiO_2 (wt%)	63.90	64.16	64.07	65.56	64.12	66.73	67.55
TiO_2	0.64	0.61	0.63	0.52	0.58	0.51	0.48
Al_2O_3	16.48	16.02	16.07	15.79	16.05	15.95	15.90
Fe_2O_3*	5.24	5.00	5.17	4.26	4.98	4.04	3.81
MnO	0.10	0.10	0.11	0.09	0.10	0.09	0.08
MgO	2.16	2.04	2.14	1.66	1.94	1.52	1.38
CaO	4.62	4.28	4.62	4.21	4.30	3.71	3.66
Na_2O	4.02	3.80	4.20	4.34	4.03	4.29	4.26
K_2O	1.90	2.17	1.66	1.55	1.99	2.01	1.84
P_2O_5	0.12	0.12	0.12	0.10	0.11	0.10	0.10
Total	99.18	98.30	98.79	98.08	98.20	98.95	99.06
Rb (ppm)	49.8	47.9	44.3	38.5	48.8	52.4	40.9
Sr	378.2	376.8	376.6	369.1	365.8	356.7	366.1
Ba	614.0	668.0	536.0	416.0	569.0	633.0	722.0
Zr	158.4	148.7	140.1	136.2	145.5	157.2	154.3
Y	-	-	-	-	-	-	-
V	-	-	-	-	-	-	-
K_2O/Na_2O	0.47	0.57	0.40	0.36	0.49	0.58	0.57
A/CNK**	0.97	0.98	0.94	0.95	0.97	1.00	1.02
K/Rb	317	376	311	334	339	318	373
Rb/Sr	0.13	0.13	0.12	0.10	0.13	0.15	0.11
M***	0.31	0.31	0.32	0.30	0.30	0.29	0.29

Sample No.	W-1	W-2	S-1	S-2	S-3	S-4	S-5
Mass Name[1]	OKU	OKU	SHI	SHI	SHI	SHI	SHI
SiO_2 (wt%)	61.75	62.41	62.91	63.50	69.67	71.07	71.36
TiO_2	0.85	0.82	0.59	0.68	0.34	0.30	0.29
Al_2O_3	16.99	16.96	18.29	15.42	14.82	14.16	14.27
Fe_2O_3*	5.47	5.25	4.33	5.45	2.83	2.47	2.39
MnO	0.15	0.14	0.16	0.09	0.05	0.05	0.05
MgO	1.79	1.78	1.04	2.66	1.14	0.88	0.96
CaO	4.23	4.33	3.29	5.49	2.87	2.66	2.09
Na_2O	5.54	5.11	6.54	3.39	3.80	3.97	3.80
K_2O	1.41	1.47	1.74	2.32	2.59	3.15	3.31
P_2O_5	0.21	0.19	0.20	0.10	0.07	0.06	0.06
Total	98.39	98.46	99.09	99.10	98.18	98.77	98.58
Rb (ppm)	34.4	30.9	42.7	69.8	80.7	97.7	111.7
Sr	412.0	429.8	462.9	352.0	291.4	273.9	272.6
Ba	400.0	656.0	651.6	546.2	414.1	523.4	476.1
Zr	268.5	250.5	370.3	157.2	109.5	99.9	99.1
Y	-	-	21.4	23.2	12.5	15.1	13.0
V	-	-	39.6	133.1	47.7	53.2	44.1
K_2O/Na_2O	0.25	0.29	0.27	0.68	0.68	0.79	0.87
A/CNK**	0.93	0.95	0.98	0.85	1.04	0.96	1.05
K/Rb	340	395	363	276	268	247	247
Rb/Sr	0.08	0.07	0.09	0.20	0.28	0.36	0.41
M***	0.27	0.27	0.21	0.35	0.31	0.28	0.31

Table 7. (continued)

Sample No.	S-6	S-7	AM-1	F-1	F-2	F-3	F-4
Mass Name[1]	SHI	SHI	SHI	FUN	FUN	FUN	FUN
SiO_2 (wt%)	68.80	69.67	64.23	70.81	70.80	73.07	74.97
TiO_2	0.37	0.38	0.56	0.35	0.21	0.20	0.14
Al_2O_3	14.14	14.07	15.97	14.36	14.73	13.71	12.96
Fe_2O_3*	3.11	3.15	4.80	3.38	2.24	2.25	1.11
MnO	0.05	0.05	0.08	0.10	0.08	0.08	0.03
MgO	1.35	1.19	2.52	0.99	0.53	0.44	0.23
CaO	2.49	2.96	4.56	2.01	1.64	1.63	0.52
Na_2O	3.17	3.22	3.45	4.29	4.36	4.19	4.36
K_2O	4.04	3.93	2.32	2.55	3.52	3.71	3.55
P_2O_5	0.06	0.06	0.09	0.09	0.06	0.06	0.05
Total	97.58	98.68	98.58	98.93	98.17	99.34	97.92
Rb (ppm)	131.3	146.2	69.6	61.9	92.1	104.7	62.8
Sr	243.6	221.9	349.6	285.9	251.4	198.3	110.7
Ba	516.8	514.5	437.0	806.7	1148.9	767.9	676.6
Zr	132.2	145.0	119.2	157.2	130.5	133.7	102.8
Y	18.2	17.9	-	17.7	16.0	17.4	5.2
V	54.3	59.0	-	48.0	43.9	43.6	31.8
K_2O/Na_2O	1.27	1.22	0.67	0.59	0.81	0.89	0.81
A/CNK**	1.00	0.94	0.97	1.07	1.06	0.99	1.08
K/Rb	250	224	276	340	317	294	469
Rb/Sr	0.54	0.66	0.20	0.22	0.38	0.53	0.57
M***	0.33	0.30	0.37	0.25	0.21	0.18	0.19

Sample No.	F-5	F-6	F-7	F-8	AS-1	AS-2
Mass Name[1]	FUN	FUN	FUN	FUN	ASU	ASU
SiO_2 (wt%)	75.52	75.29	76.97	76.06	60.31	62.97
TiO_2	0.06	0.12	0.13	0.17	0.64	0.87
Al_2O_3	13.00	13.03	12.60	12.27	17.09	15.66
Fe_2O_3*	0.48	0.81	0.93	1.04	6.21	5.16
MnO	0.02	0.06	0.02	0.03	0.12	0.07
MgO	0.10	0.14	0.00	0.15	2.26	2.25
CaO	0.58	0.43	0.61	0.68	5.99	4.41
Na_2O	4.08	4.36	3.93	3.89	4.64	5.27
K_2O	4.16	3.68	4.24	3.83	1.19	1.75
P_2O_5	0.02	0.04	0.03	0.03	0.22	0.25
Total	98.02	97.96	99.46	98.15	98.67	98.66
Rb (ppm)	84.8	99.6	85.0	71.7	27.9	35.2
Sr	103.6	82.8	63.7	63.5	885.4	1195.2
Ba	884.6	470.7	427.3	1269.5	467.3	461.5
Zr	65.2	100.8	102.8	132.7	125.9	169.7
Y	6.1	31.9	41.7	14.0	18.5	10.4
V	7.4	20.3	32.7	32.2	101.3	93.8
K_2O/Na_2O	1.02	0.84	1.08	0.98	0.26	0.33
A/CNK**	1.06	1.09	1.04	1.04	0.86	0.84
K/Rb	408	443	414	443	354	413
Rb/Sr	0.81	1.20	1.33	1.13	0.03	0.03
M***	0.19	0.16	0	0.14	0.29	0.33

Table 7. (continued)

Sample No.	Y-1	Y-2	Y-3	Y-4	Y-5	Y-6	Y-7	Y-8
Mass Name[1]	YAT	YAT	YAT	YAT	YAT	YAT	YAT	YAT
SiO_2 (wt%)	60.64	64.10	61.94	71.37	70.79	67.03	69.30	61.60
TiO_2	0.86	0.70	0.77	0.30	0.34	0.53	0.41	0.77
Al_2O_3	16.59	15.78	16.30	14.52	14.56	14.94	14.90	16.45
Fe_2O_3*	6.42	5.41	5.93	1.99	2.39	4.03	3.31	5.82
MnO	0.10	0.13	0.11	0.02	0.04	0.08	0.07	0.10
MgO	2.84	2.06	2.51	0.37	0.44	1.23	1.06	2.51
CaO	6.22	5.21	5.86	2.02	2.37	3.28	2.89	5.19
Na_2O	4.06	4.36	4.02	4.04	4.14	4.29	4.17	4.24
K_2O	1.31	0.84	1.67	3.54	3.52	2.47	2.65	1.76
P_2O_5	0.20	0.15	0.18	0.08	0.09	0.12	0.10	0.20
Total	99.24	98.74	99.29	98.25	98.68	98.00	98.86	98.64
Rb (ppm)	39.6	24.8	68.5	94.7	89.5	75.3	70.8	65.7
Sr	820.1	478.1	662.4	567.2	503.0	416.4	420.7	723.9
Ba	529.9	197.1	561.6	1134.0	777.5	1152.1	784.6	965.0
Zr	185.7	164.9	196.6	149.5	161.8	192.8	162.2	225.1
Y	13.4	28.7	24.3	14.9	16.6	15.1	17.6	-
V	114.4	84.0	112.2	25.6	39.6	61.0	47.6	-
K_2O/Na_2O	0.32	0.19	0.42	0.88	0.85	0.58	0.64	0.42
A/CNK**	0.86	0.90	0.85	1.03	0.98	0.95	0.99	0.90
K/Rb	275	307	202	327	343	272	330	222
Rb/Sr	0.05	0.05	0.10	0.17	0.18	0.18	0.17	0.09
M***	0.33	0.30	0.32	0.17	0.17	0.25	0.26	0.32

Sample No.	Y-9	Y-10	Y-11	SO-1	SO-2	SO-3	SO-5	SO-6
Mass Name[1]	YAT	YAT	YAT	SHO	SHO	SHO	SHO	SHO
SiO_2 (wt%)	69.03	61.04	63.32	73.83	62.82	66.97	66.08	56.35
TiO_2	0.44	0.77	0.57	0.15	0.84	0.49	0.56	0.97
Al_2O_3	15.43	16.58	16.28	14.10	16.92	16.36	15.58	17.44
Fe_2O_3*	3.14	6.61	5.35	1.58	4.70	3.45	4.25	7.97
MnO	0.03	0.13	0.09	0.02	0.06	0.03	0.07	0.10
MgO	0.94	2.72	1.82	0.15	1.21	0.64	1.57	3.90
CaO	3.29	5.92	5.07	1.41	4.76	3.61	4.55	7.02
Na_2O	4.87	3.74	4.34	3.86	5.16	5.33	4.09	3.87
K_2O	1.44	1.18	2.03	4.34	1.98	1.41	1.27	1.67
P_2O_5	0.10	0.16	0.15	0.04	0.28	0.10	0.13	0.23
Total	98.71	98.85	99.02	99.48	98.73	98.39	98.15	99.52
Rb (ppm)	39.5	37.5	47.5	114.2	73.3	39.4	55.9	51.2
Sr	460.6	594.2	494.3	315.9	1086.0	755.2	686.4	731.4
Ba	503.0	429.0	694.0	952.3	468.6	758.0	264.4	590.6
Zr	207.7	178.4	177.1	135.9	147.1	251.7	137.0	121.7
Y	-	-	-	9.9	12.2	4.4	13.7	23.7
V	-	-	-	25.1	72.1	49.4	61.8	129.0
K_2O/Na_2O	0.30	0.32	0.47	1.12	0.38	0.26	0.31	0.43
A/CNK**	0.99	0.91	0.88	1.04	0.88	0.97	0.95	0.83
K/Rb	303	261	355	315	224	297	189	271
Rb/Sr	0.09	0.06	0.10	0.36	0.07	0.05	0.08	0.07
M***	0.25	0.31	0.27	0.10	0.22	0.17	0.27	0.35

Table 7. (continued)

Sample No.	SO-7	SO-8	SO-9	SO-10	SO-11	SO-13	SO-15	HO-1
Mass Name[1]	SHO	SHO	SHO	SHO	SHO	SHO	SHO	HOD
SiO_2 (wt%)	68.22	71.32	73.77	71.10	73.71	67.92	57.70	60.60
TiO_2	0.43	0.26	0.15	0.25	0.10	0.42	0.90	0.66
Al_2O_3	16.74	14.94	14.00	14.46	13.71	16.17	17.61	16.14
Fe_2O_3*	2.92	1.72	1.47	2.06	1.39	3.02	7.14	7.08
MnO	0.05	0.02	0.02	0.03	0.02	0.04	0.06	0.12
MgO	0.54	0.24	0.10	0.40	0.07	0.77	3.44	2.92
CaO	2.73	1.55	1.22	1.76	0.88	3.03	6.95	5.94
Na_2O	4.97	4.50	3.81	4.18	3.61	4.53	4.08	4.21
K_2O	2.85	3.69	4.27	3.59	4.56	2.54	1.36	1.58
P_2O_5	0.11	0.07	0.04	0.07	0.02	0.14	0.21	0.17
Total	99.56	98.31	98.85	97.90	98.07	98.58	99.45	99.42
Rb (ppm)	80.9	121.7	121.8	109.5	117.0	111.5	48.7	61.1
Sr	537.0	323.8	325.7	445.4	244.0	641.1	814.4	408.4
Ba	1078.5	715.1	1047.4	864.8	1044.3	655.6	601.1	406.2
Zr	228.8	158.1	133.6	145.5	115.7	153.1	136.9	128.5
Y	16.0	9.7	16.9	10.7	13.8	11.4	20.4	24.7
V	34.9	13.1	31.7	33.8	31.4	45.0	115.3	132.4
K_2O/Na_2O	0.57	0.82	1.12	0.86	1.26	0.56	0.33	0.38
A/CNK**	1.03	1.05	1.06	1.04	1.10	1.03	0.85	0.83
K/Rb	292	252	292	272	324	189	232	215
Rb/Sr	0.15	0.38	0.37	0.25	0.48	0.17	0.06	0.15
M***	0.17	0.13	0.07	0.18	0.05	0.22	0.35	0.31

Sample No.	HO-2	HO-3	HO-4	HO-5	HO-6	TK-2
Mass Name[1]	HOD	HOD	HOD	HOD	HOD	TOK
SiO_2 (wt%)	60.98	63.48	68.61	68.78	64.61	64.42
TiO_2	0.96	0.76	0.55	0.46	0.72	0.59
Al_2O_3	17.43	16.36	14.93	15.10	16.23	16.24
Fe_2O_3*	5.64	4.50	3.36	2.95	4.18	4.90
MnO	0.10	0.07	0.05	0.04	0.06	0.16
MgO	1.89	1.31	0.77	0.74	1.33	1.22
CaO	5.58	4.63	3.16	2.85	4.26	3.83
Na_2O	5.27	5.01	4.15	4.21	4.43	4.90
K_2O	1.39	2.60	3.47	3.76	2.98	2.11
P_2O_5	0.27	0.23	0.15	0.11	0.17	0.19
Total	99.51	98.95	99.20	99.00	98.97	98.56
Rb (ppm)	69.5	72.2	106.8	116.4	72.5	70.9
Sr	886.5	664.4	577.3	526.6	765.4	540.8
Ba	360.6	681.5	737.7	742.6	977.4	752.2
Zr	296.7	165.5	156.7	157.9	175.5	277.2
Y	23.4	9.5	9.4	12.5	10.1	15.0
V	75.9	52.4	42.9	45.7	78.3	35.3
K_2O/Na_2O	0.26	0.52	0.84	0.89	0.67	0.43
A/CNK**	0.86	0.84	0.91	0.93	0.89	0.94
K/Rb	166	299	270	268	341	247
Rb/Sr	0.08	0.11	0.18	0.22	0.09	0.13
M***	0.27	0.24	0.20	0.22	0.26	0.22

Fe_2O_3* : total Fe as Fe_2O_3,
A/CNK**: molar ratio Al_2O_3 /(K_2O+Na_2O+CaO), M*** : MgO/(MgO+FeO^t)
[1] Abbreviations: KEK, Kekachidake; OKU, Okumayama; SHI, Shimonomoto; FUN, Funatsu; ASU, Asuwagawa, YAT, Yatsuo; SHO, Shogawa; HOD, Hodatsusan; TOK, Togi.

show SiO_2 content of about 60 and 63 %. They are chemically different from the granite specimens from the Shimonomoto mass: Na_2O is high at 4.6 and 5.3 %; P_2O_5 is high at 0.22 and 0.25 %; Sr is high at 885 and 1195 ppm.

The Yatsuo mass shows a broad range of SiO_2 content from 60.6 % in the tonalite of the Todamine Facies to 71.4 % in the aplitic granite, but the variation of K_2O, Rb, Sr, Zr and Y vs. SiO_2 are relatively scatter. The aplitic granite, sample Y-4, is very similar in composition to the adamellite(sample Y-5) of the Besougawa Facies.

The Shogawa mass displays a large range of SiO_2 content from 56.4 % in the quartz diorite of the Omaki Facies to 73.8 % in the adamellite of the Toga Facies (without the pyroxene gabbro and hornblende gabbro) and its chemical characteristics are comparable to those of the Yatsuo and Hodatsusan masses: MgO is rather low at 0.1-3.9 %; MnO is also low at 0.02-0.10 %; P_2O_5 is relatively high at 0.02-0.28 %; Sr is high at 244-1086 ppm.

SiO_2 content of the Hodatsusan mass ranges from 60.6 % in the tonalite of its core to 68.8 % in the adamellite of its rim. Although the variation of Fe_2O_3, CaO, K_2O, MnO and Rb vs. SiO_2 is coherent, the remainder show some scatter. TiO_2 content is higher than that of the Jurassic granites at a fixed SiO_2 value, which is compatible with abundance in sphene.

The tonalite specimen from the Togi area shows SiO_2 at about 64 %. It has elemental abundances much like the granites of the Hodatsusan mass, except for MnO content.

The Hayatsukigawa mass displays range of SiO_2 content from 66.1 to 72.2 % (without aplitic rock). It is chemically different from the Jurassic granites: Na_2O is rather high at 4.6-5.9 %; Sr is high 429-814 ppm; Ba is strongly high at 1010-1847 ppm; MgO is relatively low at 0.1-0.3 %; MnO is rather low 0.02-0.04 %; P_2O_5 is low at 0.01-0.04 %. The enrichment in Na_2O content, which have been pointed out by Kawano and Nozawa (1969), resulted in an abundance of sodic plagioclase (An_{27}-An_{15}). K_2O and Rb contents increase and the other elements decrease as SiO_2 content increases. The variation trends in Sr, Rb and Ba indicate plagioclase, potassium feldspar and biotite fractionation during crystallization of the rocks (Tanaka and Ohtsubo, 1987).

All analyzed samples of the early Mesozoic granites show a calc-alkaline trend on the AFM diagram (Fig. 20), in spite of difference in abundance of various major and minor elements between them. However, samples from the Inner Plutonic Zone are closer to the Alkali-FeO side, as compared with the data of the Outer Plutonic Zone, which reflect the rather low content of MgO in the rocks of the former. On a Kuno plot of total alkalis against SiO_2 (Fig. 21) most samples lie in the calc-alkaline field, whereas the granites of the Hayatsukigawa mass are evidently plotted in alkaline field owing to the high content of Na_2O. The early Mesozoic granites are best characterized by low K_2O/Na_2O ratios (0.19-1.27).

Table 9 shows comparison in chemical composition between the granitic rocks of the two zones (not including the Hayatsukigawa mass and the gabbroic rocks). The estimation of the major and trace element contents at 67 % SiO_2, which corresponds closely to the average SiO_2 content (67.4 %) for 71 samples, was conducted using a linear regression. On the normalized values, the granites from the Inner Plutonic Zone are richer in P_2O_5, Rb and Sr and poorer in MgO, MnO and V

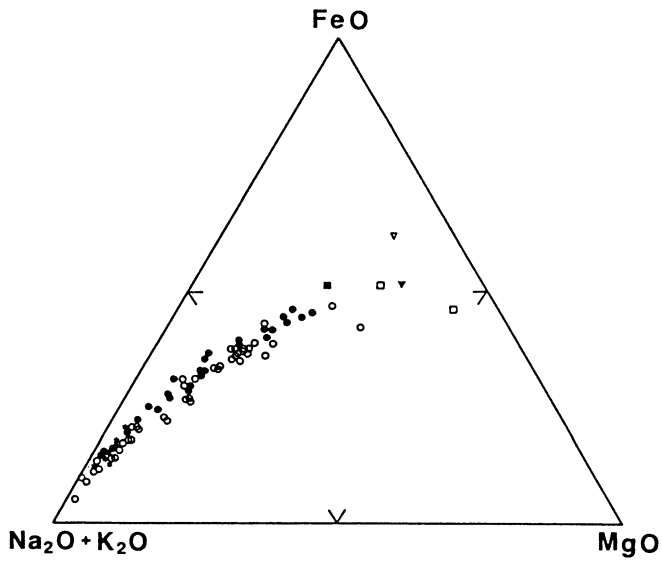

Fig. 20. AFM diagram of the early Mesozoic igneous rocks. Open circle, Jurassic granitic rocks in the Outer Plutonic Zone; Solid circle, Jurassic granitic rocks in the Inner Plutonic Zone; Asterisk, Hayatsukigawa mass rocks. Open square, pyroxene gabbro in the Outer Plutonic Zone; Solid square, pyroxene gabbro in the Inner Plutonic Zone. Open triangle, hornblende gabbro in the Outer Plutonic Zone; Solid triangle, hornblende gabbro in the Inner Plutonic Zone.

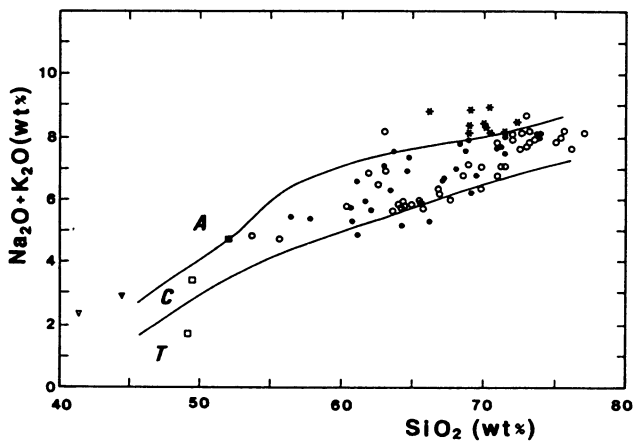

Fig. 21. Total alkalis vs. SiO_2 diagram of the early Mesozoic igneous rocks showing fields for tholeiitic (T), calc-alkalic (C) and alkalic (A) suites (boundaries from Kuno, 1969). For symbols see Fig. 20.

Table 8. Major and trace element composition of the country rocks.

Sample No.	14 KM136-1	15 KM136-2	16 KM136	17 KM139	20 TG124	21 TG170	B-7
SiO_2 (wt%)	53.73	70.27	61.67	58.26	48.06	54.60	51.81
TiO_2	0.92	0.63	0.77	0.89	2.17	1.21	0.79
Al_2O_3	17.60	11.82	14.97	17.43	21.30	20.41	22.34
Fe_2O_3	7.58	3.62	5.93	7.38	14.78	11.48	6.40
MnO	0.08	0.08	0.10	0.10	0.10	0.23	0.10
MgO	2.46	1.14	2.40	2.43	1.79	1.47	1.91
CaO	8.52	7.64	7.39	3.86	3.32	5.60	7.69
Na_2O	4.00	2.46	3.78#	4.57#	5.64#	2.94#	4.93
K_2O	2.12	2.05	1.73	2.80	1.84	0.35	1.15
P_2O_5	0.18	0.14	0.16#	0.21#	0.14#	0.23#	0.10
Total	97.19	99.85	98.90	97.93	99.14	98.52	97.22
Rb (ppm)	41.2	58.8	57.9 (59.2)	137.6 (136.7)	42.1 (40.1)	12.1 (11.0)	34.5 31.8*
Sr	315.4	268.6	305.6 (324.1)	387.6 (386.7)	358.0 (346.5)	247.9 (237.0)	1109.3 1179.0*
Ba	-	-	-	-	-	-	-
Zr	-	-	200.8	147.2	300.4	154.9	197.4
Y	-	-	29.6	20.2	27.2	38.4	20.0
V	-	-	99.0	117.8	130.0	159.3	-

Sample No.	23 73U202	133-2	136-3	218-3	8015V
SiO_2 (wt%)	58.54	74.32	72.98	73.03	75.07
TiO_2	1.42	0.02	0.06	0.12	0.15
Al_2O_3	19.68	13.96	14.20	14.40	12.85
Fe_2O_3	11.01	0.25	0.33	0.92	1.22
MnO	0.13	0.01	0.02	0.03	0.05
MgO	1.38	0.00	0.12	0.01	0.18
CaO	3.46	2.23	1.68	1.65	1.03
Na_2O	2.16#	(3.49)	(2.75)	(3.85)	4.36
K_2O	1.58	4.34	6.53	4.64	3.89
P_2O_5	0.14	0.02	0.00	0.01	0.05
Total	99.50	98.64	98.67	98.65	98.85
Rb (ppm)	49.8 (34.6)	109.5 110.1*	131.8	129.4	72.2
Sr	306.3 (287.7)	283.0 281.6*	442.9	474.1	210.2
Ba	-	573.6	1731.6	1338.3	-
Zr	173.8	79.6	108.2	136.7	-
Y	27.8	7.0	4.0	5.5	-
V	-	22.2	24.0	26.6	-

* : Isotope dilution analyses, ( ): Atomic absorption analyses,
# : after Kano (1980), X-ray fluorescence analyses unless marked.

Hida gnesses
14: Fine-grained hornblende gneiss.
15: Fine-grained clinopyroxene gneiss.
16: Alternation of biotite gneiss, hornblende gneiss and clinopyroxene gneiss.
17: Fine-grained biotite gneiss.
20: Staurolite-andalusite-garnet-sillimanite-cordierite-muscovite-biotite gneiss.
21: Garnet-sillimanite-biotite gneiss.
B-7: Garnet-biotite gneiss.

Unazuki schist
23: Garnet-staurolite schist.

Gray granites
133-2: Coarse-grained biotite adamellite.
136-3: Coarse-grained biotite adamellite.
218-3: Fine-grained biotite adamellite.

Granitic cobble
8015V: Medium-grained biotite adamellite.

Table 9. Difference in normalized chemical composition between the Jurassic granitic rocks of the Outer Plutonic Zone and those of the Inner Plutonic Zone.

	Granitic rocks from the Outer Plutonic Zone (n=41)'				Granitic rocks from the Inner Plutonic Zone (n=30)			
	Mean	S.D.	r	at 67% SiO_2	Mean	S.D.	r	at 67% SiO_2
SiO_2	68.67	4.54			66.05	4.72		
TiO_2	0.41	0.22	-0.960	0.49	0.56	0.24	-0.959	0.51
Al_2O_3	15.04	1.36	-0.929	15.51	15.76	1.05	-0.903	15.57
Fe_2O_3*	3.30	1.60	-0.982	3.88	4.16	1.84	-0.980	3.79
MnO	0.08	0.03	-0.719	0.09	0.07	0.04	-0.748	0.06
MgO	1.19	0.77	-0.932	1.45	1.39	1.04	-0.940	1.19
CaO	2.87	1.53	-0.962	3.41	3.90	1.73	-0.982	3.56
Na_2O	4.22	0.59	-0.288	4.29	4.35	0.46	-0.149	4.33
K_2O	2.79	0.99	0.900	2.46	2.46	1.07	0.813	2.64
P_2O_5	0.09	0.05	-0.863	0.11	0.14	0.07	-0.800	0.13
Rb	72.3	30.5	0.695	64.5	75.6	28.3	0.724	79.7
Sr	314.9	198.0	-0.755	369.8	580.6	187.7	-0.679	554.9
Ba	687.4	295.4	0.389	645.2	714.2	252.5	0.564	742.9
Zr	148.0	51.9	-0.566	159.5	174.2	43.7	-0.217	172.3
Y	18.1	7.1	-0.052	17.8	15.3	5.7	0.496	15.0
V	52.6	27.9	-0.830	68.6	61.2	33.8	-0.888	57.4
K/Rb	320			317	270			275
Rb/Sr	0.23			0.17	0.13			0.14
K/Ba	33.7			31.7	28.6			29.5
Sr/Ba	0.46			0.57	0.81			0.75

Note: Mean, standard deviation and 67% SiO_2 values are percent by oxides and parts per million for minor elements. Fe_2O_3* , total Fe as Fe_2O_3.
r, coefficient of correletion.

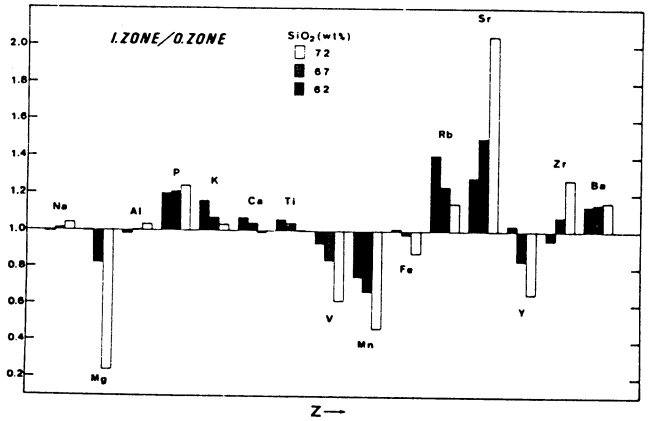

Fig. 22. Diagram showing enrichment factors for 15 elements in the Jurassic granites. The factors are based on normalized values 62, 67 and 72 wt% SiO_2 in the Inner Plutonic Zone divided by those in the Outer Plutonic Zone.

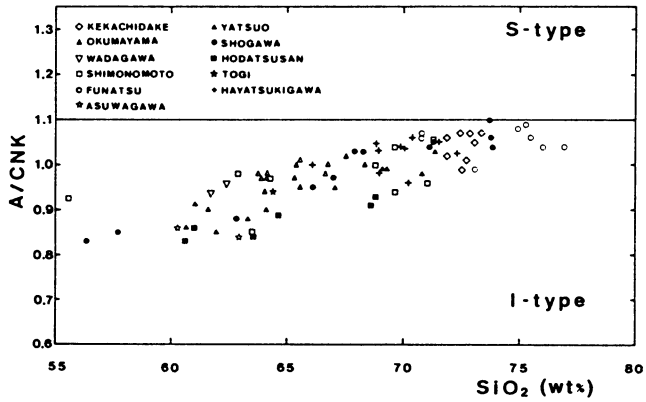

Fig. 23. Molar $Al_2O/(CaO+Na_2O+K_2O)$ vs. SiO_2 diagram of the early Mesozoic granitic rocks. Solid line represents the boundary between I-type and S-type granitoids after White and Chappell (1977).

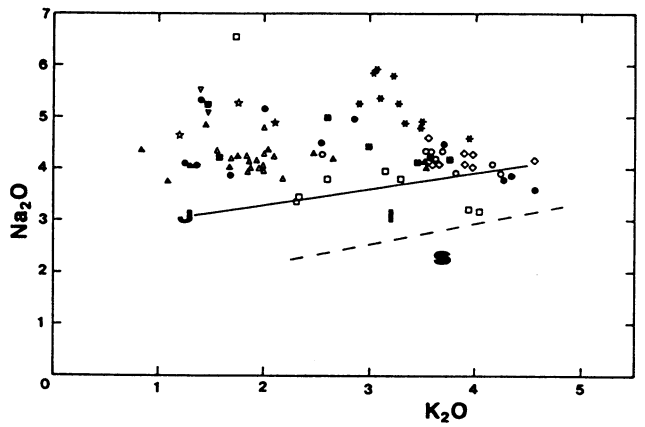

Fig. 24. Na_2O vs. K_2O diagram of the early Mesozoic granitic rocks. Solid line (J) is the average composition of the Japanese granitoids by Aramaki et al. (1972). Broken line represents the boundary between I-type (I) and S-type (S) granitoids after White and Chappell (1977). For symbols see Fig. 23. Asterisk, Hayatsukigawa mass rocks.

than those from the Outer Plutonic Zone. Elements such as Rb, Ba and Sr, that are strongly concetrated in the liquid during partial melting or fractional crystallization, are known as incompatible elements. The Sr content shows the most marked difference between the two zones, which will be in more detail discussed in the later section. The difference in MgO and V contentsis reflected by the presence of magnesio-hornblende and much more abundance of magnetite in the Outer Plutonic Zone granites. Furthermore, the estimation of the element contents at 62 % and 72 % SiO_2 was conducted using the linear regression. As shown in Fig. 22, the chemical differences between the two zones granites become much more apparent with increasing SiO_2 content (62 to 72 %),except for Rb.

Coefficients of correlation for Na_2O, Y, Zr and Ba are too low to compare using the such method (Table 9). As compared with the Outer Plutonic Zone granites, the Inner Plutonic Zone granites have lower Y and higher Zr and Ba in mean values. The granites from the Inner Plutonic Zone have lower K/Rb ratios (avg. 270) than those from the Outer Plutonic Zone (avg. 320) have.

It is note worthy that there is no significant difference in K_2O, Na_2O and CaO contents between the two zones. In addition no difference was detected in the aluminous character between the granites from the two zones: the ratio of mole $Al_2O_3/(Na_2O+K_2O+CaO)$ (hereafter to as A/CNK) is low and less than 1.1 (Fig. 23). The granites plotted above the line A/CNK=1 are commonly called to be peraluminous. They with A/CNK > 1.1 are named S-type according to the definition of Chappell and White (1974). As mentioned above the granites of the two zones have relatively high content of sodium (Na_2O more than 3.2 wt%) (Fig. 24). Consequently, it can be said that they belong to the I-type granitoids on the basis of the classification of Chappell and White (1974).

Although the granites of the Hayatsukigawa mass indicate an alkaline nature, their other chemical signatures such as $(CaO+MgO)/FeO^*$ (wt%)= (1.37-1.91), $(Na_2O+K_2O)/Al_2O_3$ (molar)=(0.70-0.81) and $Al_2O_3/(Na_2O+K_2O+CaO)$ (molar)=(0.96-1.06) are similar to those of the I-type rather than the A-type after Collins et al. (1982).

The two pyroxene gabbro (sample SO-18) in the Shogawa mass is richer in P_2O_5, Rb, Sr, Ba, Zr contents and poorer in MgO, MnO, Y and V contents than that (sample S-19) in the Shimonomoto mass (Table 7), which is entirely identical with the difference in these contents between the two zones granites. These gabbros are plotted in the tholeiite field in the FeO^*/MgO vs. SiO_2 diagram (cf. Miyashiro, 1974) and in the island arc tholeiite field in the $MnO/TiO_2/P_2O_5$ diagram (cf. Mullen, 1983).

VI. ISOTOPE RESULTS

A. ANALYTICAL PROCEDURE.

Whole rock samples used in the present study were prepared from 1 to 3 kg rock specimens, except for metamorphic rocks. Minerals (plagioclase, potassium feldspar and biotite) were separated using a combination of isodynamic separator, heavy liquid (Clerici solution) and hand pick method.

Rock powders weighing 100 to 300 mg, depending upon Sr and Nd concentrations of the sample, were dissolved in a mixture of 40 % HF (2 ml), 65 % HNO_3 (0.5 ml), 70 % $HClO_4$ (0.5 ml), 30 % HCl (0.5ml) in the Krogh's-type teflon vessel (Krogh, 1973). The vessel was loaded into a self-sealing stainless steel jaket and was heated at 210℃ for about 7 days.

Rb and Sr were separated following the procedure described by Kagami et al. (1982). REE remaining in the ion-exchange resin after Sr separation were extracted by 6 M HCl. Sm and Nd were separated from other REE in another column with a cation-exchange resin (Dowex AG. 50W-X8, 200-400 mesh, H-form) by 0.2 M hydroxy-α-isobutyric acid adjusted to pH=4.5. The column was reequilibrated with 18 ml butyric acid before loading the sample.

The extracted elements were loaded on to a Ta-filament in a double filament mode. Isotopic ratios were measured in MAT 261 mass spectrometer, which was reconstructed from MAT 260, with single collector and in new MAT 261 with 5 collectors. $^{87}Sr/^{86}Sr$ ratios were normalized to $^{86}Sr/^{88}Sr=0.1194$ and $^{143}Nd/^{144}Nd$ ratios were normalized to $^{146}Nd/^{144}Nd=0.7219$. $^{87}Sr/^{86}Sr$ and $^{143}Nd/^{144}Nd$ ratios were obtained by measurement of 200 and 400 scans respectively. The blank for the whole procedure was < 0.60 ng Rb, < 0.55 ng Sr, < 0.04 ng Sm and < 0.40 ng Nd.

Sr isotopic ratios for NBS987 were measured 10 times during this study. The average of all these ratios was 0.710256±0.000020 (2 σ mean). Rb and Sr concentrations were determined by isotope dilution using a ^{87}Rb-^{86}Sr mixed spike and X-ray fluorescence analysis (Tanaka and Maruyama, 1985b; Ichikawa et al., 1987). Analytical uncertainties in $^{87}Rb/^{86}Sr$ ratios were taken at 2 % and 5 % for X-ray fluorescence analysis and isotope dilution, respectively, and that in $^{87}Sr/^{86}Sr$ ratios were 0.015 %.

The average of the $^{143}Nd/^{144}Nd$ ratio for BCR-1 was 0.512649±0.000020 (2 σ mean). This average ratio agrees, within the limit of error, with 0.512640 determined by Wasserburg et al. (1981). The error for each sample was 0.005 % on the 2 σ level. Sm and Nd concentrations of each sample were determined using a ^{149}Sm-^{150}Nd mixed spike. Analytical uncertainties in Sm/Nd ratios were taken at 1%.

Internal and whole-rock isochrons were calculated using the least square regression technique of York (1966). Isochrons were identified when the mean square of weighted deviates (MSWD) was less than the F-variate, approximately 2.5, for the number of points regressed, whereas when MSWD was more than the F-variate, the data defined an errorchron (Brooks et al., 1972). Errors of the calculated ages and initial ratios were given on the 2 σ level. These decay constants used in age calculation are $^{87}Rb\ \lambda = 1.42 \times 10^{-11}/y$ (Steiger and Jäger, 1977) and $^{147}Sm\ \lambda = 6.54 \times 10^{-12}/y$ (Lugmair and Marti, 1978).

The initial $^{143}Nd/^{144}Nd$ and $^{87}Sr/^{86}Sr$ ratios are also reported in the ε notation (DePaolo and Wasserburg, 1976) as deviations in parts in 10^4 from a model chondritic uniform reservoir (CHUR) and a model reservoir thought to be representative of the total earth (UR) (it is not a chondritic uniform reservoir), respectively:

$$\varepsilon Nd = \left[\frac{(^{143}Nd/^{144}Nd)^{T}_{ROCK}}{(^{143}Nd/^{144}Nd)^{T}_{CHUR}} - 1 \right] \times 10^4$$

The ratio $(^{143}Nd/^{144}Nd)^{T}_{CHUR}$ is given by the following expression:

$$(^{143}Nd/^{144}Nd)^{T}_{CHUR} = 0.512638 - 0.1967\ [\exp(\lambda_{Sm} T) - 1]$$

where T is time measured backward from the present (age). Present day reference values are $(^{143}Nd/^{144}Nd)^{0}_{CHUR}=0.512638$ and $(^{147}Sm/^{144}Nd)^{0}_{CHUR}=0.1967$ (Jacobsen and Wasserburg, 1984). An equivalent notation for $^{87}Sr/^{86}Sr$ is:

$$\varepsilon Sr = \left[\frac{(^{87}Sr/^{86}Sr)^{T}_{ROCK}}{(^{87}Sr/^{86}Sr)^{T}_{UR}} - 1 \right] \times 10^4$$

The ratio $(^{87}Sr/^{86}Sr)^{T}_{UR}$ is given by:

$$(^{87}Sr/^{86}Sr)^{T}_{UR} = 0.7045 - 0.0839\ [\exp(\lambda_{Rb} T) - 1]$$

where the numbers are $(^{87}Sr/^{86}Sr)^{0}_{UR}$ and $(^{87}Rb/^{86}Sr)^{0}_{UR}$, respectively (Kagami et al., 1987). The initial isotopic ratios have been calculated using a Rb-Sr whole rock isochron age for the Kekachidake, Shimonomoto, Funatsu and Utsubo masses. For the remaining masses, an assumed age of 190 Ma was used, except for the Hayatsukigawa mass. This value is an average of Rb-Sr whole rock ages from the Jurassic Granitic masses in the Hida Terrane, which were reported by Shibata and Nozawa (1984) and this study. The initial isotopic ratios reported below are thought to correspond to be primary magmatic values, because the analysed samples show no evidence of significant mineralogical alteration induced during the post-crystallization stage.

The model age is determined by the intersection between the isotopic vector of a crustal rock and the isotopic evolution curve of the mantle. Originally the evolution curve of the mantle was chosen to be the chondritic evolution curve (McCulloch and Wasserburg, 1978), but, later on, many authors have indicated that the evolution curve of the depleted oceanic mantle is a better choice, since continental crust is considered to be extracted via complex mechanisms from such a

Table 10. Rb and Sr concenrations and $^{87}Sr/^{86}Sr$ ratios.

Sample No.	Lithology[1]	Rb[2] (ppm)	Sr[2] (ppm)	$^{87}Rb/^{86}Sr$	$^{87}Sr/^{86}Sr$	2σ
	Kekachidake Mass					
K-1	Bt adm	60.7	237.4	0.7397	0.70689	0.00002
K-2	Bt gd	79.2	245.1	0.9349	0.70717	0.00002
K-3	Bt gd	98.8	182.2	1.5691	0.70927	0.00004
K-4	Bt adm	112.2	148.1	2.1926	0.71088	0.00003
K-5	Bt adm	114.5	198.9	1.6658	0.70924	0.00003
K-6	Bt adm	127.2	157.2	2.3419	0.71121	0.00002
	Okumayama Mass					
O-1	Hb-bt gd	50.2*	373.4*	0.3888	0.70576	0.00003
O-2	Hb-bt ton	43.4*	394.0*	0.3186	0.70568	0.00002
O-3	Hb-bt ton	45.9* 44.2	371.3* 373.6	0.3577 0.3426	0.70581	0.00003
O-4	Hb-bt ton	55.3* 54.1	332.2* 332.9	0.4814 0.4706	0.70622	0.00002
O-4	Pl	31.3*	642.5*	0.1410	0.70541	0.00002
O-4	Kf	157.7*	350.1*	1.3033	0.70832	0.00004
O-4	Bt	397.0*	9.0*	132.25	1.05002	0.00005
O-5	Hb-bt ton	58.5* 57.3	347.3* 347.2	0.4871 0.4779	0.70613	0.00002
	Hayatsukigawa Mass					
H-1	Hb-bt gd	42.4	757.5	0.1619	0.70665 0.70664	0.00003 0.00002
H-1	Pl	12.3*	881.6*	0.0404	0.70630	0.00003
H-1	Kf	165.8*	761.7*	0.6298	0.70806	0.00002
H-2	Hb-bt qmd	63.5	739.7	0.2483	0.70673	0.00004
H-3	Hb-bt gd	60.3	501.1	0.3481	0.70710	0.00003
H-4	Bt gd	87.8* 86.2	424.5* 420.8	0.5982 0.5927	0.70832 0.70834	0.00002 0.00002
H-5	Hb-bt qmd	68.5	664.6	0.2982	0.70707	0.00005
	Shimonomoto Mass					
S-1	Bt qd	42.7	462.9	0.2668	0.70539	0.00004
S-2	Bt-hb gd	69.8* 71.1	352.0* 357.3	0.5672 0.5758	0.70641	0.00003
S-3	Hb-bt gd	80.7	291.4	0.8012	0.70697	0.00004
S-4	Hb-bt adm	97.7* 99.3	273.9* 274.3	1.0320 1.0474	0.70769	0.00003
S-5	Hb-bt adm	111.7	272.6	1.1856	0.70825	0.00002
S-6	Hb-bt adm	131.3	243.6	1.5597	0.70925	0.00002
S-7	Hb-bt adm	146.2* 146.1	221.9* 215.5	1.9067 1.9611	0.71017	0.00002
S-19	Py gab	5.0*	536.2*	0.0270	0.70486	0.00003
S-20	Py gab	7.3*	423.4*	0.0497	0.70491	0.00001

Table 10. (continued)

Sample No.	Lithology[1]	Rb[2] (ppm)	Sr[2] (ppm)	$^{87}Rb/^{86}Sr$	$^{87}Sr/^{86}Sr$	2σ
	Funatsu Mass					
F-1	Bt gd	61.9	285.9	0.6263	0.70653	0.00004
F-2	Bt gd	92.1	251.4	1.0599	0.70738	0.00003
F-3	Bt gd	104.7* 104.5	198.3* 204.9	1.5283 1.4762	0.70899	0.00003
F-4	Bt adm	62.8	110.7	1.6416	0.70916	0.00002
F-5	Bt adm	84.8	103.6	2.3690	0.71101	0.00003
F-6	Bt adm	99.6	82.8	3.4823	0.71358	0.00004
F-7	Bt adm	85.0* 88.3	63.7* 63.6	3.8679 4.0244	0.71500	0.00002
	Wadagawa Mass					
W-1	Hb-bt qd	34.4	412.0	0.2415	0.70548	0.00002
	Asuwagawa Mass					
AS-1	Hb-bt qd	27.9*	885.4*	0.0911	0.70495	0.00002
AS-2	Bb-hb qd	35.2*	1195.2*	0.0853	0.70474	0.00003
	Utsubo Mass					
U-06	Hb-bt gd	72.5* 72.3	463.3* 447.8	0.4528 0.4672	0.70631	0.00003
	Yatsuo Mass					
Y-1	Hb-bt ton	39.6* 41.4	820.1* 804.6	0.1396 0.1488	0.70724	0.00005
Y-2	Hb-bt ton	24.8	478.1	0.1501	0.70689	0.00005
Y-3	Hb-bt ton	68.5* 69.2	662.4* 656.4	0.2991 0.3049	0.70769	0.00002
Y-4	Bt-gd	94.7	567.2	0.4833	0.71256	0.00003
Y-5	Bt-adm	89.5	503.0	0.5149	0.70987	0.00002
Y-6	Hb-bt gd	75.3* 75.4	416.4* 409.1	0.5232 0.5298	0.70812	0.00002
Y-6	Pl	8.3*	465.1*	0.0516	0.70692	0.00003
Y-6	Kf	196.5*	543.2*	1.0466	0.70938	0.00003
Y-7	Hb-bt gd	70.8	420.7	0.4869	0.70827	0.00002
Y-8	Hb-bt ton	65.7	723.9	0.2626	0.70720	0.00001
	Shogawa Mass					
SO-1	Mus-bt adm	114.2*	315.9*	1.0466	0.71278	0.00004
SO-2	Hb-bt ton	73.3*	1086.0*	0.1952	0.70706	0.00002
SO-3	Bt ton	39.4*	755.2*	0.1509	0.70670	0.00003
SO-5	Hb-bt ton	55.9*	686.4*	0.2356	0.70906	0.00004
SO-6	Bt-hb qd	51.2*	731.4*	0.2027	0.70717	0.00001
SO-7	Bt gd	80.9	537.0	0.4359	0.70763	0.00002
SO-7	Bt	510.3*	14.8*	102.82	0.98960	0.00005
SO-11	Mus-bt-adm	117.0	244.0	1.3882	0.71424	0.00003

Table 10. (continued)

Sample No.	Lithology[1]	Rb[2] (ppm)	Sr[2] (ppm)	$^{87}Rb/^{86}Sr$	$^{87}Sr/^{86}Sr$	2σ
SO-14	Hb gab	44.2	749.5	0.1706	0.70573	0.00002
SO-18	Py gab	16.0	780.4	0.0593	0.70656	0.00003
	Hodatsusan Mass					
HO-1	Bt-hb ton	61.1*	408.4*	0.4324	0.70715	0.00005
HO-2	Hb-bt ton	69.5	886.5	0.2268	0.70843	0.00004
HO-3	Hb-bt gd	72.2*	664.4*	0.3135	0.70717	0.00005
HO-4	Hb-bt adm	106.8*	577.3*	0.5353	0.71096	0.00002
HO-4	Bt	615.7*	17.4*	105.24	0.97052	0.00007
HO-5	Hb-bt adm	116.4*	526.6*	0.6400	0.71128	0.00002
HO-6	Hb-bt gd	72.5*	765.4*	0.2740	0.70990	0.00002
	Small mass in Togi area					
TK-2	Bt ton	70.9	540.8	0.3791	0.70775	0.00003
	Country Rock; Hida gneisses					
B-7	Ga-bt gn	31.8*	1179.0*	0.0781	0.71126	0.00003
14	Hb gn	41.2	315.4	0.3779	0.70622	0.00002
15	Py gn	58.8	268.6	0.6337	0.71268 0.71265	0.00002 0.00002
16	Py-hb-bt gn	57.9	305.6	0.5485	0.71543	0.00003
17	Bt gn	137.6	387.6	1.0277	0.71119	0.00003
20	St-bt gn	42.1	358.0	0.3404	0.70581	0.00005
21	Ga-bt gn	12.1	247.9	0.1413	0.70583	0.00002
	Country Rock; Unazuki schist					
23	Ga-St sch	49.8	306.3	0.4704	0.70620	0.00002
	Country Rock; Gray granite					
133-2	Bt adm	110.1* 109.5	281.6* 283.0	1.1322 1.1206	0.71407	0.00004
	Country Rock; Granite cobble					
8015V	Bt adm	72.2	210.2	0.9942	0.70749	0.00002

1 Abbreviations: Bt, biotite; Hb, hornblende; Pl, plagioclase; Mus, muscovite; Kf, k-feldspar; St, staurolite; Ga, garnet; Py pyroxene qd, quartz diorite; ton, tonalite; gd, granodiorite; qmd, quartz monzodiorite; adm, adamellite; gn, gneiss; sch, schist

2 X-ray fluorescence analyses unless marked.
* Isotope dilution analyses for Rb and Sr concentrations

Table 11. Nd and Sm concentrations and $^{143}Nd/^{144}Nd$ ratios.

Sample[1] No.	Sm (ppm)	Nd (ppm)	$^{147}Sm/^{144}Nd$	$^{143}Nd/^{144}Nd$[2]		ε Nd(T)	ε Sr(T)	T (Ma)
	Outer Plutonic Zone							
H-1	1.97	13.40	0.0890	0.512312	(18)	-3.33	27.06	220
H-4	1.33	9.41	0.0852	0.512260	(24)	-4.24	31.53	220
K-5	3.27	17.39	0.1138	0.512698	(20)	+3.25	4.73	196
O-1	3.00	15.23	0.1191	0.512698	(26)	+3.05	6.20	190
S-2	3.55	16.39	0.1309	0.512710	(29)	+3.13	7.45	201
S-19	2.33	9.54	0.1477	0.512771	(25)	+3.85	7.42	201
S-20	0.89	3.63	0.1481	0.512713	(43)	+2.71	7.15	201
F-3	2.76	16.04	0.1042	0.512683	(27)	+3.05	10.03	184
U-06	3.45	19.43	0.1073	0.512603	(16)	+1.41	12.06	183
	Inner Plutonic Zone							
HO-1	3.47	15.95	0.1316	0.512640	(31)	+1.62	24.32	190
HO-3	4.51	25.00	0.1092	0.512500	(18)	-0.57	29.09	190
Y-8	4.71	25.22	0.1128	0.512396	(19)	-2.69	31.41	190
TK-2	3.68	23.94	0.0930	0.512378	(13)	-2.56	34.84	190
Y-5	3.69	23.70	0.0941	0.512126	(16)	-7.50	59.70	190
HO-4	3.92	23.79	0.0997	0.512043	(19)	-9.26	74.45	190
SO-1	3.26	18.99	0.1037	0.512119	(19)	-7.87	80.57	190
SO-11	2.92	17.56	0.1004	0.512062	(28)	-8.90	88.32	190
SO-14	2.31	7.16	0.1948	0.512798 0.512815	(39) (50)	+3.34	14.08	190
SO-18	3.75	17.87	0.1268	0.512454	(27)	-1.89	30.18	190
	Country Rock; Hida gneisses							
B-7	7.03	29.87	0.1425	0.512230	(20)	-6.65	96.26	190
14	7.71 7.74	40.48 40.40	0.1155	0.511926	(14)	-11.92	13.08	190
15	7.38 7.36	40.91 40.67	0.1092	0.511706	(21)	-16.07	94.86	190
16	6.86	36.71	0.1129	0.511944	(14)	-11.51	137.37	190
17	4.59	24.89	0.1115	0.512679 0.512652	(15) (17)	+2.62	58.83	190
20	4.45	21.00	0.1280	0.512840	(19)	+5.61	8.79	190
21	7.01	29.79	0.1423	0.512895	(18)	+6.34	16.70	190
	Country Rock; Unazuki schist							
23	5.01	20.47	0.1479	0.512824	(25)	+4.82	9.36	190
	Country Rock; Gray granite							
133-2	0.61	2.95	0.1258	0.512010	(22)	-10.54	95.63	190

1 All are whole-rock samples.
2 Numbers in parentheses refer to the last digit and the error in 95% confidence.

type of mantle (e.g., DePaolo, 1980; Allègre, 1982). Initial ε Nd values of as much as +4 in this study area also provide evidence that the depleted mantle was involved in a magma genesis. Therefore, the present writer calculated Sm-Nd and Rb-Sr model ages using "depleted" mantle parameters. Nd model ages (T_{DM}^{Nd}) were calculated on the basis of the evolution of a "depleted" mantle (DM) (DePaolo, 1981a) by solving the following equation for T (age in Ga):

$$\varepsilon Nd(T) = 0.25T^2 - 3T + 8.5$$

where $\varepsilon Nd(T) = \varepsilon Nd(0) - f_{Sm/Nd} Q_{Nd} T$. The $\varepsilon Nd(0)$ and $f_{Sm/Nd}$ values are measured for each sample. The Q_{Nd} value is defined as:

$$Q_{Nd} = \frac{10^4 \lambda_{Sm} (^{147}Sm/^{144}Nd)^0_{CHUR}}{(^{143}Nd/^{144}Nd)^0_{CHUR}} = 25.09 \text{ b.y.}^{-1}$$

The $f_{Sm/Nd}$ value is defined as:

$$f_{Sm/Nd} = \frac{(^{147}Sm/^{144}Nd)_{Sample} - (^{147}Sm/^{144}Nd)_{CHUR}}{(^{147}Sm/^{144}Nd)_{CHUR}}$$

Sr model ages (T_{DM}^{Sr}) were calculated on the basis of the evolution of a "depleted" mantle (DM) (Ben Othman et al., 1984) by solving the following equation for T (age in Ga):

$$(^{87}Sr/^{86}Sr)^T = AT^2 + BT + C$$

where $(^{87}Sr/^{86}Sr)^T = (^{87}Sr/^{86}Sr)_{Sample} - (^{87}Rb/^{86}Sr)_{Sample}(e^{\lambda T} - 1)$. $A = -1.54985776 \times 10^{-4}$; $B = -1.6007234 \times 10^{-4}$; $C = 0.70273029$.

If a crust is derived from a mantle with no admixture of older crust, then a model age for the former is actually the crust formation age (e.g., DePaolo, 1981a). But if an orogenic terrane is produced by mixing of crustal material and mantle-derived products, the model age for the terrane reflects a weighted average of contributing components. This is the interpretation of Patchett and Arndt (1986). They suggested that such a model age is unlikely to specify the timing of a particular geological event, but rather it provides an estimate of the average period (crustal residence age) when the Rb, Sr, Sm and Nd components of constituent sediments or granites had been resident in the continental crust for them. Especially, owing to the apparent resistance of Sm-Nd to disturbance during sedimentation, diagenesis and high-grade metamorphism (e.g., McCulloch and Wasserburg, 1978), the Sm-Nd model age provides an estimate of provenance age. Goldstein et al. (1984) calculated Nd model ages assuming a linear evolution of depleted mantle from $\varepsilon Nd = 0$ at 4.5 Ga to $\varepsilon Nd = +10$ at the present day. Such model ages are greater approximately by 0.2 Ga than Nd model ages of DePaolo (1981a).

B. MESOZOIC GRANITIC ROCKS

1. STRONTIUM ISOTOPE

Rubidium, strontium, and $^{87}Sr/^{86}Sr$ ratios for the Mesozoic granitic rocks investigated in this paper and for each of minerals separated from the rocks are summarized in Table 10.

Six whole-rock samples from the Kekachidake mass give a valid Rb-Sr isochron (MSWD=0.6) with an age of 196.1±16.8 Ma and an initial $^{87}Sr/^{86}Sr$ ratio of 0.70472±0.00032 (Fig. 25). This age is in well agreement with a K-Ar age of 192±8 Ma, recalculated using the decay constants by Steiger and Jäger (1977), for muscovite separate of pegmatite from the mass reported by Suwa (1966a). A Rb-Sr whole-rock age of granite is commonly considered to indicate the time of its emplacement, whereas Rb-Sr and K-Ar mineral ages represent the time of its uplift and cooling, during which the mineral. Thus, it seems very likely that the figure of 196 Ma reflects the primary age of emplacement of the Kekachidake mass.

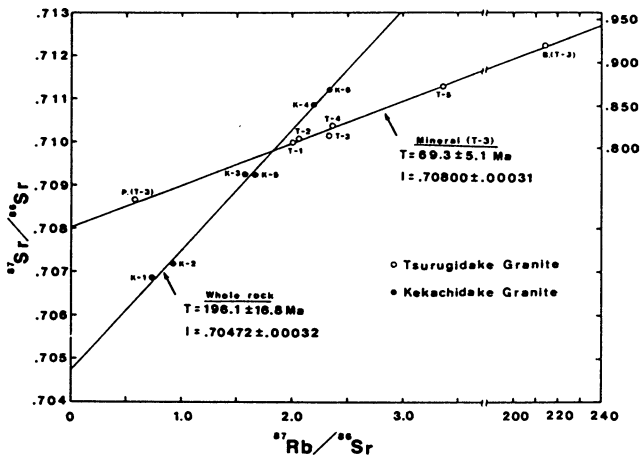

Fig. 25. Rubidium-strontium isochron diagram for the Kekachidake mass and the Tsurugidake Granite. P.=plagioclase; B.=biotite.

Five whole-rock samples and three minerals (biotite, potassium feldspar and plagioclase) from the Okumayama mass have been analysed for Rb/Sr and $^{87}Sr/^{86}Sr$ ratios. It was impossible to derive a meaningful Rb-Sr whole rock isochron age from the obtained data because of the extremely restricted range of $^{87}Rb/^{86}Sr$ ratios (0.32-0.49). A four-point internal isochron for sample O-4 defines an age of 182.6±3.8 Ma with an initial $^{87}Sr/^{86}Sr$ ratio of 0.70499±0.00008 and an MSWD of 0.3 (Fig. 26). This age is controlled by the biotite data and indicates that the cooling of the Okumayama mass had occurred below the Rb-Sr closure temperature of biotite (320±40℃, Harrison and McDougall, 1980) by ~180 Ma. The Rb-Sr mineral age is disconcordant with the Rb-Sr internal isochron age of 174.2±3.4 Ma (biotite, whole-rock and plagioclase) for quartz diorite in the Unazuki district indicated by Katoh et al. (1989). Using an assumed age of 190 Ma and the whole-rock Rb, Sr and $^{87}Sr/^{86}Sr$ data, the mass has initial $^{87}Sr/^{86}Sr$ ratios in the range of 0.70471 to 0.70492 showing an average value of 0.70482.

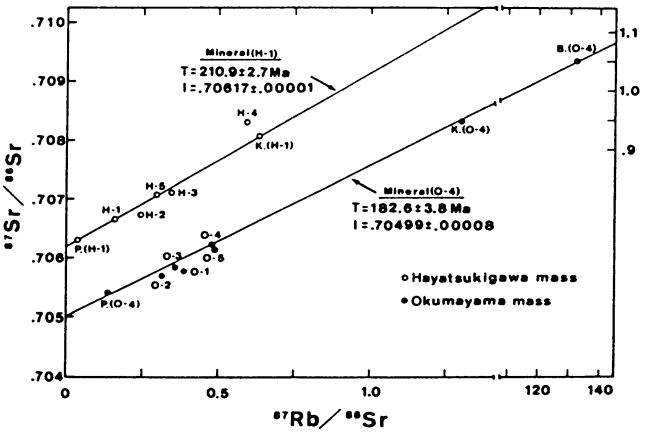

Fig. 26. Rubidium-strontium isochron diagram for the Okumayama mass and the Hayatsukigawa mass. P.=plagioclase; K.=k-feldspar; B.=biotite.

For the Hayatsukigawa mass Rb-Sr isotope data were obtained from five whole-rock samples and two minerals (potassium feldspar and plagioclase). These data define a statistically acceptable Rb-Sr whole-rock isochron, giving an age of 281.4± 60.8 Ma, an initial $^{87}Sr/^{86}Sr$ ratio of 0.70585± 0.00031 and an MSWD of 1.6 (Fig. 26). The author is reluctant to attach much meaning to this age because of the large resulting error. This scatter probably reflects some initial isotopic heterogeneity or crustal contamination during magma ascent. A three-point internal isochron for sample H-1 defines an age of 210.9±2.7 Ma with an initial $^{87}Sr/^{86}Sr$ ratio of 0.70617±0.00001 and an MSWD of 0.1 (Fig. 26). The internal isochron age indicates that the Hayatsukigawa mass is older by ca. 30 Ma than its spatially associated one, Okumayama mass. This result is concordant with the estimation based on the field observation for these masses (see the section III). Shibata and Nozawa (1984) reported Rb-Sr whole-rock and internal isochron ages of 296.7±25.6 Ma and 210.8±1.8 Ma, respectively, for the Mizunashi granite of the Amo area, and pointing out that the granite is older in age than the Jurassic granitic rocks. There is a possibility that the Hayatsukigawa mass is not correlative with the Jurassic granites but the Triassic ones, although the emplacement age is poorly constrained by the whole-rock Rb-Sr isotope data (281.4±60.8 Ma). A three-point internal isochron age of 211 Ma is probably related closely to its crystallization age. Thus, using an assumed emplacement age of 220 Ma and the whole-rock Rb, Sr, and $^{87}Sr/^{86}Sr$ data, the initial $^{87}Sr/^{86}Sr$ ratio for the mass range from 0.70595 to 0.70647 with an average of 0.70614. The initial $^{87}Sr/^{86}Sr$ ratios of the Hayatsukigawa mass are evidently higher than those of the Okumayama mass, suggesting that the Hayatsukigawa and Okumayama mass do not share the same source or magmatic evolution.

One sample (W-1: quartz diorite) from the Wadagawa mass has been analysed for Rb/Sr and $^{87}Sr/^{86}Sr$ ratios. A 177 Ma K-Ar age for biotite from this mass (Kawano and Ueda, 1966) can merely be considered as minimum estimates of the age of igneous emplacement. Using an assumed age of 190 Ma, an initial $^{87}Sr/^{86}Sr$ ratio of 0.70483 is indicated.

For the Shimonomoto mass nine whole-rock samples (two samples from the gabbroic rocks, two samples from the Kanekido Facies, two samples from the Kuwasaki Facies and three samples from the Ikenoo Facies) define an excellent isochron with a whole-rock Rb-Sr age of 201.2±5.7 Ma, an initial $^{87}Sr/^{86}Sr$ ratio of 0.70474±0.00007 and an MSWD of 0.3 (Fig. 27). This estimate of the whole-rock age involves the assumption that all facies of the mass were emplaced at the nearly same time. Seven

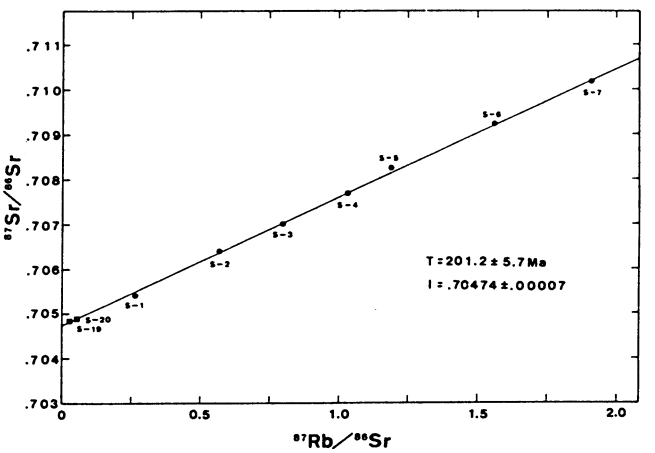

Fig. 27. Rubidium-strontium isochron diagram for the Shimonomoto mass. Solid circle=granitic rocks; Solid square=gabbroic rocks.

samples, excluding two gabbroic samples, yield a 204.9±7.8 Ma age and an initial $^{87}Sr/^{86}Sr$ ratio of 0.70468±0.00011, being identical to the result obtained for all facise. Therefore the gabbroic rocks can be regarded as cogenetic and contemporaneous with host rocks. The 201.2±5.7 Ma age and initial ratio are believed to be better estimates than the age of 197.9±15.4 Ma and initial $^{87}Sr/^{86}Sr$ ratio of 0.70481±0.00016 (MSWD=0.6) for a 13-point whole-rock isochron reported by Shibata and Nozawa (1984). They analysed no samples from the gabbroic rocks with low $^{87}Rb/^{86}Sr$ ratio and from the Kuwazaki Facies with high $^{87}Rb/^{86}Sr$ ratios. Shibata and Nozawa (1984) obtained also K-Ar ages of 181±6 Ma and 177±6 Ma for hornblende and biotite separates, respectively. The difference between the Rb-Sr whole-rock isochron and the K-Ar biotite ages is 24 Ma, which is significantly larger than the range of 4-9 Ma reported by Shibata and Ishihara (1979) for the Cretaceous granitic plutons of Japanese Island, which are considered to be of simple cooling history. This may be ascribed to the long duration of magmatic activity in the Hida Terrane during the early Jurassic age.

Seven whole-rock samples from the Funatsu mass have been analyzed for Rb/Sr and $^{87}Sr/^{86}Sr$ ratios.

These data fit a straight line within analytical error giving an age of 184.1±9.1 Ma with an initial $^{87}Sr/^{86}Sr$ ratio of 0.70485±0.00023 and an MSWD of 0.8 (Fig. 28). These results are substantiated by the results of analyses of nine whole-rock samples of the same mass by Shibata and Nozawa (1984), which yield an age of 188.9±4.4 Ma and an initial $^{87}Sr/^{86}Sr$ ratio of 0.70480±0.00009 (MSWD=0.7). The data of this study indicate that the Funatsu mass is somewhat younger in Rb-Sr whole-rock age than the Shimonomoto mass. This result is consistent with the field relations for these masses.

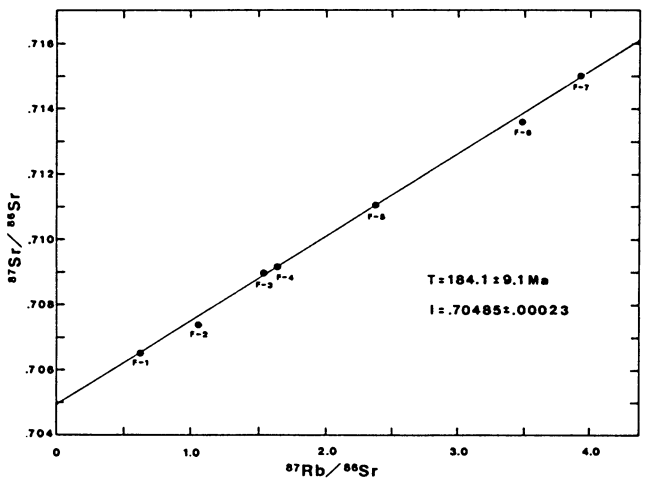

Fig. 28. Rubidium-strontium isochron diagram for the Funatsu mass.

Two samples from the Asuwagawa mass have been analysed for Rb/Sr and $^{87}Sr/^{86}Sr$ ratios (AS-1: 35° 58′ 54″ N, 136° 22′ 18″ E; AS-2: 35° 57′ 12″ N, 136° 21′ 19″ E). In the absence of isotopic ages for the mass, initial $^{87}Sr/^{86}Sr$ ratios have been calculated using an assumed age of 190 Ma. They are relatively low at 0.70471 and 0.70451

For the Utsubo Mass, Shibata et al. (1988) determined a Rb-Sr whole-rock age of 182.5±6.8 Ma and an initial $^{87}Sr/^{86}Sr$ ratio of 0.70544±0.00011 (MSWD=1.0). Arakawa (1988) reported the same results: Rb-Sr whole-rock age of 183.2±9.8 Ma and an initial $^{87}Sr/^{86}Sr$ of 0.70529±0.00005. These whole-rock ages are considered to represent the time of intrusion. One sample (U-06) from the Nariteyama Facies has been analysed for Rb/Sr and $^{87}Sr/^{86}Sr$ ratios. Using the Rb-Sr whole-rock age (183 Ma) and this data, it gives an initial $^{87}Sr/^{86}Sr$ ratio of 0.70512.

Eight whole-rock samples (four samples from the Todamine Facies, three samples from the Besougawa Facies and one sample from the aplitic granite) and two minerals (potassium feldspar and plagioclase of sample Y-6) from the Yatsuo mass have been analysed for Rb/Sr and $^{87}Sr/^{86}Sr$ ratios. These whole-rock data exhibit a restricted range of $^{87}Rb/^{86}Sr$ ratios, 0.14-0.52, being ploted as a scatter in the isochron diagram (Fig. 29). They

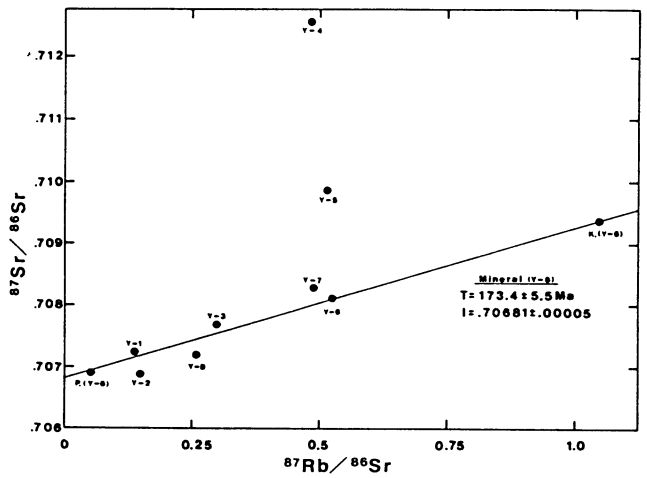

Fig. 29. Rubidium-strontium isochron diagram for the Yatsuo mass. P.=plagioclase; K.=k-feldspar.

define no meaningful isochron. For instance, three whole-rock samples, Y-2, Y-8 and Y-6, yield a statistically acceptable Rb-Sr isochron age of 234.7±26.4 Ma. While, the other three whole-rock samples, Y-1, Y-3 and Y-7, give a Rb-Sr isochron age of 208.7±10.3 Ma. There is no sufficient geological and petrographical evidence to show that the whole-rock age is better. Samples from the acidic facies, especially Y-4 and Y-5, have the higher present-day $^{87}Sr/^{86}Sr$ ratios. A three-point internal isochron for sample Y-6 gives an age of 173.4±5.5 Ma with an initial $^{87}Sr/^{86}Sr$ ratio of 0.70681±0.00005 and an MSWD of 0.1. The mineral isochron age is roughly the same as a three-point internal isochron age of 171.5±3.2 Ma (potassium feldspar, whole-rock and plagioclase) for the Funatsu mass yielded by Shibata and Nozawa (1984). However, the initial $^{87}Sr/^{86}Sr$ ratio is evidently higher than that of the Funatsu mass (0.70625±0.00013). Using an assumed age of 190 Ma and the whole-rock Rb, Sr and $^{87}Sr/^{86}Sr$ data, initial $^{87}Sr/^{86}Sr$ ratios for the mass range from 0.70649 in sample Y-8 of the Todamine Facies to 0.71129 in sample Y-4 of the aplitic granite and come to an average of 0.70753. Such a large range of initial $^{87}Sr/^{86}Sr$ ratios is thought to reflect variation in the composition and age of the magma source materials, which will be in more detail discussed in the later section.

Nine whole-rock samples (two samples from gabbroic rocks, four samples from the Omaki Facies and three samples from the Toga Facies) and one mineral (biotite of sample SO-7) from the Shogawa mass have been analysed for Rb/Sr and $^{87}Sr/^{86}Sr$ ratios. These data also yield a notable scatter in the isochron diagram (Fig. 30). Samples from the Toga Facies, especially SO-1 and SO-11, have higher present-day Sr-isotopic ratios. Whatever age was assumed for these samples, a substantial range of initial $^{87}Sr/^{86}Sr$ ratios is obtained. Sample SO-7 gives an isochron age of 193.9± 15.5 Ma by biotite and whole-rock. Following the fact that four whole-rock samples, SO-18, SO-3, SO-2 and SO-6, are plotted close to the isochron,

it can be pointed out that the biotite age of 194 Ma is closest to the time of the granite emplacement. The hornblende gabbro (sample SO-14), on the other hand, falls well below this line. Initial $^{87}Sr/^{86}Sr$ ratios have been calculated using an assumed age of 190 Ma. These range in value from 0.70629 to 0.71049 with an average value of 0.70782, except for gabbroic rocks. Tonalite SO-3 has the lowest value of 0.70629, whereas adamellite SO-11 has the highest value of 0.71049. The initial $^{87}Sr/^{86}Sr$ ratio (0.70527) of the hornblende gabbro (sample SO-14) is lower than that (0.70640) of the pyroxene gabbro (sample SO-18). The different initial ratios suggest that the pyroxene and the hornblende gabbros were derived from different sources or formed at different ages, indicating that these rocks are not strictly cogenetic.

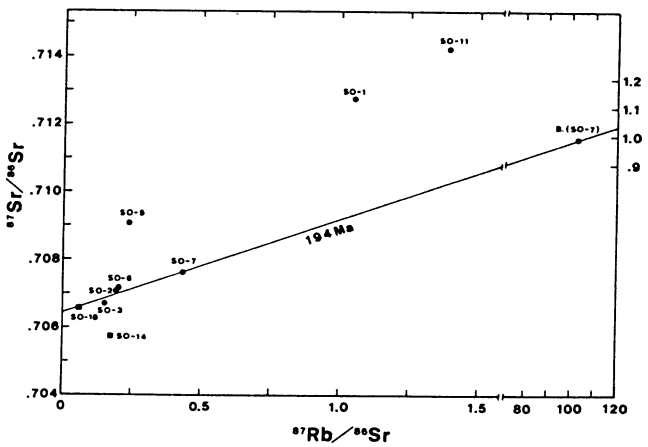

Fig. 30. Rubidium-strontium isochron diagram for the Shogawa mass. Solid circle = granitic rocks; Solid square = gabbroic rocks; B. = biotite.

For the Hodatsusan mass, six whole-rock data (two samples from tonalitic core, one sample from granodioritic mantle and three samples from granitic rim) are scatter in an extreme wide range on the isochron diagram (Fig. 31). Thus, the Rb-Sr whole-rock isochron age can not be defined for the mass. Samples from granitic rim, HO-4, HO-5 and HO-6, have particularly, high present-day Sr-isotopic ratios. Their data form a statistically acceptable Rb-Sr whole-rock isochron giving an age of 269.8±33.5 Ma (MSWD=0.3), which is older than that of the main regional metamorphism in the Hida Terrane (ca. 240 Ma). However, the Hodatsusan mass postdated the metamorphism. Sample HO-4 gives an isochron age of 174.6±15.0 Ma by biotite and whole-rock. Kawano and Ueda (1966) determined 166 and 159 Ma K-Ar ages for biotite separates from slightly altered rocks, which were recalculated using the decay constants by Steiger and Jäger (1977). It is generally expected that the Rb-Sr biotite age agrees closely with the K-Ar biotite age for the same closing temperature at 300℃ (Harrison et al., 1979). The younger K-Ar biotite

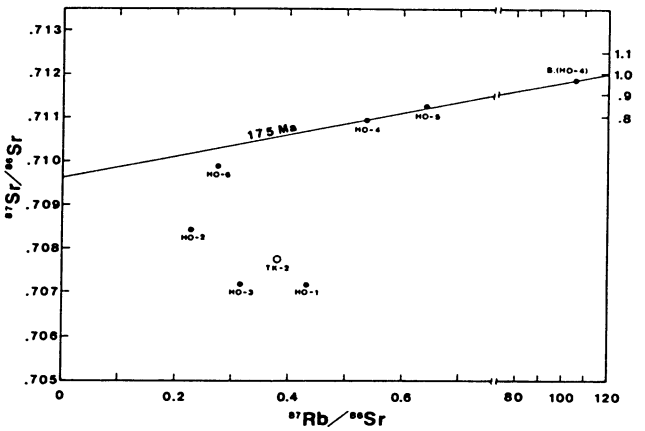

Fig. 31. Rubidium-strontium isochron diagram for the Hodatsusan mass and Togi area. Solid circle = Hodatsusan mass rocks; Open circle = Togi area rock; B. = biotite.

ages presumably present partial resetting during cooling. Using an assumed age of 190 Ma and the whole-rock Rb, Sr and $^{87}Sr/^{86}Sr$ data, initial $^{87}Sr/^{86}Sr$ ratios for the mass range from 0.70599 in sample HO-1 of the tonalitic core to 0.70955 in sample HO-5 of the granitic rim with an average of 0.70806.

One sample was collected from a small mass at the Shishizu coast of the Togi area. (TK-2: 37° 10′ 59″ N, 136° 40′ 44″ E). Kawano and Ueda (1966) reported 184 Ma K-Ar age for biotite separate from biotite tonalite at the Daifukuji area of 3 km to the east of the Togi area. This age was recalculated using the decay constants by Steiger and Jäger (1977). Using an assumed age of 190 Ma and the whole-rock Rb, Sr and $^{87}Sr/^{86}Sr$ data, an initial $^{87}Sr/^{86}Sr$ ratio of 0.70673 is estimated for the mass.

The analyzed Jurassic granites have initial $^{87}Sr/^{86}Sr$ ratios in the range of 0.70451 to 0.71129 (not including gabbroic rocks). Such the variation of the initial $^{87}Sr/^{86}Sr$ ratios appears to be clearly related to the geological position in the Hida Terrane (Fig. 32): The granitic masses of the Outer Plutonic Zone have lower and relatively uniform initial $^{87}Sr/^{86}Sr$ ratios, ranging from 0.70451 to 0.70544, whereas these of the Inner Plutonic Zone have higher initial $^{87}Sr/^{86}Sr$ ratios of 0.70599 to 0.71129. Furthermore, individual masses of the Inner Plutonic Zone show internal variation in initial $^{87}Sr/^{86}Sr$ ratio (Fig. 33). The gabbroic rocks, as well as the granites, also exhibit spatial variation in initial $^{87}Sr/^{86}Sr$ ratio, suggesting that the difference in isotopic composition between the gabbroic rocks of the two zones reflects a fundamental difference in geochemical properties between their source materials.

The overall range of the initial $^{87}Sr/^{86}Sr$ ratios for the Jurassic granites is roughly comparable to that found in magmatic arcs of convergent plate margins. Some magmatic arcs along continental margins that are underlain by older continental crust have higher values of the

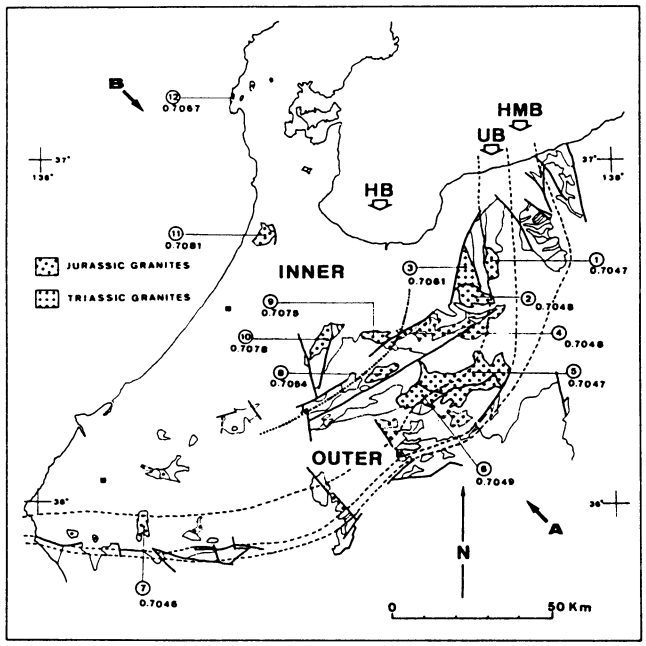

Fig. 32. Diagram showing regional variation of initial $^{87}Sr/^{86}Sr$ ratios of early Mesozoic granitic rocks in the Hida Terrane. HB=Hida Gneiss Belt; UB=Unazuki Belt; HMB=Hida Marginal Belt. For numbers circled see Fig. 1.

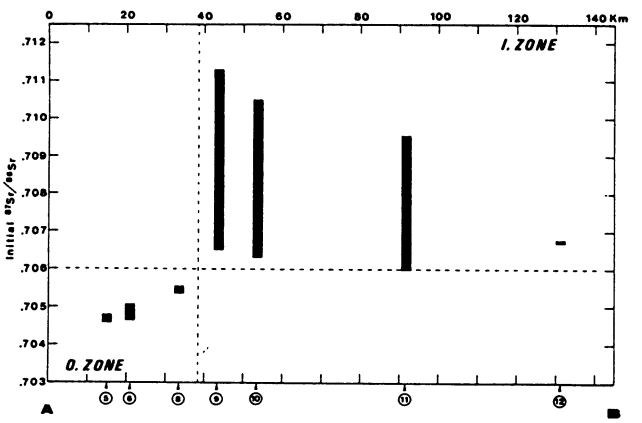

Fig. 33. Diagram showing initial $^{87}Sr/^{86}Sr$ ratios of early Mesozoic granitic rocks vs. distance from Hida Marginal Belt to Hida Gneiss Belt (A-B in Fig. 49). For numbers circled see Fig. 1.

initial $^{87}Sr/^{86}Sr$ ratios ranging to 0.708 (e.g. Hawkesworth, 1982). Initial $^{87}Sr/^{86}Sr$ ratios greater than 0.710 are found in some western North America batholiths such as Pioneer batholith (Arth et al., 1986) and parts of Idaho batholith (Fleck and Criss, 1985) which were emplaced in to the area underlain by Precambrian continental crust.

It may be said from these observations that some granitic magmas in the Inner Plutonic Zone probably were derived from or interacted with significant amounts of crust of the Precambrian age, whereas many granitic magmas in the Outer Plutonic Zone were derived from the less radiogenic crust of Paleozoic or younger age.

2. NEODYMIUM ISOTOPE

Samarium, neodymium and $^{143}Nd/^{144}Nd$ ratios for the Mesozoic granitic rocks investigated in this paper are given in Table 11. Their variation are displayed on the Sm-Nd isochron diagram (Fig. 34) and on the diagram of initial ε Nd vs. ε Sr in Fig. 35.

Present-day $^{143}Nd/^{144}Nd$ ratios for the Jurassic granites exhibit a variation from 0.512043 to 0.512710 and $^{147}Sm/^{144}Nd$ ratios range from 0.0930 to 0.1309. The initial Nd isotope ratios, expressed as ε Nd, have been calculated from the times of their emplacement, and these values range from -9.3 to $+3.3$. Adamellite HO-4 of the Hodatsusan mass has the lowest value of -9.3 for ε Nd, whereas adamellite K-5 of the Kekachidake mass has the highest value of $+3.3$ for ε Nd. The initial ε Nd values show a systematic spatial variation. The Outer Plutonic Zone samples exhibit a small range of $+1.4 < \varepsilon Nd < +3.3$, whereas the Inner Plutonic Zone samples have less radiogenic Nd within $-9.3 < \varepsilon Nd < +1.6$. As shown in Fig. 35, the filed of the former is distinct from that of the latter.

The granites from the Outer Plutonic Zone are essentially uniform in both Nd concentrations (about 16 ppm) and initial $^{143}Nd/^{144}Nd$ ratios (approximately $\varepsilon Nd = +3.1$), except for sample U-06 from the Utsubo mass exposed nearby the Inner Plutonic Zone. These samples, F-3, K-5, O-1 and S-2, are plotted parallel to the isochron of 190 Ma (Fig. 34). Thus, it is said that the Outer Plutonic Zone granites were initially uniform not only in Sr isotopic composition but also in Nd isotopic composition. Such limited variations in ε Nd and ε Sr are significant because they require for the source rocks to have had a reasonably uniform isotopic compositions over a considerable extent (about 150 km), or if the variations are a hybrid, they represent a high degree of homogenization. These rocks have Nd model ages (T_{DM}^{Nd}) of 0.522 to 0.647 Ga (Table 12), which are invariably older than Sr model ages (0.278 to 0.579 Ga).

The granites from the Inner Plutonic Zone exhibit substantial variations in both Nd concentration and initial $^{143}Nd/^{144}Nd$ ratios. Nd concentration ranges from about 16 to 25 ppm, which are higher than that of the Outer Plutonic Zone granites. This is reflected by the presence of abundant sphene and allanite in the Inner Plutonic Zone granites (Table 6).

Calculated initial $^{143}Nd/^{144}Nd$ ratios, ε Nd values, show a large range from approximately $+1.6$ for the Hodatsusan mass tonalite to -9.3 for the Hodatsusan mass adamellite, and the corresponding Nd model ages for these samples range from 0.765 to 1.340 Ga, which are significantly older than those of the Outer Plutonic Zone granites. Especially high silicic rocks (SiO_2 > 68 wt%) have unradiogenic Nd composition with

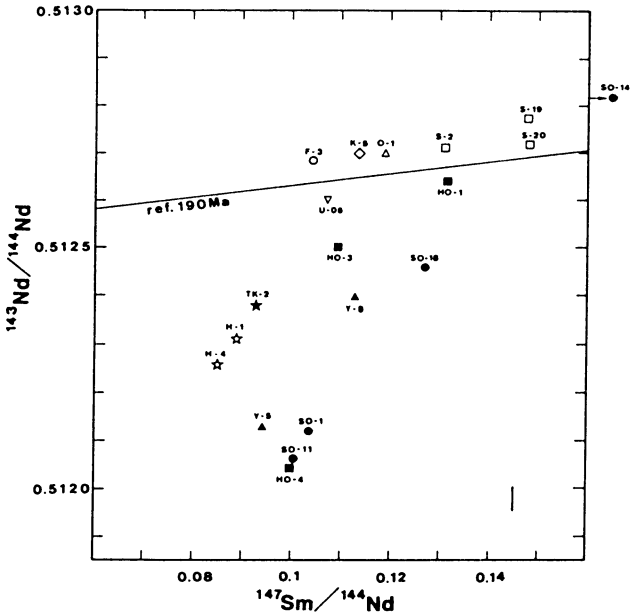

Fig. 34. Samarium-neodymium isochron diagram for the early Mesozoic igneous rocks. Bar in the lower right corner shows average 2σ error. Straight line is the reference isochron of 190 Ma. For symbols see Fig. 35.

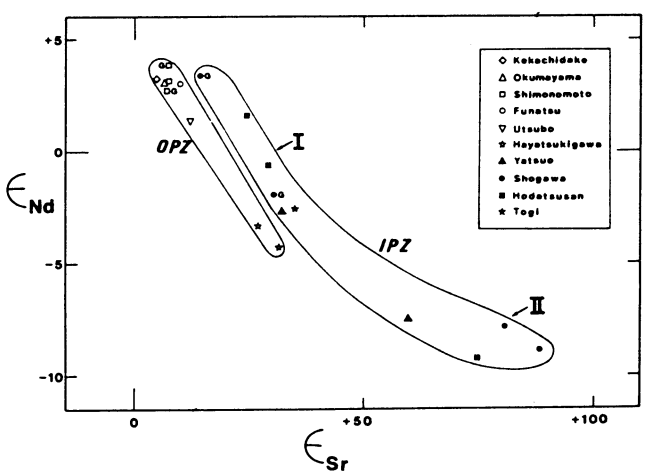

Fig. 35. Initial ϵ Nd and ϵ Sr diagram of the early Mesozoic igneous rocks from the Outer Plutonic Zone (OPZ) and Inner Plutonic Zone (IPZ) of the Hida Terrane. Symbols with "G" represent the gabbroic rocks. Group I (I) and Group II (II) note granitic rocks with different isotopic compositions.

$-9.3 < \epsilon Nd < -7.5$. The lower values of ϵ Nd for the Inner Plutonic Zone granites would reflect a larger component of older or more silicic crustal rocks in their source. This inference is supported by higher initial $^{87}Sr/^{86}Sr$ ratios for these.

For the Hayatsukigawa mass Sm-Nd isotope data were obtained from two samples. They have the lowest $^{147}Sm/^{144}Nd$ ratios (0.0852 and 0.0890) of the early Mesozoic granitic rocks (Fig. 34). Using an assumed age of 220 Ma and these data, initial

Table 12. Summary of model ages (in 10^9 years).

Sample No.	T^{Nd}_{CHUR} [1]	T^{Nd}_{DM} [2]	T^{Sr}_{DM} [3]	T^{Nd}_{DM} [4]
Outer Plutonic Zone				
K-5	-	0.548	0.278	0.700
O-1	-	0.578	0.575	0.739
S-2	-	0.635	0.471	0.821
F-3	-	0.522	0.291	0.660
U-06	0.060	0.647	0.579	0.792
Inner Plutonic Zone				
HO-1	-	0.765	0.754	0.956
HO-3	0.240	0.804	1.076	0.955
Y-8	0.440	0.985	1.329	1.144
TK-2	0.383	0.850	0.990	0.981
Y-5	0.761	1.172	1.021	1.307
HO-4	0.935	1.340	1.133	1.481
SO-1	0.851	1.283	0.689	1.430
SO-11	0.912	1.322	0.591	1.465
Hayatsukigawa Mass				
H-1	0.462	0.902	2.176	1.030
H-4	0.517	0.937	0.680	1.061
Hida gneiss				
B-7	1.147	1.741	-	1.962
14	1.335	1.735	0.683	1.894
15	1.620	1.954	1.147	2.097
16	1.261	1.663	1.725	1.819
17	-	0.591	0.590	0.731
20	-	0.394	0.674	0.565
21	-	0.358	2.022	0.560
Unazuki schist				
23	-	0.540	0.539	0.770
Gray granite				
133-2	1.348	1.793	0.717	1.970

[1] T^{Nd}_{CHUR} is calculated relative to CHUR parameters.
[2] T^{Nd}_{DM} is calculated using the equation of DePaolo (1981a).
[3] Sr model ages are calculated relative to a depleted mantle (Ben Othman et al., 1984).
[4] T^{Nd}_{DM} is calculated assuming a linear evolution of depleted mantle (Goldstein et al., 1984).

ϵ Nd values are determined to be -3.3 and -4.2, which are obviously lower than those of the Outer Plutonic Zone masses (Fig. 35). The rocks have essentially the same initial ϵ Sr values as some samples (HO-3 and Y-8) from Inner Plutonic Zone, but the initial ϵ Nd values of the former are significantly lower than those of the latter (Fig. 35). Nd model ages relative to a depleted mantle (T_{DM}^{Nd}) are 0.902 and 0.937 Ga. The negative initial ϵ Nd values indicate that the granites incorporated significant amount of older continental crust during their formation.

Initial ϵ Nd values ($+3.9$ and $+2.7$) of two gabbroic samples, S-19 and S-20, from the Shimonomoto mass in the Outer Plutonic Zone are roughly the same as their host granitic samples. While two gabbroic rocks, SO-14 and SO-18, from the Shogawa mass in the Inner Plutonic Zone have slightly lower initial ϵ Nd values ($+3.4$ and -1.9) than the gabbroic rocks in the Shimonomoto mass have.

The Sr and Nd isotopic data emphasize the distinction between the Outer Zone masses and the Inner Zone masses and also suggest that the latter and the Hayatsukigawa mass may contain components of the Precambrian crust in their sources.

For the Mesozoic granites, the Sr model ages (Table 12) are roughly younger than or equal to T_{DM}^{Nd}, except for one sample (H-1) from the

Hayatsukigawa mass, indicating that the formation of these rocks were associated with the larger increase of Rb/Sr. This would be expected from partial melting of plagioclase-rich source rocks, or from the crystallization stage including plagioclase fractionation. In contrast, the difference between the Sr and the Nd model ages for the sample H-1 indicates that the formation of this rock participated in the decrease of Rb/Sr. Since the sample H-1 is one of the most non-differentiated rocks in the Hayatsukigawa mass, this would be expected from partial melting of plagioclase-poor source materials.

C. COUNTRY ROCKS

Isotopic analyses of eight samples of the metamorphic rocks in the Hida Gneiss and Unazuki Belts, one sample of the grey granite from the Kubusu-gawa district in the Hida Gneiss Belt and one sample of the granitic cobble in the Hida Marginal Belt have been performed in attempt to estimate the involvement of their country rocks either as source materials or as contaminants for the early Mesozoic granites. Sample locations are shown in Fig. 36, and their isotopic data are presented in Tables 10 and 11.

The Rb-Sr and Sm-Nd data for the country rocks are shown in Figs. 37 and 38, except for the gray granite and granitic cobble. It was not the objective of measurements to accurately date these metamorphic rocks but to characterize them isotopically. The data do not form a linear array, indicating their variable initial ratios and/or their open system behavior during the metamorphism. The metamorphic rocks generally have relatively low Rb content (about 12 to 138 ppm) and high Sr content (about 248 to 1179 ppm) with limited Rb/Sr dispersion (Table 10). The Hida gneisses generally have higher present-day $^{87}Sr/^{86}Sr$ ratios in relatively higher values than the Unazuki schists (sample 23) have. However, Sr-isotopic ratios of samples from the Koshimizu formation (sample 20 and 21) and Makawadani formation (sample 14) are approximately the same as Sr-isotopic ratio of the Unazuki schists. This is consistent with the resemblance in major and trace elements feature between the Unazuki schists and the metapelites of the Koshimizu formation (Table 8). These metamorphic rocks have $^{87}Sr/^{86}Sr$ ratios at the time of the emplacement of Jurassic granitoidos (T=190 Ma) of 0.70489 to 0.71395, which are broadly similar to the ratios obtained by Shibata et al. (1970), Yamaguchi and Yanagi (1970), Arakawa (1984) and Shibata and Nozawa (1986).

These metamorphic rocks exhibit a substantial variation in present-day $^{143}Nd/^{144}Nd$ ratios of 0.511706 to 0.512895 ($\varepsilon Nd = +5.0$ to -18.2). In addition, the Sm/Nd ratios are variable and some what higher than those of the Mesozoic granitic rocks: The metamorphites have a range in $^{147}Sm/^{144}Nd$ of 0.1092 to 0.1479, whereas they typically exhibit uniform $^{147}Sm/^{144}Nd$ ratios of 0.10 to 0.12, (Table 11; Fig. 38).

A pelitic sample from the Unazuki schists (sample 23) has high $^{147}Sm/^{144}Nd$ ratio (0.1479) and initial $^{143}Nd/^{144}Nd$ ratio of 0.512252 ($\varepsilon Nd(T) = +5.5$) at the time of their original sediment deposition (T=300 Ma). The Nd isotope data for two analysed metapelites of the Koshimizu formation (sample 20 and 21) is similar to that for the Unazuki schists, showing relatively high $^{147}Sm/^{144}Nd$ ratios (0.1280 and 0.1423) and present-day $^{143}Nd/^{144}Nd$ ratios of 0.512840 and 0.512895 ($\varepsilon Nd = +3.9$ and $+5.0$). The metapelites have Nd model ages (T_{DM}^{Nd}) of 0.358 to 0.540 Ga (Table 12; Fig. 56), suggesting that they include a substantial component of young mantle-derived volcanic detritus. In contrast, three samples from the Makawadani formation (sample 14, 15 and 16) exhibit lower $^{147}Sm/^{144}Nd$ ratios of 0.1092 to 0.1155 and less radiogenic present-day $^{143}Nd/^{144}Nd$ ratios of 0.511706 to 0.511944 ($\varepsilon Nd = -13.5$ to -18.2), giving Nd model ages (T_{DM}^{Nd}) of 1.663 to 1.954 Ga (Table 12; Fig. 39). Some Sm-Nd isotopic investigations of metamorphosed continental rocks have provided the general impression that, on

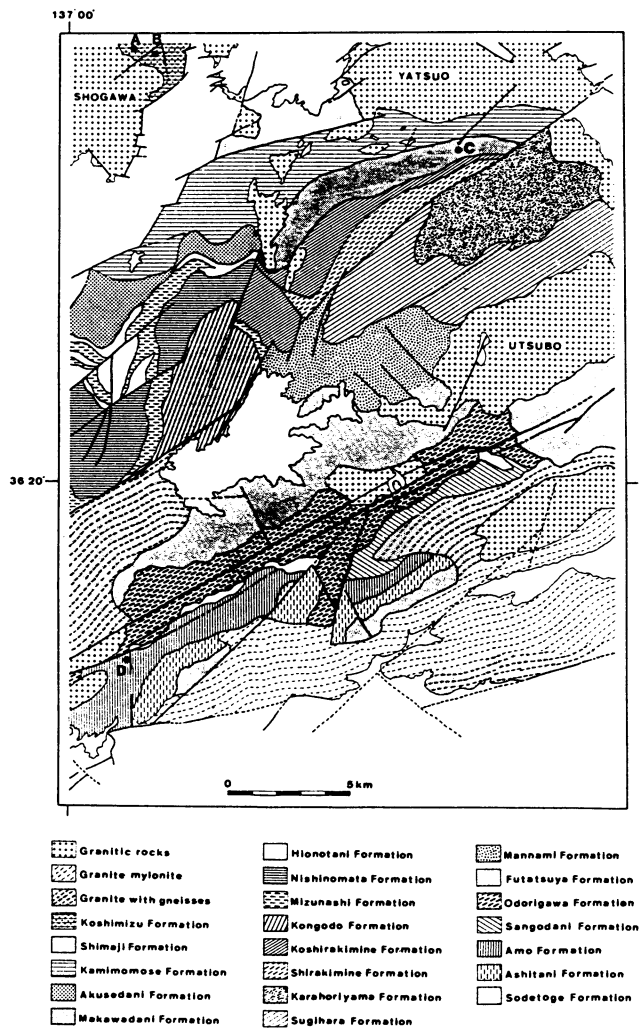

Fig. 36. Diagram showing locations of Hida gneisses and Gray granite samples for isotopic study (Geological map after Nozawa et al., 1975; 1981). A=20; B=21; C=14,15,16,17,133-2; D=B-7.

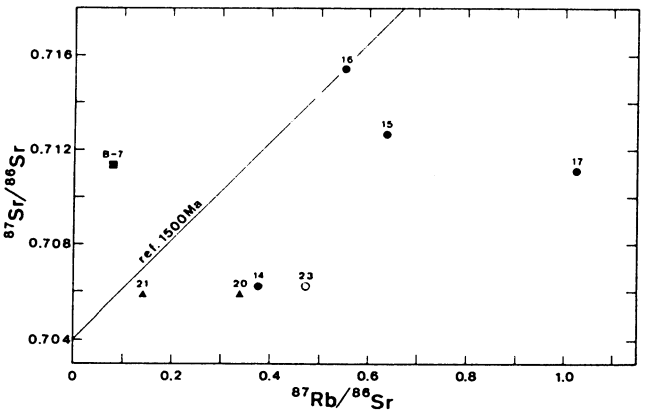

Fig. 37. Rubidium-strontium isochron diagram for the Hida metamorphic rocks. Straight line is the reference isochron of 1500 Ma. For symbols see Fig. 38.

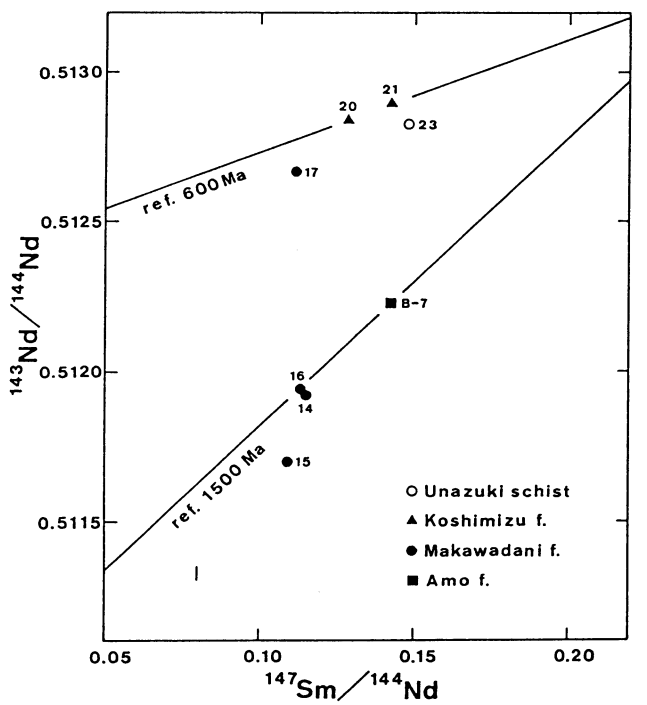

Fig. 38. Samarium-neodymium isochron diagram for the Hida metamorphic rocks. Straight lines are the reference isochron of 600 Ma and 1500 Ma. Bar in the lower left corner shows average 2σ error.

scale larger than that of local mineral equilibria, metamorphic processes had only small effect on Sm-Nd systematics (Hamilton et al., 1978 and 1979). Therefore, the metamorphites with older Nd model ages appear to have been derived from materials that include a significant amount of pre-Phanerozoic continental component. The period around 1.8 Ga has been considered by some authors (DePaolo, 1981a; Nelson and DePaolo, 1985; Patchett and Arndt, 1986) to be an important time of the crust generation in the Northen Hemisphere.

All metamorphic rocks analysed in the present study show a wide variation in ε Nd values (at 190 Ma) of +6.4 to −16.1. Sm-Nd isotopic data for the Hida metamorphic rocks reported by Tanaka and Adachi (1987) and Asano et al., (1988) fall within the range mentioned just above.

As the emplacement age of the gray granite is not known, it is impossible to determine their initial isotopic ratio, the only one gray granite (sample 133-2) was analysed. Using the 190 Ma age, calculated Sr-isotopic ratio and ε Nd value are 0.71101 and −10.5, respectively. This isotopic data fall within the range of that for the Gray granite, reported by Shibata et al. (1989). The Nd model age of 1.793 Ga (Table 12) coincides with the older model ages of the Hida metamorphic rocks (ca. 1.8 Ga).

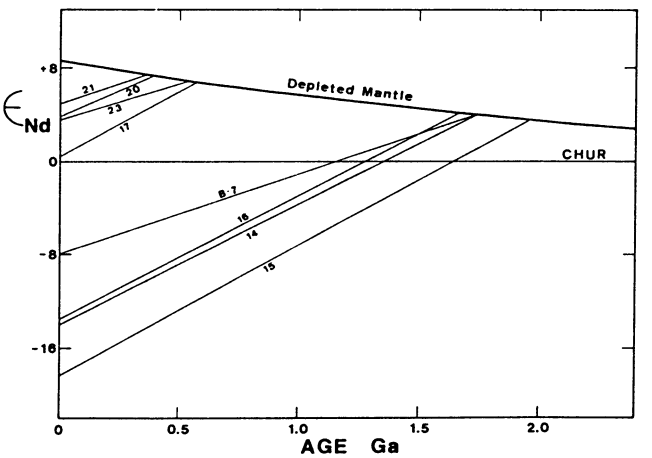

Fig. 39. Neodymium isotopic evolution diagram for the Hida metamorphic rocks. Heavy curve represents isotopic evolution of a depleted mantle (Depaolo, 1981a). Horizontal line shows isotopic evolution of a chondritic uniform reservoir (CHUR). Intersection of the evolution path for samples (straight lines) with the depleted mantle curve defines T_{DM} model age.

VII. DISCUSSION

A. GEOCHRONOLOGY

Isotopic data presented in this study provide farther evidence defining early Jurassic age for the main phase of the magmatism in the Hida Terrane. For individual masses in the Outer Plutonic Zone, Rb-Sr whole-rock isochron data exhibit that first igneous activities began at 201 Ma with the formation of the Shimonomoto mass, were followed by the intrusion of the Kekachidake mass at 196 Ma and of the Funatsu mass at 184 Ma and ended at 183 Ma with the intrusion of the Utsubo mass. Rb-Sr biotite ages range from 183 Ma of the Okumayama mass to 174 Ma of the quartz diorite in the Unazuki district. Thus, Rb-Sr biotite ages date the cooling of these masses to 320±40℃ which appeared at ca. 170 Ma.

For individual masses in the Inner Plutonic Zone were unfortunately determined no Rb-Sr whole-rock isochron ages, since whole-rock data yielded notable scatters in the isochron diagrams. Rb-Sr mineral isochron ages, however, were obtained ranging from 194 Ma of the Shogawa mass to 173 Ma of the Yatsuo mass, which are roughly the same as those of the Outer Plutonic Zone (Fig. 40). K-Ar ages show also no difference between the two zones, except for altered biotite ages from the Hodatsusan mass (166 and 159 Ma). Judging from these mineral ages, it can be said that the Jurassic granitic intrusions in the Inner Plutonic Zone probably occurred concurrently with those in the Outer Plutonic Zone, and so that the early Jurassic magmatic activity continued through ca. 20 Ma.

The Rb-Sr potassium feldspar age of 211 Ma for the Hayatsukigawa mass is older by ca. 40 Ma than that for the Jurassic granitic rocks (172 and 173 Ma for the Funatsu and Yatsuo masses, respectively). Taking into account the difference between the Rb-Sr whole-rock and the potassium feldspar ages (e.g. ca. 10 Ma for the Funatsu mass), the emplacement time of the Hayatsukigawa mass may be estimated to be ca. 220 Ma indicating late Triassic age. If the intrusion age is free from error, it may be pointed out that there is a time gap of ca. 20 Ma between the late Triassic and the early Jurassic igneous activities in the Hida Terrane.

In conclusion, the time for the intrusion, crystallization, uplift and cooling of the Triassic - Jurassic granitic rocks in the Hida Terrane ranges from ca. 220 to ca. 170 Ma and is evidently but only a little younger than the phase (ca. 240 Ma) of the main regional metamorphism in the Hida Terrane. It can be clearly stated that regional metamorphism was followed by the granite intrusions of vast volume with a time gap of ca. 20 Ma and that the granite intrusions occurred episodically during the period of ca. 40 Ma.

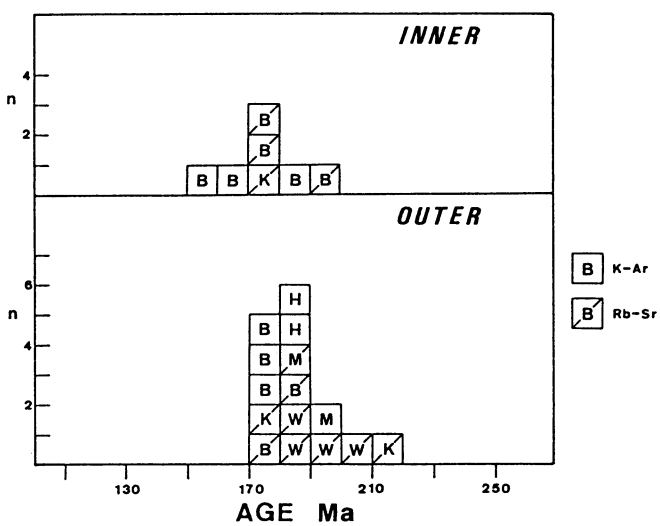

Fig. 40. Histograms showing the variation of isotopic ages for the early Mesozoic granitic rocks. Two younger K-Ar ages (142 and 146 Ma) in the Outer Plutonic Zone are excluded for their alteration or rejuvenation by Cretaceous granites. B=biotite; H=hornblende; M=muscovite; K=k-feldspar; W=whole-rocks. Data are of Kawano and Ueda (1966), Suwa (1966), Hayase and Ishizaka (1968), Shibata and Nozawa (1978;1984), Shibata et al. (1984; 1988), Kato et al. (1989) and this study.

B. PETROGENESIS

1. TRIASSIC GRANITES

The Sm-Nd data of two whole-rock samples from the Triassic Hayatsukigawa mass have ε Nd(T) values of -3.3 and -4.4 at 220 Ma. The negative initial ε Nd values suggest that the formation of its related magma was incorporated by significant amount of an older continental crust. There are several ways to interpret such the isotopic data indicating involvement of old continental crust: 1) the granitic magmas were derived from mantle-origin melts, though they were considerably contaminated by old crust components or mixed with crustal melts (e.g. DePaolo, 1981c; Gray, 1984; Juteau et al., 1986). And 2) the magmas may simply be the products of crustal anatexis without direct involvement of mantle-derived melts (e.g. McCulloch and Chappell, 1982; Domenick et al., 1983; Chen et al., 1985).

The first hypothesis is examined with a simple

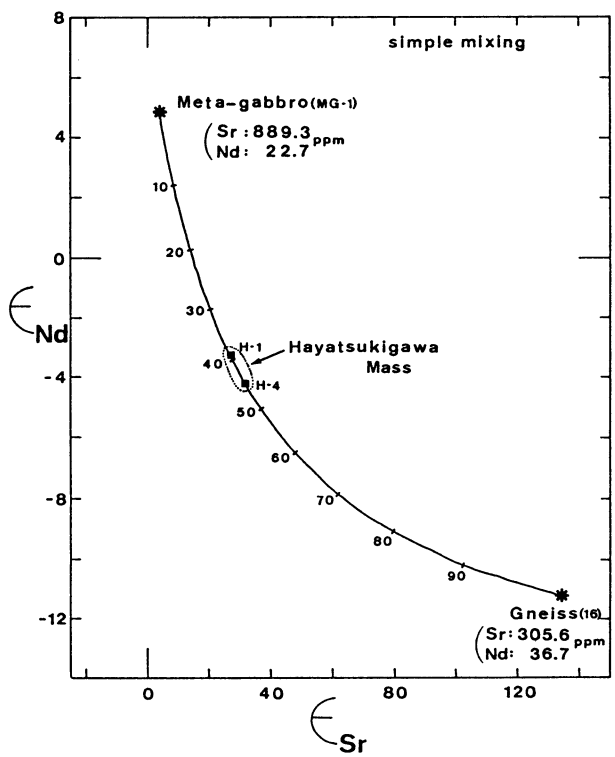

Fig. 41. Mixing curve showing the effect of mixing of a meta-gabbro (MG-1) with high initial ε Nd and low ε Sr values presumably derived from sub-crustal sources and a Hida gneiss (16). Marks show the proportion (%) of the Hida gneiss in a mixture. The curve seems to fit the data of the Hayatsukigawa mass.

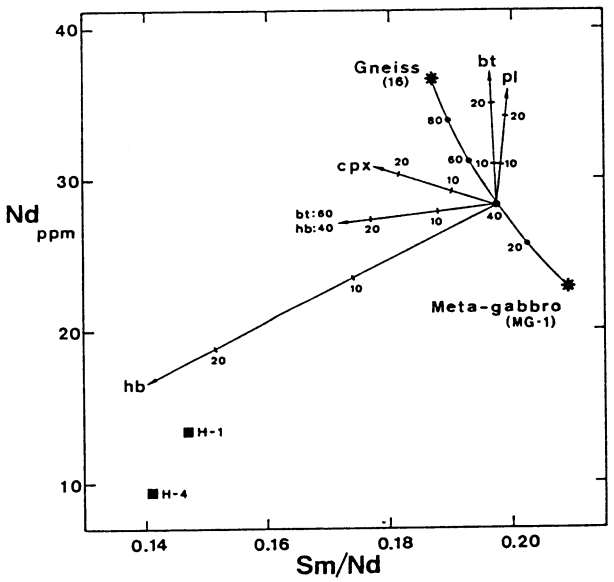

Fig. 42a. Nd vs. Sm/Nd diagram for the Hayatsukigawa mass. Vectors are shown for fractional crystallization of indicated assemblages of minerals. Pl, plagioclase; bt, biotite; cpx, clinopyroxene and hb, hornblende. The percentage of fractional crystallization of the melt to produce corresponding changes in Nd and Sm/Nd is marked along the vectors. The end point of vectors represents 25 % crystallization. The curve shows the effects of mixing the meta-gabbro (MG-1) and the Hida gneiss (16). Marks on the curve show the proportion (%) of the Hida gneiss in a mixture.

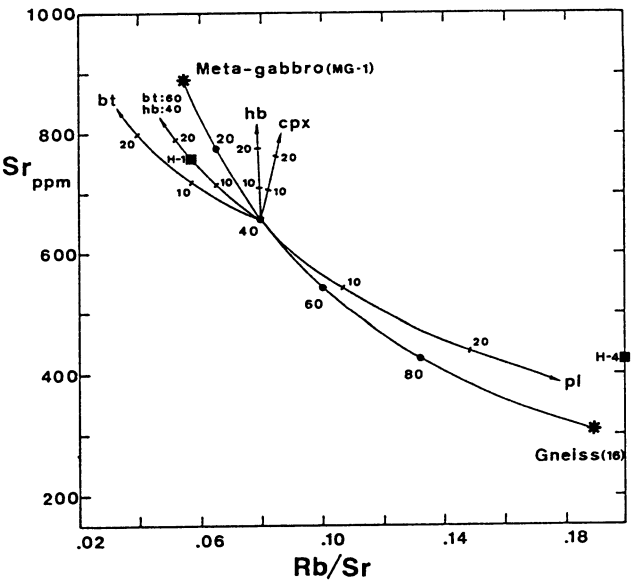

Fig. 42b. Sr vs. Rb/Sr diagram for the Hayatsukigawa mass. For symbols see Fig. 42a. Sample H-1 can be explained by about 15 % crystallization of the assemblage of 60 % biotite and 40 % hornblende. However, Fig. 42a illustrates that the fractional crystallization of the assemblage is unlikely to account for the Nd and Sm contents of the sample H-1.

Table 13. Distribution coefficients used in model calculation.

	Rb	Sr	Sm	Nd
Plagioclase	0.048 (1)	2.84 (1)	0.13 (1)	0.17 (1)
Orthopyroxene	0.022 (2)	0.017(2)	0.074(3)	0.046(3)
Clinopyroxene	0.032 (1)	0.318(1)	0.681(3)	0.427(3)
Hornblende	0.304 (1)	0.241(1)	3.99 (1)	2.80 (1)
Biotite	3.28 (1)	0.12 (1)	0.058(1)	0.044(1)
Magnetite	-	-	0.9 (4)	0.9 (4)
Sphene	-	0.874(5)	102.0 (5)	88.3 (5)
Garnet	0.0085(1)	0.015(1)	2.66 (1)	0.53 (1)

Sources-(1) Arth (1976); (2) Philpotts and Schnetzler (1970); (3) Schnetzler and Philpotts (1970); (4) Henderson (1983); (5) Simmons and Hedge (1978).

two component mixing model. These components would have been a relatively young (~220 Ma) isotopically mantle-like igneous component and an old (Precambrian age) continental crust component. The possible mantle-like component is represented by the meta-gabbro (sample MG-1) in the Unazuki district (Katoh, 1989). He presumed that the gabbro was emplaced during Triassic time based on the field evidence. The initial ε Nd and ε Sr values (+4.9 and +3.3, respectively) are different from those of the typical depleted mantle component (+8.8 and −24.0, respectively, after White et al., 1987). The Nd and Sr contents are 22.7 and 889.3 ppm, respectively. The Hida gneisses, on the other hand, are appropriate for the possible crustal endmember. The isotopic character of this component is represented by the analyses of sample 16 (ε Nd(220 Ma) = −11.2, Nd = 36.7 ppm, ε Sr(220 Ma) = +134.6, Sr = 305.6 ppm) which roughly correspond to the average of the Sr isotopic composition for the Hida gneisses (ε Sr(220 Ma) = ca. +120, Sr = ca. 300 ppm) reported by Shibata et al. (1970), Arakawa (1984), Shibata and Nozawa (1986) and Shibata et al. (1989). The mixing of the meta-gabbro and Hida gneiss components in various proportions can be drawn as a curve for ε Nd vs. ε Sr using standard mixing equations (Faure, 1986), as shown in Fig. 41. The amount of crustal component in the source rocks of the Hayatsukigawa mass must be about 40 % to explain the observed isotopic character of the mass.

Chemical trends produced by fractional crystallization of particular minerals are displayed on diagrams in Fig. 42. The vectors were constructed using the data on distribution coefficients given in Table 13 and the method summarized by Hanson (1978). The mixing line between two end members does not fall near the granitic data on the Nd vs. Sm/Nd plot (Fig. 42a), which could be interpreted that hornblende fractionation during crystallization occurred after mixing or concurrently with mixing processes. However, the Sr vs. Rb/Sr plot (Fig. 42b) suggests that the dominant hornblende fractionation does not adequately explain the granitic data, but biotite or plagioclase are also fractionating phases.

Consequently, it would be said that the first hypothesis involving igneous differentiation can not explain both the geochemical and isotopic data, although only the Nd- and Sr-isotope data for the Hayatsukigawa mass are consistent with the mixing model.

While the second hypothesis appears to be supported not only by the Nd- and Sr-isotope data, but also by the geochemical data, giving a preliminary model for the generation of the Hayatsukigawa mass by derivation from late Proterozoic crustal rocks (ca. 900 Ma in terms of the Nd model ages). The I-type nature of the granitic rocks indicates that the source of the mass is igneous rocks which had not been subject to any significant amount of chemical weathering (White and Chappell, 1977). The mass is characterized by low K_2O/N_2O ratios, Rb and MgO contents and high Sr and Ba contents, showing low Rb/Sr ratios. If it was derived from partial melting of lower crustal materials, the sources must have had even lower Rb/Sr ratios, since the Rb/Sr ratio of a partial melt would normally be greater than that of the residual fraction, especially if plagioclase was a residual phase. It is well established that high grade metamorphic rocks, such as granulites, are depleted in K, Rb, Cs, Th and U relative to other crustal rocks but such rocks have normal or high abundances of Sr and Ba (e.g. Lewis and Spooner, 1973; Tarney and Windley, 1977; Weaver and Tarney, 1983). Therefore, partial melting of a granulite facies igneous lower crust may give rise to such geochemical trends as observed in the Hayatsukigawa mass.

2. JURASSIC GRANITES

(a). The Outer Plutonic Zone Granites.

The initial $^{87}Sr/^{86}Sr$ ratios and ε Nd values of all analysed Jurassic rocks from the Outer Plutonic Zone vary between 0.7045 and 0.7054 and between +3.1 and +1.1, respectively, which display a signature different from a 190 Ma old depleted mantle ($\varepsilon Nd = +8$, $\varepsilon Sr = -18$). The Kekachidake and Funatsu masses are composed of very felsic rocks (SiO_2 > 70 wt%). It hardly seems possible that such large quantities of acidic magmas are brought from an upper mantle (cf. Wyllie, 1983). From their isotopic data and geochemical characteristics, it is difficult to consider that these granites originated directly from a depleted MORB type or an undepleted mantle (mantle peridotite or oceanic-island basalts) except for gabbroic and dioritic rocks.

Any model related to the assimilation of crustal material by mantle-derived magmas is not suitable to explain the regional uniformity of Sr and Nd isotopic compositions in the Outer Plutonic Zone granites. Especially, these compositions of the Funatsu and Shimonomoto masses provide a very important insight in to the mixing model. The masses are emplaced spatially in the close association but at different ages separated by ca. 20 Ma. However, they have essentially identical Sr- and Nd-isotopic signatures to each other (Fig. 35) in spite of their age difference and important geochemical differences. The mixing model would require the process to occur in exactly the same manner at two different times. This seems unlikely to occur. In addition, such a model would be inconsistent with the difference in geochemical data between the two masses. It seems much more reasonable to separately derive the Funatsu and the Shimonomoto mass by melting of the crust with the same or similar provenance age. The difference in geochemistry between them could be ascribed to difference of physical condition (e.g. pressure and temperature) of magma generation or to somewhat different source rock compositions or perhaps to differences in degree of partial melting and fractionation. Thus, it seems likely that both Funatsu and Shimonomoto masses were formed by anatexis of the same or similar crust but at different ages.

The affinity of island-arc or continental margin volcanics with these granitoids is shown in

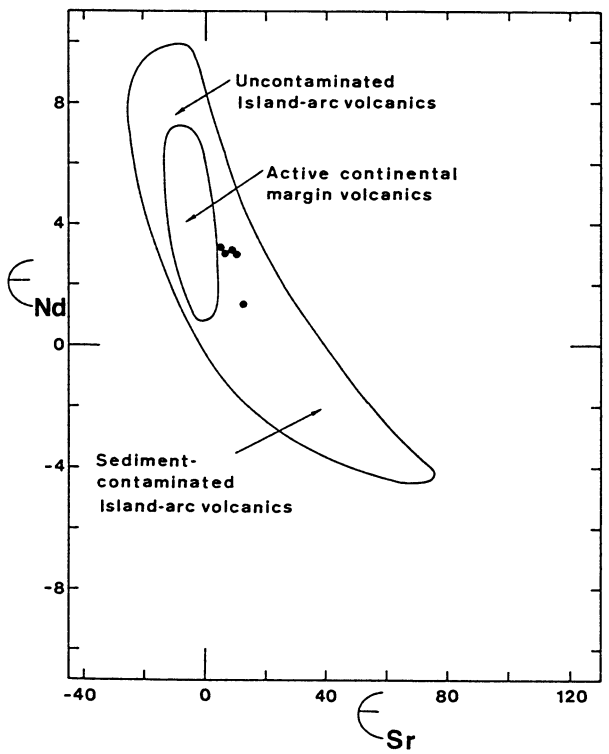

Fig. 43. Initial ε Nd and ε Sr diagram for the Jurassic granitic rocks in the Outer Plutonic Zone (solid circles). The fields for island-arc volcanics and active continental margin volcanics are shown for reference. Data sources are: South Sandwich (Hawkesworth et al., 1977), New Britain (DePaolo and Johnson, 1979; White and Patchett, 1984), Mariana (White and Patchett, 1984), Japan (Nohda and Wasserburg, 1981), Aleutians (McCulloch and Perfit, 1981; Morris and Hart, 1983; White and Patchett, 1984), Lesser Antilles (Hawkesworth et al., 1979; White and Patchett, 1984), Sunda and Banda (Whiteford et al., 1981) and northern and southern volcanic zones in Andes (Hawkesworth et al., 1979; Hickey et al., 1986).

Fig. 43, which is a plot of initial ε Nd and ε Sr. The fields for active continental margin and island-arc volcanic rocks are shown for reference. The region of island-arc volcanic rocks uncontaminated by continental sediments (for instance, arcs such as the Aleutians, the Marianas and New Britain) and island-arc volcanics heavily contaminated by sediments (parts of the Banda and Sunda arcs, for example) are also shown in the figure. Since the South American Andes have been regarded as a typical example of active continental margins (cf. Mitchell and Reading, 1969), the field for active continental margin volcanics is based on Andean data (not including the central volcanic zone data). The central volcanic zone data with higher initial ε Sr and lower ε Nd values require contamination of mantle derived magmas by continental crust (James, 1982). In Fig. 43 all samples from the Outer Plutonic Zone are either in the island-arc volcanics field or near active continental margin volcanics field. The Nd model ages for the Outer Plutonic Zone granites range from 550 to 650 Ma with an average age of ca. 590 Ma and are older than their emplacement ages (Table 12). Thus, it may be concluded that these granitoids were derived from Phanerozoic basic igneous rocks (e.g. basaltic composition) with island-arc or continental margin character.

(b). The Inner Plutonic Zone Granites.

All analysed samples from the Inner Plutonic Zone have a large range of initial $^{87}Sr/^{86}Sr$ ratios from 0.7060 to 0.7113 and variable initial ε Nd values ranging from +1.6 to −9.3. As mentioned above, the Sr contents in the Inner Plutonic Zone granites are of about two times higher than those in the Outer Plutonic Zone granites, except for the Asuwagawa mass. The higher initial $^{87}Sr/^{86}Sr$ ratios and Sr contents of these rocks suggest that they cannot be derived from the Outer Plutonic Zone type magmas. If the igneous rocks of the Inner Plutonic Zone were derived from the Outer Plutonic Zone type magmas, the magmas should have assimilated crustal material with high $^{87}Sr/^{86}Sr$ ratio and Sr content. However, such the crustal material is not observed within the Inner Plutonic Zone (Table 8). If high Sr contents (> 1000 ppm) rocks, some mafic granulites, were common in deeper parts of crust, then their contamination with the Outer Plutonic Zone type magmas at such depth parts should result in Sr enrichment. However, high-Sr mafic granulites commonly have low $^{87}Sr/^{86}Sr$ ratios of 0.704-0.705 (at 190 Ma) (e.g. Rogers and Hawkesworth, 1982; Cohen et al., 1984; Ruiz et al., 1988), showing that it could not cause the initial $^{87}Sr/^{86}Sr$ ratios of ca. 0.706. In the case of the assimilation of high Sr contents crust or of mixing with high Sr contents magmas, moreover, there is a possibility that plagioclase with reverse zoning of Sr is found in the granitic rocks. The Sr zoning trends of plagioclase from the Hodatsusan mass show normal pattern (Fig. 14) and so may be explained in terms of fractional crystallization (cf. Michael, 1984).

Consequently, it has to be assumed that the igneous rocks in the Inner Plutonic Zone is independent in origin on these in the Outer Plutonic Zone. This assumption is in accordance with the Nd- and Sr-isotopic relationships mentioned above (Fig. 35).

Furthermore, individual masses show considerably internal variations of initial $^{87}Sr/^{86}Sr$ ratios and ε Nd values (Figs. 35, 44). Fractional crystallization can account for the variation of major and trace elements in these masses but dose not seem to adequately to explain such the isotopic variations. Variation in initial $^{87}Sr/^{86}Sr$ ratio may be induced by ^{87}Rb decay in slowly cooled granitic magma, whose cooling continued during the period of ca. 20 Ma, (e.g. Clarke and Halliday, 1980; McCarthy and Cawthorn, 1980), whereas it is impossible to account for the variation of initial ε Nd value by ^{147}Sm decay in such a magma (commonly, the ε Nd value will decrease by only 0.2 during the period of 20 Ma). The granitic rocks can be divided into two groups, Group I and Group II, on the basis of their initial $^{87}Sr/^{86}Sr$ ratios and ε Nd values: The Group I rocks have initial $^{87}Sr/^{86}Sr$ ratios of less than 0.708 and ε Nd values of greater than −3 (Fig. 35). Their SiO_2 contents are less than 69 wt% (Fig. 44). While the Group II rocks have initial $^{87}Sr/^{86}Sr$ ratios of greater than 0.708 and ε Nd values of less than −3 (Fig. 35). Their SiO_2 contents are greater than 64 wt% (Fig. 44). As for individual granitic masses, the Group II rocks are slightly younger in intrusion age than the Group I ones as based on the field evidence.

The source material of the Group I is inferred to have been enriched in ^{87}Sr than that of the granites in the Outer Plutonic Zone (Fig. 35). The incorporation of basalts of ancient oceanic crust altered by seawater and of their associated metasediments into the subcontinental mantle, which may occur in a subduction zone, may be related to the enrichment of ^{87}Sr at source

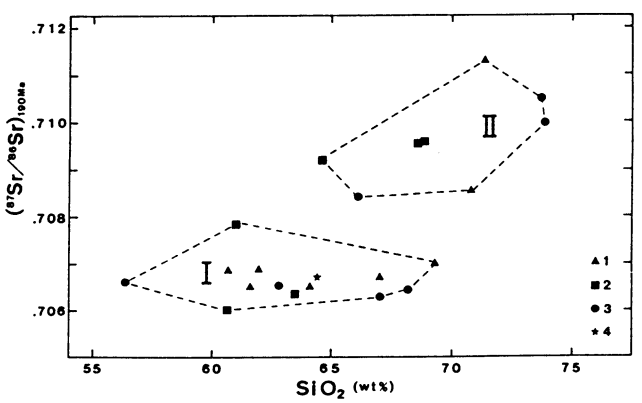

Fig. 44. Plot of initial $^{87}Sr/^{86}Sr$ vs. SiO_2 content of the Group I (I) and Group II (II) rocks from the Inner Plutonic Zone. 1, Yatsuo mass; 2, Hodatsusan mass; 3, Shogawa mass; 4, Togi area.

materials. Since seawater has a relatively high Sr concentration of about 8 ppm whereas its Nd concentration is only 2.6×10^{-6} ppm (Faure, 1986), the interaction of seawater with volcanic rocks on the ocean floor alters their $^{87}Sr/^{86}Sr$ much more effectively than their $^{143}Nd/^{144}Nd$ ratios.

While the origin of the Group II rocks could be interpreted in two ways: (1) the rocks with the lower initial $^{87}Sr/^{86}Sr$ ratios (Group I) approximate the compositions of the original parent magmas, and the contamination of the parent magmas by crustal materials, which may occur as the magmas rise through the crust, causes the higher initial $^{87}Sr/^{86}Sr$ ratios (Group II), and (2) the Group II rocks were primarily derived from the Precambrian crust.

For the Yatsuo mass, the Group II rocks (two samples from the adamellite in the Besougawa facies and aplitic rock) are plotted in higher Sr content field in comparison with a trend of the Group I rocks (nine samples from the Todamine and Besougawa Facies), as shown in Fig. 45. Thus, the Group II rocks in the Yatsuo mass with higher initial $^{87}Sr/^{86}Sr$ ratios and Sr content are hardly explained by the contamination model as mentioned above.

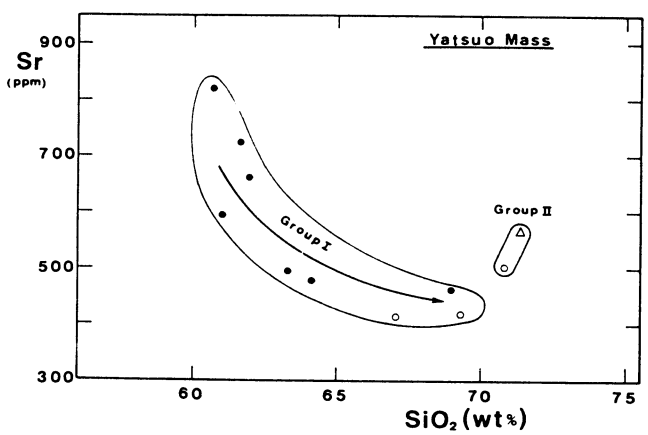

Fig. 45. Sr vs. SiO_2 diagram for the Yatsuo mass. Solid circles, Todamine Facies. Open circles, Besougawa Facies. Open triangle, aplitic granite.

For the Hodatsusan mass, plagioclase in the Group II rocks (three samples from the granitic rim) is more calcic than that in the Group I (two samples from the tonalitic core and granodioritic mantle) (Fig. 46). The compositional variation of the plagioclase may be hardly explained in terms of magmatic crystallization with contamination, implying that the original parent magma of the Group II rocks is substantially different from that of the Group I in the Hodatsusan mass.

For the Shogawa mass, the Group I rocks are composed of the Omaki Facies and the medium-grained granodiorite and adamellite in the Toga Facies, while the Group II rocks consist only of the fine-grained adamellite in the Toga Facies at

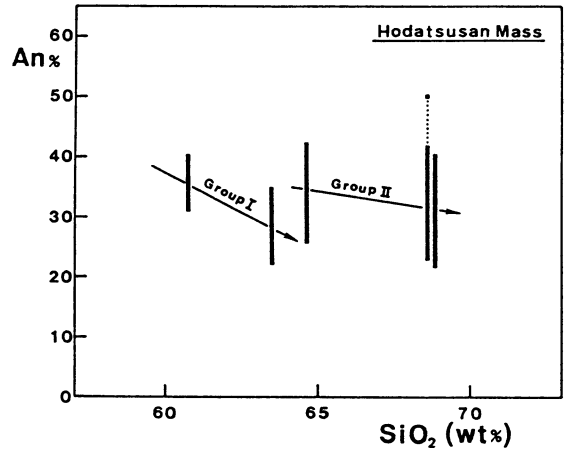

Fig. 46. Diagram showing anorthite content of plagioclase vs. SiO_2 content of host rock for the Hodatsusan mass.

the western part of the mass. The mineralogical and petrochemical differences between the Group I and the Group II rocks in the Toga Facies are uncertain.

The contamination (assimilation) of country rock during emplacement may provide a mechanism to explain isotopic data of the Group II rocks in the Shogawa mass, since the Hida gneisses have relatively higher $^{87}Sr/^{86}Sr$ ratios (T=190 Ma) of 0.7040 to 0.7130 and lower ε Nd values of of +6.3 to −16.1 than the Group II rocks have. If the contamination hypothesis is available for the origin of the Group II rocks in the Shogawa mass, a question remains as to how much of the country rocks were digested by the Group I magma? Assuming that the initial magma is chemically comparable with the hornblende gabbro (sample SO-14: Sr=750 ppm, ε Sr=+14, Nd=7.2 ppm, ε Nd=+3.4) in the Omaki Facies, which can be considered to be representative of the Group I primitive magma, mixing curves for the gabbro (sample SO-14) and the Hida gneisses (sample 16 and B-7) do not pass through isotopic data of the Group I rocks (Fig. 47). Whereas a mixing model between the hornblende gabbro (sample SO-14) and the mixed Hida gneisses (sample 16 (50 %) plus B-7 (50 %)) is also shown in Fig. 47. The mixing model has a hyperbolic form which shows roughly agreement with the isotopic data of the Group II rocks. Although the two-component mixing model satisfies the isotopic constraints, the large proportion (over 80 % in some sample of Group II) of the country rocks estimated by this model is not supported by field evidence for the Toga Facies (see the section III). Even if the initial magma is the pyroxene gabbro (sample SO-18: Sr=780 ppm, ε Sr=+30, Nd=17.9 ppm, ε Nd=−1.9), the large proportion (over 70 % in some sample of Group II) of the country rocks such as the mixed Hida gneisses (sample 16 (60 %) plus B-7 (40 %)) (Fig. 47) necessitates to explain the isotopic data of the Group II rocks.

There are some above mentioned problems posed by the two-component mixing model. Therefore, the

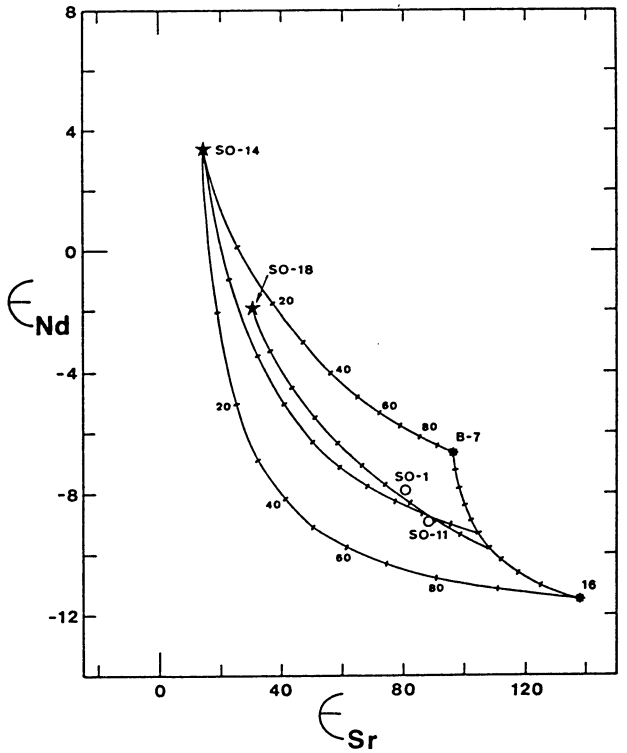

Fig. 47. Initial εNd vs. εSr diagram for the Shogawa mass and simple mixing model curves. The curves with solid star show the effect of mixing the gabbroic rocks (SO-18; SO-14) and the Hida gneisses (16; B-7; mixtures). Marks on the curves show the proportion (%) of the Hida gneiss in a mixture. The curves connecting asterisks show the effect of mixing the Hida gneisses (sample 16 and B-7).

author now considers the assimilation-fractional crystallization (AFC) model. Several authors (Bowen, 1928; Taylor, 1980; Depaolo, 1981b) have stressed that simple mixtures may not be appropriate for contamination of magmas. Since heat required for assimilation can be provided by the laten heat of crystallization of the magma, the chemical and isotopic characters of the resulting contaminated magma must be controlled by simultaneous fractional crystallization and assimilation. The Group II data on Fig. 44 show an excellent positive correlation between the initial $^{87}Sr/^{86}Sr$ ratio and SiO_2 content. Such a relation can be interpreted in terms of crustal contamination of a basic magma with low initial $^{87}Sr/^{86}Sr$ ratio during fractional crystallization (AFC), or magma mixing between a basic magma with low initial $^{87}Sr/^{86}Sr$ ratio and an acidic magma with high initial $^{87}Sr/^{86}Sr$ ratio.

DePaolo (1981b) presented equations to such assimilation and fractional crystallization processes: Considering a magma body of mass Mm which is assimilating wall rock at a rate Ma (mass/unit time) and crystallizing with a rate Mc at which fractionating phases are being effectively separated from the magma, the concentration of the element (Sr or Nd) in the magma (Cm) will be written (Ma≠Mc):

$$Cm/Cm^{\circ}=F^{-z}+(r/(r-1))(Ca/ZCm^{\circ})(1-F^{-z})$$

with:

$$Z=(r+D-1)/(r-1),\quad F=Mm/Mm^{\circ}$$

where Cm° is the original concentration of element in the magma, Ca is the concentration of the element in the assimilated wall rock, D is the bulk solid/liquid partition coefficient for the element between the fractionating crystalline phases and the magma, Mm° is initial mass of magma and r is the ratio Ma/Mc. The isotopic ratio ($^{87}Sr/^{86}Sr$, $^{147}Nd/^{144}Nd$, εSr, εNd) of the magma (εm) can be written:

$$(\varepsilon m-\varepsilon m^{\circ})/(\varepsilon a-\varepsilon m^{\circ})=1-(Cm^{\circ}/Cm)F^{-z}$$

where εm° = isotopic ratio in the original magma and εa = isotopic ratio in the wall rock.

The lack of data on the distribution coefficient between bulk solid and melts for strontium (D_{Sr}) and neodymium (D_{Nd}) severely restricts the application of DePaolo's equations. In order to estimate D_{Sr} and D_{Nd}, taking textural observations into consideration, therefore, fractionating phases and their proportions were decided using major element modelling by least-squares methods (cf. Le Maitre, 1981). The composition of fractionating minerals was determined by microprobe analysis for the pyroxene gabbro and quartz diorite (Tables 1, 2, 3, 4 and 5). The program also calculates the sum of the squares of the residuals (ΣR^2), its low value indicating a good fit.

A summary of the calculations for four models is given in Table 14. For models 1 and 2 the "parent" magma compositions chosen are the sample SO-6 from diorite of the Omaki Facies and the residual liquids are the sample SO-7 from adamellite of the Toga Facies. The two models are different from each other, because the model 1 is free from pyroxenes unlike the case of the model 2. Whereas, for models 3 and 4, the "parent" magma compositions chosen are the sample SO-18 from two pyroxene gabbro of the Omaki Facies. As the samples, SO-6, SO-7 and SO-18, are plotted close to the isochron of 194 Ma (Fig, 30), the major elements variation can be roughly explained from the fractional crystallization. The model 2 has the lowest value of ΣR^2, and, based on the calculated proportion in the fractionating solids, the D_{Sr} and D_{Nd} are determined to be 1.59 and 2.03, respectively.

Taylor (1980) has calculated that the assimilation of 1 g of country rock (specific heat = 0.25 cal/g℃ plus heat of dissolution = 75 cal/g) initially at 150℃ into a magma at 1150℃ is thermally balanced by crystallization of 3.25 g of crystals having an aggregate latent heat of 100 cal/g. He estimated an upper limit value of r (mass assimilated = r × mass crystallized), therefore, to be about 0.3(≒1/3.25). This calculation, however, is for cold country rock and hot magma. An analogous calculation for country rock, around

Table 14. Major element modelling.

Model	Initial magma	Fractionating phases *							Residual magma	Σ R²
		Opx	Cpx	Pl	Hb	Bt	Mt	Sph		
1	SO-6	-	-	45.6	47.3	7.2	-	-	SO-7 39.6%	0.254
2	SO-6	9.9	3.6	52.8	24.1	7.2	0.9	1.4	SO-7 34.8%	0.017
3	SO-18	-	-	53.2	40.1	4.9	1.4	0.4	SO-7 16.4%	0.906
4	SO-18	14.5	7.5	65.7	-	4.9	4.3	3.1	SO-7 8.1%	0.446

* Recalculated to 100%; abbreviations, Opx = orthopyroxene, Cpx = clinopyroxene, Pl = plagioclase, Hb = hornblende, Bt = biotite, Mt = magnetite, Sph = sphene.

middle continental crust, at 300℃ (Wyllie, 1983) and for magma at 900℃ (temperature estimates based on two-pyroxene pairs in the gabbro, sample SO-18, see the section IV) would result in an upper limit r of ca. 0.5(≒1/2.25).

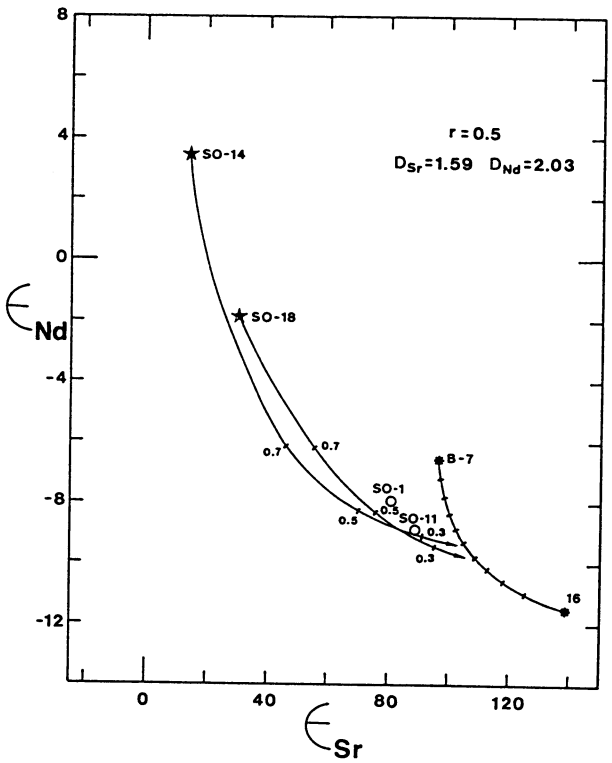

Fig. 48. Initial ε Nd vs. ε Sr plot illustrating assimilation fractional crystallization (AFC) evolution of primary magmas with isotopic composition similar to gabbroic rocks (SO-18; SO-14) towards isotopic compositions of the Group II rocks in the Shogawa mass (open circles). For the AFC calculations was used a fractionating assemblage of model 2 in Table 14 which yielded bulk crystal-liquid distribution coefficients of 2.03 for Nd (D_{Nd}) and 1.59 for Sr (D_{Sr}). The two curves show evolution under "r" (rate of assimilation/rate of fractionation) value of 0.5. The assimilants are the same as those in Fig. 47. The numbers along the AFC curves represent the relative amount of magma remaining.

Using these bulk distribution coefficients and the r value, the AFC model (Fig. 48) might explain the isotopic data of the Group II rocks. The initial magma and contaminant components are identical to those for the simple mixing model as mentioned above. However, this model is not supported by Fig. 49, where initial ε Nd values are plotted against Nd contents. From this diagram, it can be said that the AFC model is inadequate to explain the high Nd contents of the Group II rocks.

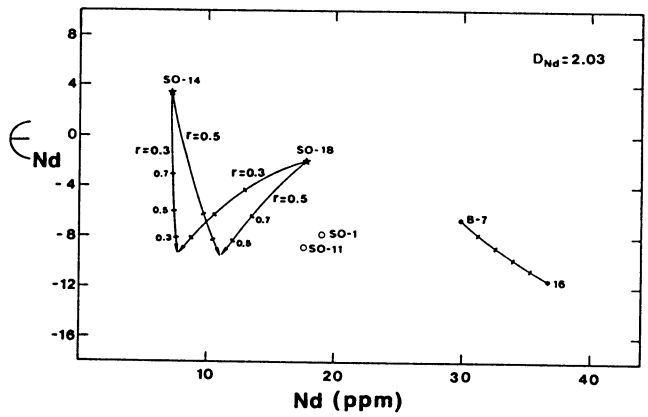

Fig. 49. Initial ε Nd vs. Nd concentration diagram for the Shogawa mass and AFC model curves. The curves show evolution under "r" values of 0.5 and 0.3. The assimilants are the same as those in Fig. 47. The numbers along the AFC curves represent the relative amount of magma remaining. The Group II rocks data (open circles) are apart from these curves.

From the geological, mineralogical and petrochemical considerations on the individual granitic masses, therefore, the distinction between the Group I and the Group II rocks may be attributable to the difference between of the primitive source materials. The Group II rocks with higher initial $^{87}Sr/^{86}Sr$ ratios and lower ε Nd values appear to have primarily been derived from the Precambrian continental basement. Available Hida gneiss Nd model ages (Table 12; Fig. 39) suggest that the formation age (T_{CF}) of the basement source for the Group II rocks is early Proterozoic in age (ca. 1.8 Ga). If this crust formation age is valid, the Sm/Nd ratio in the source material can be estimated by the next equation:

$$Sm/Nd_{SOURCE} = (Sm/Nd)_{CHUR} \times \left[1 + \frac{\varepsilon Nd(Tm) - \varepsilon Nd(T_{CF})}{Q_{ND}(T_{CF} - Tm)}\right]$$

where Sm/Nd_{CHUR}=0.325 (by weight) and Tm is the age of formation of the granite. Using an average value of ε Nd(Tm) of -8.38 and Tm=0.19 Ga, it is calculated that Sm/Nd_{SOURCE} ($^{147}Sm/^{144}Nd$)=0.226 (0.137) (Fig. 50). The calculated Sm/Nd ratio in the source material corresponds to that in the

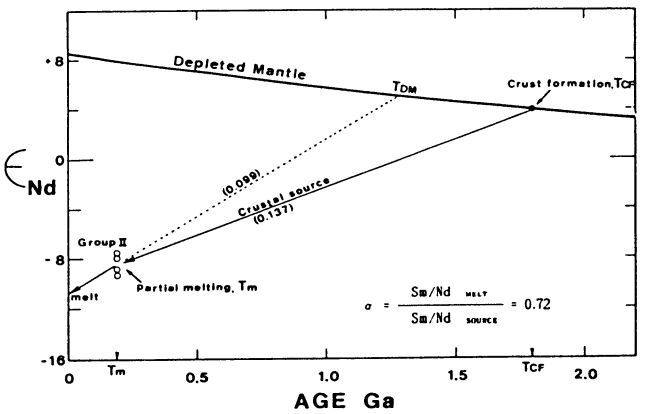

Fig. 50. Neodymium isotopic evolution diagram for the Group II rocks in the Inner Plutonic Zone. Heavy curve represents isotopic evolution of a depleted mantle (Depaolo, 1981a). Solid line connecting the T_{CF} and Tm represents isotopic evolution of crustal source derived from the mantle during an event at time T_{CF}. Solid line connecting the Tm and the present shows isotopic evolution of material produced at time Tm by partial melting of crust. Model ages (T_{DM}) of material (Group II rocks) produced at Tm are given by the intersection of the dotted line and the mantle evolution curve. Numbers in parentheses represent $^{147}Sm/^{144}Nd$ ratio.

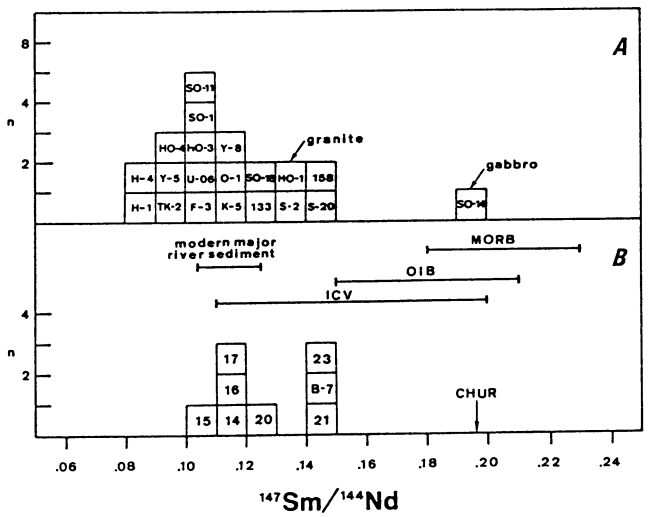

Fig. 51. Histograms showing $^{147}Sm/^{144}Nd$ ratios of igneous rocks (A) and metamorphic rocks (B) in the Hida Terrane. The ranges of OIB (ocean island basalt), MORB (mid-ocean ridge basalt), ICV (island arc and continental margin volcanics) and modern river sediment are shown for reference. Data sources are: OIB (O'Nions et al., 1977; White and Hofmann, 1982), MORB (Cohen et al., 1980; Cohen and O'Nions, 1982), ICV (Hawkesworth et al., 1977, 1979; DePaolo and Johnson, 1979; Nohda and Wasserburg, 1981; McCulloch and Perfit, 1981; Whiteford et al., 1981; Morris and Hart, 1983; White and Patchett, 1984; Hickey et al., 1986) and modern river sediment (Goldstein et al., 1984).

basaltic or andestic rocks generated in island-arc or active continental margin environments, but not to that in continental material sediments, oceanic basalts (MORB and OIB) and Hida gneisses with older Nd model ages (Fig. 51).

The Sm/Nd fractionation (α) that occurs during the generation of the the Group II magmas by melting of a crustal source is therefore:

$$\alpha = \frac{Sm/Nd_{ROCK}}{Sm/Nd_{SOURCE}} = 0.72$$

Such substantial Sm/Nd fractionation would be consistent with the Sm/Nd ratios for rocks generated by partial melting leaving a hornblende and clinopyroxene-bearing residue, which we reevaluated by batch partial melting calculations carried out using the equation presented by Allègre and Minster (1978). The concentration C_L^i of a trace element i in a magma is given by:

$$C_L^i = \frac{C_o^i}{D^i + F(1-D^i)}$$

where C_o^i = concentration of element i in the initial solid, F = weight proportion of melted material = degree of partial melting and D^i = bulk distribution coefficient for the residual solid (at the moment when the melt is removed from the system). A partly molten rock can be mobilized to become a magma when it has the critical melt fraction. The critical melt fraction in rocks containing granitic melt has been evaluated between 30 and 50 % (Wickham, 1987). Thus, if the magmas parental to the Group II rocks were produced by 30 % batch melting and if the residual mineral assemblage consisted of 45 % hornblende, 30 % plagioclase and 25 % clinopyroxene (amphibolitic assemblage), then $\alpha = 0.72$ is calculated. However, a 30 % partial melting of granulitic assemblage (residue: 40 % plagioclase and 40 % clinopyroxene, $\alpha = 0.85$) and eclogitic assemblage (residue: 60 % clinopyroxene, 30 % garnet and 10 % hornblende, $\alpha = 0.57$) rocks would hardly satisfy the Sm/Nd fractionation.

According to Green and Ringwood (1968), the conditions for producing granulitic residue by partial melting of a basalt are of relatively shallow depth and dry condition, while the conditions for producing amphibolitic residue are of relatively shallow depth and wet condition (Helz, 1976).

Based on field evidence and petrochemical and isotopic characteristics, many workers (Suzuki, 1977; Sohma, 1979; Shibata et al, 1989) have considered that the gray granites formed by melting of the Hida gneisses or of its equivalent at depth. As shown in Fig. 52, the $CaO-Na_2O-K_2O$ field of the gray granites is apparently different from that of the Group II rocks. And a Nd model age of the gray granite (sample 133-2) is older than that of the Group II rocks (Table 12). These evidences imply that the source material of the

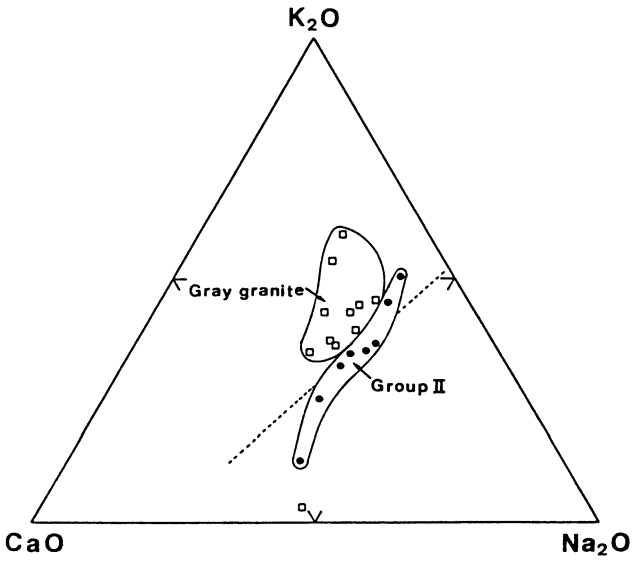

Fig. 52. CaO-Na_2O-K_2O diagram for the Group II rocks (solid circles) and Gray granites (open squares). Dotted line is the average composition of the Japanese granitoids by Aramaki et al. (1972). Data for Gray granites are from Kano (1974) and this study (Table 8)

Group II rocks is different from the Hida gneisses. This inference is in accordance with the consideration about the calculated Sm/Nd ratio for the source material.

The Group II rocks are characterized by a deficiency in basic inclusions and by plagioclase with high-calcic core (An_{60}-An_{50}), respectively (see the sections III and IV). Recently, many authors have considered that mafic enclaves (basic inclusions) found within calc-alkaline batholiths are a product of magma mixing during which more mafic magmas were quenched against the silicic host (e.g. Eichelberger, 1980; Whitney, 1988). According to their opinion, the calcic core may not be refractory xenocrysts derived from the basic magmas but from the source material.

In summary, the Group II rocks are thought to have been originated from a basic or intermediate igneous material extracted from a depleted mantle source at about 1.8 Ga, leaving a hornblende-bearing residue. The presence of xenocrystic calcic plagioclase also prefers to an intermediate igneous source for the Group II granitic magmas.

C. TECTONIC MODEL

Numerous studies on the geochemical characteristics of intermediate-acid intrusive rocks from various tectonic environments have indicated that their major and trace elements may be used as discriminants for understanding tectonics related to their generation (e.g. Petro et al., 1979; Pearce et al., 1984; Batchelor and Bowden, 1985). In Batchelor and Bowden's (1985) diagram (Fig. 53), the Jurassic granite samples mainly fall in the pre-plate collision (destructive plate margin) field, while the Triassic Hayatsukigawa

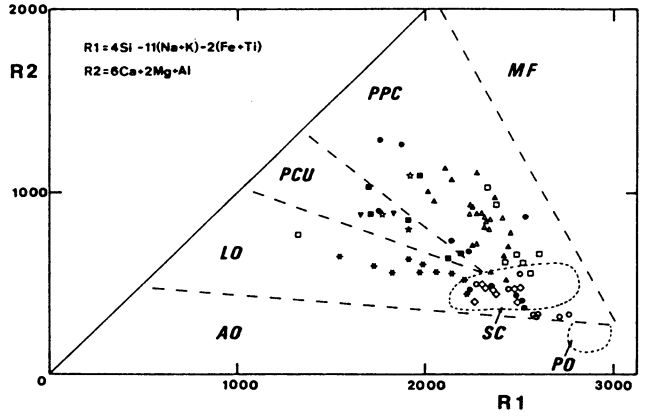

Fig. 53. R1-R2 diagram after Batchelor and Bowden (1985) for the early Mesozoic granitic rocks. Field abbreviations: MF=Mantle fractionates, PPC=Pre-plate collision, PCU=Post collision uplift, LO=Late-orogenic, AO=Anorogenic, SC=Syn-collision, and PO=Post orogenic. For symbols see Fig. 24.

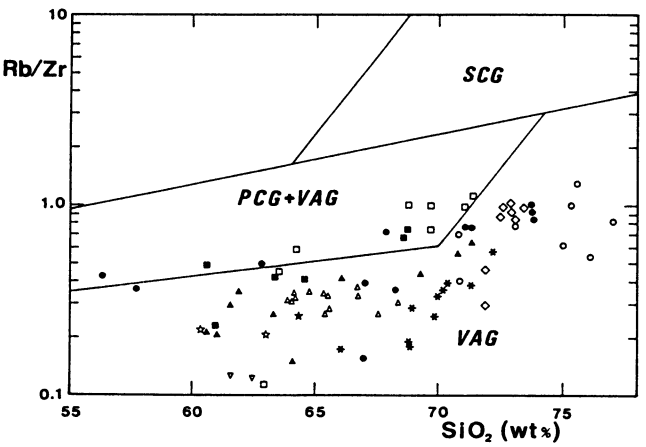

Fig. 54. Rb/Zr vs. SiO_2 diagram after Harris et al. (1986) for the early Mesozoic granitic rocks. Field abbreviations: SCG=Syn-collision granites, PCG=Post-collision granites, and VAG=Volcanic arc granites. For symbols see Fig. 24.

mass samples fall in the Late orogenic field. In this diagram the overlap around the Syn-collision filed is inevitable since all granitoids evolve towards minimum melting compositions (Tuttle and Bowen, 1958). In the Rb/Zr versus SiO_2 diagram (Fig. 54) which has been proposed by Harris et al. (1986), the early Mesozoic granitic rocks are plotted predominantly within the Volcanic arc granites (Pre-plate collision) field with some overlap into the Post collision granites filed. From the chemical criteria it may be roughly assumed that the Jurassic granites were generated in a destructive plate margin, though the tectonic environment of the Triassic Hayatsukigawa mass is not clear.

The temporal relation between the main

regional metamorphism in the Hida terrane (ca. 240 Ma) and the emplacement of the Hayatsukigawa mass (ca. 220 Ma) suggests that both metamorphism and Triassic magmatism resulted essentially from the same thermal anomalies. And a source of the Hayatsukigawa mass is thought to be composed of rocks metamorphosed in the granulite facies. If the Rb-Sr whole rock age of 237 Ma (Tanaka and Adachi, 1987) and the $^{206}U/^{238}Pb$ zircon ages of 238-241 Ma (Ishizaka and Yamaguchi, 1969) from the Hida gneisses in the Outer region represent the peak of metamorphism at 730℃ and 7 kb (Suzuki, 1989), then those ages are also considered to correspond to the beginning age of their cooling. Mattinson (1978) has estimated the closure temperature range for the $^{206}U/^{238}Pb$ system in zircon from a Cretaceous plutonic terrane to be in the range of 650-750℃. From the hornblende K-Ar ages for the Hida gneisses it may be inferred that at ca. 220 Ma the Outer region were emplaced into shallow tectonic position (=depth for confining pressure of about 3 kb) (Suzuki et al., 1989). The muscovite Rb-Sr ages of 230-220 Ma (Shibata et al., 1970; Yamaguchi and Yanagi, 1970) from the Unazuki schists and the feldspar Rb-Sr age of ca. 230 Ma from the Eboshiyama mylonite (Katoh, 1989) also suggest the beginning of uplifting in the Unazuki belt. The ages correspond to these of the uplifting of the Suo crystalline schists (Suo Terrane) (Shibata and Nishimura, 1989), which are developed on the south of the Hida Terrane.

In general, the amount of pore fluid in the deep continental crust is likely to be so small that partial melting of rocks takes place under vapour-absent condition (Rutter and Wyllie, 1988). The solidus temperatures of the dry granite and tonalite decrease with decrease of the pressure (Fig. 55). Thus, the main partial melting in the lower crust may be induced by adiabatic decompression resulting from rapid uplifting (Fig. 55). If such the rapid uplifting occurred in the Outer Plutonic Zone, the lower crustal material may have crossed the solidus of tonalite or granodiorite, consequently giving rise to such a magma that is comparable with the Hayatsukigawa granitic rocks.

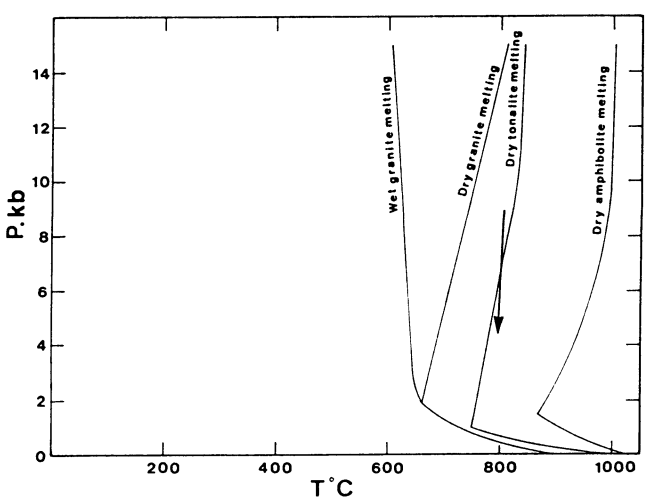

Fig. 55. Phase diagram for crustal rocks after Wyllie (1977). A vector represents the adiabatic decompression resulting from the rapid uplifting.

A subduction-related origin has been so far assumed for the early Jurassic granitic rocks in the Hida Terrane by some authors (e.g. Takahashi, 1983; Charvet et al., 1985), being supported by the chemical criteria stated above. Some geological and geophysical evidences have clarified that numerous basaltic sills injected into the lower to middle crust in the past (e.g. Fountain and Salisbury, 1981; Hauser et al., 1987). Since, at Moho pressure (about 10 kb), basaltic magmas may be denser than typical continental crust (Herzberg et al., 1983), it seems likely that the magmas form various sills in the vicinity of the continental Moho. The ponding or underplating of basaltic magmas of subduction-related origin into the continental crust may play an important part in the generation of the granitic batholiths (e.g. Hildreth, 1981; Cobbing and Pitcher, 1983; Hyndman and Foster, 1987).

Therefore, accepting the subduction-related model for the Jurassic granitic rocks (Fig. 56), the basic igneous rocks (gabbroic rocks) in the Hida Terrane are considered to have been derived directly from the basaltic magmas. Particularly the hornblende gabbro may haven been derived from some early basaltic magmas. During such process, the crust may have been thickened and the ponded magmas may have produced the source area for the granitic rocks of the Outer Plutonic Zone and the Group I rocks of the Inner Plutonic Zone.

Since the lithosphere beneath this zone must have contained remnants of ancient subducted slabs induced during the earlier cycle of subduction (Fig. 56), which was responsible for the formation of the Unazuki Belt, the basaltic magmas in the Inner Plutonic Zone are considered to have incorporated partial melts of the enriched lithosphere or fluid as they rose in the subcontinental mantle. Thus, the gabbroic rocks in the Inner Plutonic Zone are chemically more enriched than those in the Outer Plutonic Zone.

As the lower crust including the ponded rocks continues to be heated by the basic magmas, its anatexis begins to occur over larger region such as the Hida Terrane. In addition, the voluminous high temperature and hydrous basaltic magmas were emplaced into the Proterozoic continental lower crust of the Inner Plutonic Zone, causing melting of the crustal rocks with wet condition, ie, generation of the Group II rocks of the Inner Plutonic Zone. This model could explain the remarkable regional variation in isotopic characteristics of the igneous rocks.

D. AGE AND PROVENANCE OF THE HIDA TERRANE

In the light of the Nd model age data for the early Mesozoic granitic rocks and Hida gneisses including the gray granite, the author suggests the presence of early Proterozoic basement beneath

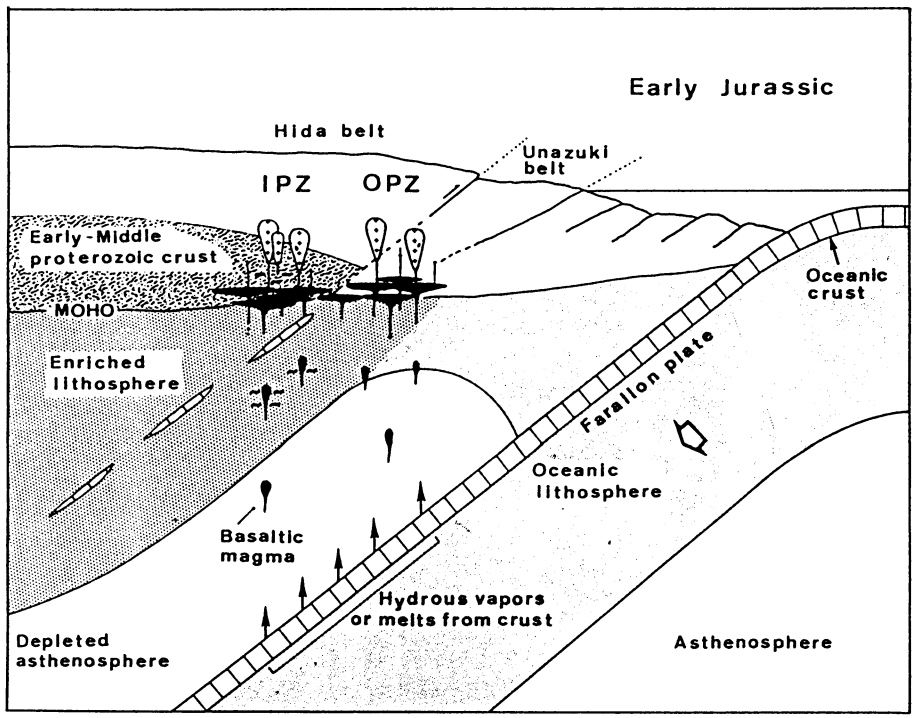

Fig. 56. Schematic diagram showing tectonic cross-section at time of generation of the Jurassic granitic rocks in the Hida Terrane.

the Inner Plutonic Zone of the Hida Terrane. Fig. 57 shows the inferred evolution band for Archean crustal material and the field of the evolution for all samples analyzed from the Hida Terrane. PAAS (Post-Archean average Australian Shale), whose Sm/Nd ratio was defined by Nance and Taylor (1976), was taken as typical Archean crustal material, since sediments are widely regarded as excellent bulk samples of crustal composition, and PAAS is the best-documented and widely used sediment average (McLennan and Taylor, 1982). The absence of Archean Nd signatures in the Hida terrane is clearly shown in Fig. 57.

The connection between the Hida Terrane and the Sino-Korean craton has been pointed out by some authors (Hurley et al., 1973; Hiroi., 1981; Nakazawa et al., 1982). This craton comprises northern China and northern Korea and is bounded to the north by the Tienshan-Tumen accretionary fold belt and to the south by the Caledonia-Variscan fold belts of the Kunlun-Qinling (Fig. 58). The oldest greenstones of the craton have a Rb-Sr whole-rock age of 3670±230 Ma. Thus, its nucleus is considered to have formed in the early Archean. Isotopic data have yielded ages of ~2.5 Ga (Fuping orogeny) for the basement rocks throughout the craton (Zhang et al., 1984; Ren et al., 1987). This evidence is not consistent with the hypothesis that the Hida Terrane was a part of the Sino-Korean craton.

Hayasaka and Hara (1986) pointed out that the structural direction of the Hida terrane seems to have been parallel to that of the basement complex of the northeastern end of Korean Peninsula, in the vicinity of the Kwanmobong Massif and Tanchon Folded Belt, before the opening of the Japan Sea (Fig. 58). This region is intruded by the Triassic and Jurassic granites (Won, 1987). The Triassic granitic series is called Songrim granite series accompanied with the Songrim disturbance. The Songrim granite series is distributed restrictive-

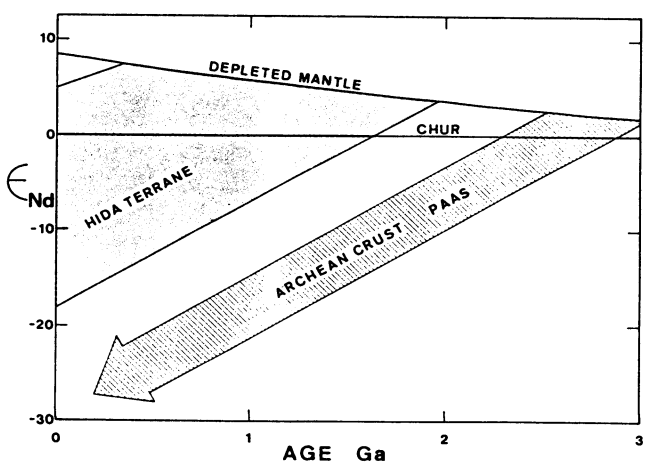

Fig. 57. Diagram showing Nd isotopic evolution of the Hida Terrane rocks and Archean crust. PAAS= Post-Archean average Australian Shale ($^{147}Sm/^{144}Nd=0.106$) used as a model for late Archean crustal materials. The field for the Hida Terrane is based on the early Mesozoic granitic rocks, gray granites and Hida metamorphic rocks.

ly as irregular masses in the northern half of the Korean peninsula. No exposures of the Songrim granite series have been found in the southern half of the peninsula. The intrusion age of the Songrim granite series is estimated to be ranging from 225 to 190 Ma (Lee, 1981). The Songrim granite series in this region is the Hysean Rock Group composed of porphyritic granite, granodiorite, diorite and syenite (Won, 1987). While the Jurassic granite is called the Tanch'on Granite in north Korea. The major rock assemblage of the Tanch'on Granite in this region is granodiorite, quartz monzonite, hornblende-biotite granite, biotite granite, two-mica granite and others (Won, 1987). Thus, the early Mesozoic igneous activity in the Hida Terrane appears to be well correlated with that of the northeastern end of Korean Peninsula.

It was inferred from the isotopic and geochemical considerations that the probable source material of the Group II rocks, that is, the basement rocks of the Inner Plutonic Zone in the Hida Terrane, was andesitic rocks with island-arc or continental margin affinity which formed during early Proterozoic age. The Hida Terrane appears to have been a micro-continent or island arc which collided with the eastern edge of the Sino-Korean craton, although the precise age of the collision remains unknown. In the eastern margin of Asian continent, there are some microcontinents such as the Sobaeksan, Khanka, Jiamusi and Songliano (Fig. 58). Lee (1980) has proposed that the

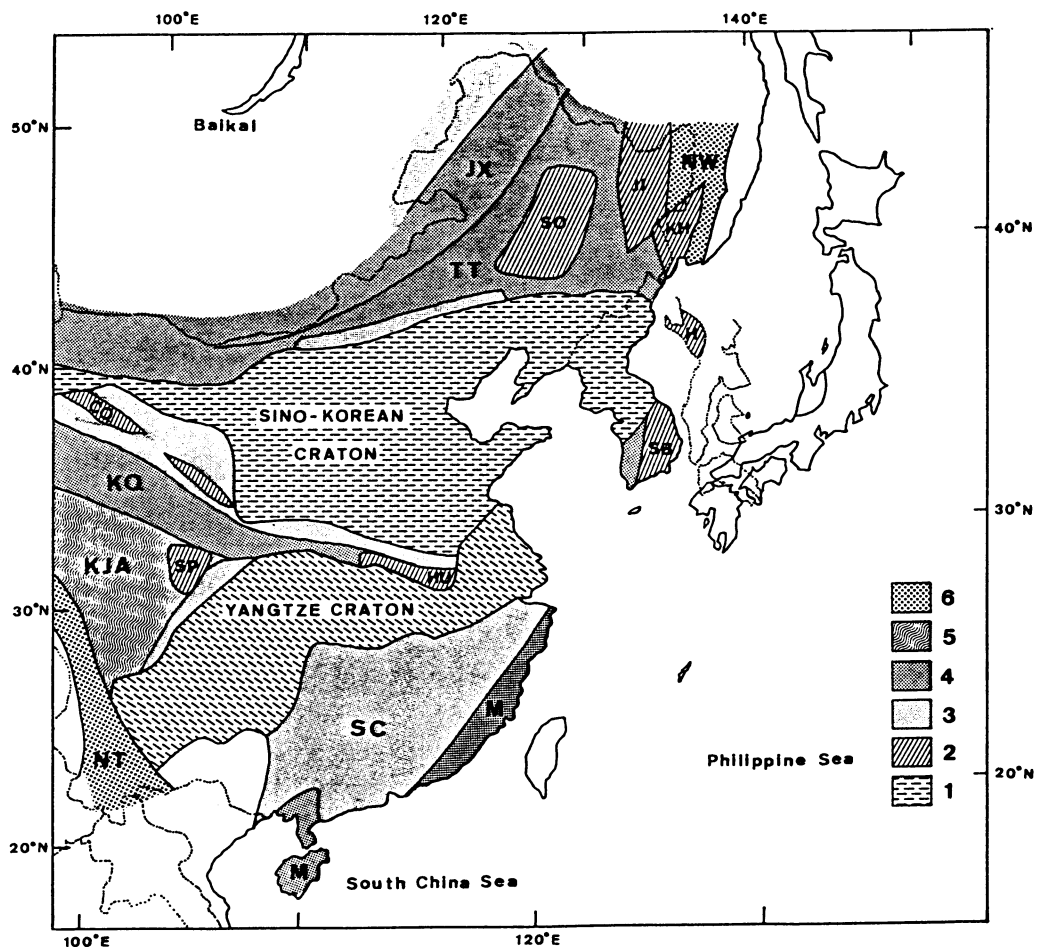

Fig. 58. Generallized tectonic map of east Asia compiled from Zhang et al. (1984), Kojima (1988), Ernst et al. (1988) and Maruyama et al. (1989). Southwest Japan before the opening of the Japan Sea after Otofuji and Masuda (1983) is shown by dotted line. 1, Precambrian craton; 2, Microcontinent; 3, Caledonian (early Paleozoic) fold belt; 4, Variscan (Late Paleozoic) fold belt; 5, Indosinian (Triassic) fold belt; 6, Early Yanshanian (Jurassic) fold belt; SB, Sobaeksan microcontinent; H, Hida microcontinent; KH, Khanka microcontinent; JI, Jiamusi microcontinent; SO, Songliao microcontinent; CQ, Central Qilian microcontinent; HU, Huaiyang microcontinent; SP, Songpan microcontinent; SC, South China accretionary fold belt; JX, Junggar-Xingan accretionary fold belt; TT, Tienshan-Tumen accretionary fold belt; KQ, Kunlun-Qinling accretionary fold belt; M, Maritime accretionary fold belt; KJA, Kekexili-Jinsha-Ailao accretionary fold belt; NT, North Tibet-West Yunnan accretionary fold belt; NW, Nadanhada-Western Sikhote-Alin accretionary fold belt.

Sobaeksan microcontinent collided with Sino-Korean craton at about 250 Ma. The collision age of the Hida microcontinent or island arc may be older than that of the Sobaeksan block. Lin et al. (1985) have described paleomagnetic data from the Sino-Korean and Yangtze cratons and suggested that the Yangtze craton was accreted to the Sino-Korean craton during the middle Triassic to early Jurassic age. The Hida Terrane appears to consist of two domains, Hida Terrane of the Hida Mountain range and Hida Terrane of the Oki-Dogo island, and the latter appears to be an eastern extension of the Sobaeksan block of Korea (Hara, 1982), which may be a part of the Yangtze craton (Ernst et al., 1988). The younger Nd model ages of the Hida metamorphic rocks are around 0.5 Ga (Fig. 39). The oldest Rb-Sr and Sm-Nd whole-rockisochron ages of the Hida metamorphic rocks are about 420 Ma (Fig. 2). And the emplacement age of the gray granite is assumed to be about 500 Ma (Shibata et al., 1989). These isotopic ages suggest that the Hida block (Inner Plutonic Zone) collided with the Sino-Korean craton during the early Paleozoic (late Cambrian ~ early Ordovician).

References

Allègre, C.J.(1982):Chemical geodynamics. Tectonophysics, 81, 109-132.

Allègre, C.J. and Minster, J.F.(1978): Quantitative models of trace element behavior in magmatic processes. Earth Planet. Sci. Lett., 38, 1-25.

Allègre, C.J. and Ben Othman, D.(1980): Nd-Sr isotopic relationship in granitoid rocks and continental crust development: a chemical approach to orogenesis. Nature, 286, 335-342.

Anderson, J.L.(1980): Mineral equilibria and crystallization conditions in the late Precambrian Wolf River Rapakivi Massif, Wisconsin, Am. J. Sci., 280, 289-332.

Arakawa, Y.(1984): Rb-Sr ages of the gneiss and metamorphosed intrusive rocks of the Hida metamorphic belt in the Urushiyama area, Gifu Prefecture, central Japan. J. Japan. Assoc. Min. Petr. Econ. Geol., 79, 431-442.

Arakawa, Y.(1988): Two contrasting types of Rb-Sr isotope systems for the Funatsu granitic rocks in the northwestern part of the Hida belt, central Japan. Ibid., 83, 374-387.

Aramaki, S., Hirayama, K. and Nozawa, T.(1972): Chemical composition of Japanese granites, Part 2. Variation trends and average composition of 1,200 analyses. J. Geol. Soc. Japan, 78, 39-49.

Arth, J.G.(1976): Behavior of trace elements during magmatic processes - A summary of theoretical models and their applications. J. Res. U.S. Geol. Surv., 4, 41-47.

Arth, J.G., Zen, Ean, Sellers, G. and Hammarstrom, J.(1986): High initial Sr isotopic ratios and evidence for magma mixing in the Pioneer batholith of southwest Montana. J. Geol., 94, 419-430.

Asami, M.(1979): Pelitic metamorphic rocks from the Arashima-dake area, Toga area and Wada-gawa area of the Hida metamorphic belt. Memorial Vol. Prof. H. KANO "The basement of the Japanese Islands", 41-49 (in Japanese).

Asami, M. and Adachi, M.(1976): Staurolite-bearing cordierite-sillimanite gneiss from the Toga area in the Hida metamorphic terrane, central Japan. J. Geol. Soc. Japan, 82, 259-271.

Asano, M., Tanaka, T. and Suwa, K.(1988): Sm-Nd and Rb-Sr ages of Hida metamorphic rocks in the Wada-gawa area, Toyama Prefecture. Abst. 95th Meeting Geol. Soc. Japan, 375 (in Japanese).

Batchelor, R.A. and Bowden, P.(1985): Petrogenetic interpretation of granitoid rock series using multicationic parameters. Chem. Geol.,48, 43-55.

Ben Othman, D., Polvé, M. and Allègre, C.J.(1984): Nd-Sr isotopic composition of granulites and constraints on the evolution of the lower continental crust. Nature, 307, 510-515.

Bowen, N.L.(1928): The evolution of the igneous rocks. Reprinted, 1956. New York: Dover, 332 p.

Brooks, C., Hart, S.R. and Wendt, I.,(1972): Realistic use of two-error regression treatments as applied to rubidium-strontium data. Rev. Geophys. Space Phys., 10, 551-577.

Chappell, B.W. and White, A.J.R.(1974): Two contrasting granite types. Pacific Geol., 8, 173-174.

Charvet, J., Faure, M., Caridroit, M. and Guidi, A.(1985): Some tectonic and tectogenetic aspects of SW Japan: An Alpine-type orogen in an island-arc position. In Formation of Active Ocean Margins (N. Nasu et al., eds.) 791-817. Terra Sci. Publ., Tokyo.

Chen, J.F., Foland, K.A. and Zhow, T.X.(1985): Mesozoic granitoids of the Yangtze foldbelt, China: Isotopic constraints on the magma sources. The crust-The significance of Granites gneisses in the lithosphere. Theophrastus publications S.A Athens. 217-237.

Clarke, D.B. and Halliday, A.N.(1980): Strontium isotope geology of the South Mountain batholith, Nova Scotia. Geochim. Cosmochim. Acta, 44, 1045-1058.

Cobbing, E.J. and Pitcher, W.S.(1983): Andean plutonism in Peru and its relationship to volcanism and metallogenesis at a segmented plate edge. Geol. Soc. Am. Mem., 159, 277-292.

Cohen, R.S., Evensen, N.M., Hamilton, P.J. and O'Nions, R.K.(1980): U-Pb, Sm-Nd, and Rb-Sr systematics of mid-ocean ridge basalt glasses. Nature, 32, 149-153.

Cohen, R.S. and O'Nions, R.K.(1982): The lead, neodymium, and strontium isotopic structure of ocean ridge basalts. J. Petrol., 23, 299-324.

Cohen, R.S., O'Nions, R.K. and Dawason, J.B.(1984) Isotope geochemistry of xenoliths from East Africa: Implications for development of mantle reservoirs and their interaction. Earth Planet. Sci. Lett., 68, 209-220.

Collins, W.J., Beam, S.D., White, A.J.R. and Chappell, B.W.(1982): Nature and origin of A-type granites with particular reference to southeastern Australia. Contrib. Mineral. Petrol., 80, 189-200.

Czamanske, G.K. and Wones, D.R.(1973): Oxidation during magmatic differentiation, Finnmarka

Complex, Oslo Area, Norway: Part II, The mafic silicates. J. Petrol., 14, 349-380.
Czamanske, G.K., Ishihara, S. and Atkin, S.A. (1981): Chemistry of rock-forming minerals of the Cretaceous-Paleocene batholith in Southwestern Japan and implications for magma genesis. J. Geophys. Res., 86, 10431-10469.
DePaolo, D.J.(1980): Crustal growth and mantle evolution: inferences from models of element transport and Nd and Sr isotopes. Geochim. Cosmochim. Acta, 44, 1185-1196.
DePaolo, D.J.(1981a): Neodymium isotopes in the Colorado Front Range and crust-mantle evolution in the Proterozoic. Nature, 291, 193-196.
DePaolo, D.J.(1981b): Trace element and isotopic effects of combined wallrock assimilation and fractional crystallization. Earth Planet. Sci. Lett., 53, 189-202.
DePaolo, D.J.(1981c): A neodymium and strontium isotopic study of the Mesozoic calc-alkaline granitic batholiths of the Sierra Nevada and Peninsular Ranges, California. J. Geophys. Res., 86, 10470-10488.
DePaolo, D.J. and Wasserburg, G.J.(1976): Nd isotopic variations and petrogenetic models. Geophys. Res. Lett., 3, 249-252.
DePaolo, D.J. and Johnson, R.W.(1979): Magma genesis in the New Britain island-arc: constraints from Nd and Sr isotopes and trace-element patterns. Contrib. Mineral. Petrol.,70, 367-379.
Domenick, M.A., Kistler, R.W., Dodge, F.C.W. and Tatsumoto, M.(1983): Nd and Sr isotopic study of crustal and mantle inclusions from the Sierra Nevada and implications for batholith petrogenesis. Geol. Soc. Amer. Bull., 94, 713-719.
Eichelberger, J.C.(1980): Vesiculation of mafic magma during replenishment of silicic magma reservoirs. Nature, 288, 446-450.
Ernst, W.G., Cao, R. and Jiang, J.J.(1988): Reconnaissance study of Precambrian metamorphic rocks, northeastern Sino-Korean shield, People's Republic of China. Geol. Soc. Am. Bull., 100, 692-701.
Farmer, G.L. and DePaolo, D.J.(1983): Origin of Mesozoic and Tertiary Granite in the Western United States and Implications for Pre-Mesozoic Crustal Structure, 1, Nd and Sr isotopic studies in the geocline of the northern Great Basin, J. Geophys. Res., 88, 3379-3401.
Faure, G.(1986): Principles of Isotope Geology: New York, John Wiley & Sons, 589 p.
Fleck, R.J. and Criss, R.E.(1985): Strontium and oxygen isotopic variations in Mesozoic and Tertiary plutons of central Idaho. Contrib. Mineral. Petrol., 90, 291-308.
Fountain, D.M. and Salisbury, M.H.(1981): Exposed cross-sections through the continental crust: implications for crustal structure, petrology, and evolution. Earth Planet. Sci. Lett., 56, 263-277.
Fujiyoshi, A.(1973): On the occurrence of the characteristic minerals from the pelitic gneisses in the Tateyama-gawa (upper Hayatsuki-gawa) area, central Japan. J. Geol. Soc. Japan, 79, 761-770 (in Japanese with English abstract).
Gilbert, M.C., Helz, R.T., Popp, R.K. and Spear, F.S.(1982): Experimental studies of amphibole stability. In: Velblen, D.R. & Ribbe, P.H., eds. Amphibloes: Petrology and experimental phase relations. Rev. Mineralogy 9b, Mineralogical Soc. Am., 229-354.
Gill, J.B.(1981): Orogenic andesites and plate tectonics. Berlin: Springer-Verlag, 358 pp.
Goldstein, S.L., O'Nions, R.K. and Hamilton, P.J. (1984): A Sm-Nd isotopic study of atmospheric dusts and perticulates from major river systems. Earth Planet. Sci. Lett., 70, 221-236.
Gray, C.M.(1984): An isotopic mixing model for the origin of granitic rocks in southeastern Australia. Ibid., 70, 47-60.
Green, T.H. and Ringwood, A.E.(1968): Genesis of the calc-alkaline igneous rock suite. Contrib. Mineral. Petrol., 18, 105-162.
Gromet, L.P. and Silver, L.T.(1983): Rare earth distribution among minerals in a granodiorite and their implications. Geochim. Cosmochim. Acta, 47, 925-939.
Guidotti, C.V., Cheney, J.T. and Conatore, P. D. (1975): Interrelationship between Mg/Fe ratio and octahedral Al content in biotite. Am. Mineralogist, 60, 849-853.
Hamilton, P.J., O'Nions, R.K., Evensen, N.M., Bridgewater, D and Allart, J.H.(1978): Sm-Nd isotopic investigations of Isua supracrustals and implications for mantle evolution. Nature, 272, 41-43.
Hamilton, P.J., Evensen, N.M., O'Nions, R.K. and Tarney, J.(1979): Sm-Nd systematics of Lewisian gneisses: implications for the origin of granulites. Ibid., 277, 25-28.
Hanson, G.N.(1978): The application of the trace elements to the petrogenesis of igneous rocks of granitic composition. Earth Planet. Sci. Lett., 38, 26-43.
Hara, I.(1981): Tectonic framework of paired metamorphic belts -Hida belt and Sangun belt-. Tectonics of Paired Metamorphic Belts, I. Hara, Ed., 147-153.
Hara, I.(1982): Evolutional processes of paired metamorpic belts -Hida belt and Sangun belt-. Mem. Geol. Soc. Japan, 21, 71-89.
Hart, W.K.(1985): Chemical and isotopic evidence for mixing between depleted and enriched mantle, northwestern U.S.A. Geochim. Cosmochim. Acta, 49, 131-144.
Harris, N.B.W, Pearce, J.A. and Tindle, A.G.(1986) Geochemical characteristics of collision-zone magmatism. Collision Tectonics, Geological Societiy Special Publication, 19, 67-81.
Harrison, T.M. and McDougall, I.(1980): Investigations of an intrusive contact, northwest Nelson, New Zealand-I. Thermal, chronological and isotopic constraints. Geochim. Cosmochim. Acta, 44, 1985-2003.
Harrison, T.M., Armstrong, R.L., Naeser, C.W. and Harakal, J.E.(1979): Geochronology and thermal history of the Coast Plutonic Complex, near Prince Rupert, British Columbia. Can. Jour. Earth Sci., 16, 400-410.
Hattori, I.(1984): Alternating clastic limestone and red chert as olistolith in the Mino terrane, central Japan. J. Geol. Soc. Japan, 90, 43-54.
Hauser, E.C., Potter, C., Hauge, T., Burgess, S., Burtch, S., Mutschler, J., Allmendinger, R.,

Brown, L., Kaufman, S. and Oliver, J.(1987): Crustal structure of eastern Nevada from COCORP deep seismic reflection data. Geol. Soc. Am. Bull., 99, 833-844.
Hawkesworth, C.J.(1982): Isotope characteristics of magmas erupted along destructive plate margins. In. Thorpes, R. S., ed., Andesites. New York, John Wiley & Sons, 549-571.
Hawkesworth, C.J., O'Nions, R.K., Pankhurst, R.J., Hamilton, P.J. and Evensen, N.M.(1977): A geochemical study of island-arc and back-arc tholeiites from the Scotia Sea. Earth Planet. Sci. Lett., 36, 253-262.
Hawkesworth, C.J., O'Nions, R.K. and Arculus, R.J. (1979): Nd and Sr isotopic geochemistry of island arc volcanics, Grenada, Lesser Antilles. Ibid., 45, 237-248.
Hayasaka, Y. and Hara, I.(1986): Permian -Jurassic tectonic evolution of the Southern front of the Hida - Hida Marginal Belt, Southwest Japan. International Symposium on Pre-Jurassic East Asia. IGCP Project 224. Rep. and Abst., 76-81.
Hayasaka, Y., Nishimura, Y. and Hara, I.(1987): Formational Process of the "Sangun metamorohic rocks", Southwest Japan. Abst. 94th Meeting Geol. Soc. Japan, 62-63 (in Japanese).
Hayase, I. and Ishizaka, K.(1967): Rb-Sr dating on the rocks in Japan (I), South Western Japan. J. Japan. Assoc. Min. Petr. Econ. Geol., 58, 201-212 (in Japanese with English abstract).
Henderson, P.(1984): Rare Earth Element Geochemistry, Elsevier, Amsterdam, 510p.
Herz, R.T.(1973): Phase relations of basalts in their melting range at P_{H_2O} = 5 kb as a function of oxygen fugacity, Part I. mafic phases. J. Petrol., 14, 249-302.
Herz, R.T.(1976): Phase relations of basalts in their melting ranges at P_{H_2O} = 5 kb, Part II. Melt compositions. Ibid., 17, 139-193.
Herzberg, C.T.(1978): Pyroxene geothermometry and geobarometry: experimental and thermodynamic evaluation of some subsolidus phase relations involving pyroxenes in the system CaO-MgO-Al_2O_3-SiO_2. Geochim. Cosmochim. Acta, 42, 945-957.
Herzberg, C.T.(1983): Density constraints on the formation of the continental Moho and Crust. Contrib. Mineral. Petrol., 84, 1-5.
Hickey, R.L., Frey, F.A. and Gerlach, D.C.(1986): Multiple sources for basaltic arc rocks from the southern volcanic zone of the Andes (34° - 41° S): trace element and isotopic evidence for contributions from subducted oceanic crust, mantle, and continental crust. J. Geophys. Res., 91, 5963-5983.
Hildreth, W.(1981): Gradients in silicic magma chambers: implications for lithospheric magmatism: J. Geophys. Res., 86, 10153-10192.
Hiroi, Y.(1978): Geology of the Unazuki district in the Hida metamorphic terrain, central Japan. J. Geol. Soc. Japan, 84, 521-530 (in Japanese with English abstract).
Hiroi, Y.(1980): Geological and petrological study on the Unazuki Crystalline Schist of Hida Belt. Hida Marginal Belt, 1, 64-71 (in Japanese).
Hiroi, Y.(1981): Subdivision of the Hida metamorphic complex, Central Japan and its bearing on the geology of the Far East in pre-Sea of Japan time. Tectonophysics, 76, 317-333.
Hiroi, Y.(1983): Progressive metamorphism of the Unazuki pelitic schists in the Hida Terrane, Central Japan. Contrib. Mineral. Petrol., 82, 334-350.
Hiroi, Y., Fuji, N. and Okimura, Y.(1978): New fossil discovery from the Hida metamorphic rocks in the Unazuki area, central Japan. Proc. Jpn. Acad., Ser. B, 54: 268-271.
Hirooka, K., Nakajima, T., Sakai. H., Date, T., Nittamachi, K and Hattori, I.(1983): Accretion tectonics inferred from paleomagnetic measurements of Paleozoic and Mesozoic rocks in central Japan, in M. Hashimoto and S. Uyeda, eds., Accretion tectonics in the circum-Pacific regions: Tokyo, Terra Scientific Publishing Company, 179-194.
Hurley, P.M., Fairbairn, H.W., Pinson, W.H. and Lee, J.H.(1973): Middle Precambrian and older apparent age values in basement gneisses of South Korea, and relations with Southwest Japan. Geol. Soc. Am. Bull., 84, 2299-2304.
Hyndman, D.W. and Foster, D.A.(1987): The role of tonalites and mafic dikes in the generation of the Idaho batholith. J. Geol., 96, 31-46.
Ichikawa, H., Sakai, T., Watanabe, T. and Iizumi, S.(1987): Quantitative analysis of seven trace elements in Silicate rocks using fused disk-samples by X-ray fluorescence method (Rh-tube). Geol. Rept. Shimane Univ., 6, 161-169 (in Japanese with English abstract).
Igo, H.(1961): On the disconformity and aluminous shales of the Carboniferous Ichinotani Formation, Hida massif. J. Geol. Soc. Japan, 67, 261-273 (in Japanese with English abstract).
Inazuki, T.(1980): Metamorphism of calc-siliceous rocks in the Momose-Mizunashi district, Hida metamorphic belt, central Japan. Ibid., 86, 727-740 (in Japanese with English abstract).
Inazuki, T.(1982): Contact metamorphism accompanying fluid exchange —with special reference to the Funatsu Granitic Rocks, Hida Metamorphic Belt, central Japan—. Mem. Geol. Soc. Japan, 21, 51-69.
Inoue, K., Ikeda, Y. and Minami, A.(1985): Determination of sodium, potassium, magnesium, calcium, manganese and iron in the silicate rocks by atomic absorption spectrophotometry. Memorial Volume of Prof. H. Yoshida, Hiroshima Univ., 355-363 (in Japanese).
Ishihara, S.(1977): The magnetite-series ilmenite-series granitic rocks. Mining Geol., 27, 293-305.
Ishioka, K. and Suwa, K.(1954): Fabric of hornblende in a schistose amphibolite from the Kurobe-gawa area, centrla Japan. J. Earth Sci. Nagoya Univ., 2, 191-199.
Ishioka, K. and Suwa, K.(1956): Metasomatic development of staurolite schist from rhyolite in the Kurobe-gawa area, central Japan. A preliminary report. Ibid., 4, 123-140.
Ishizaka, K. and Yamaguchi, M.(1969): U-Th-Pb ages of sphene and zircon from the Hida metamorphic terrain, Japan. Earth Planet. Sci. Lett., 6, 179-185.
Jacobsen, S. B., and Wasserburg, G. J.(1984): Sm-Nd isotopic evolution of chondrites and achondrites, II. Ibid., 67, 137-150.
James, D.E.(1982): A combined O, Sr, Nd, and Pb

isotopic and trace element study of crustal contamination in central Andean lavas. 1, Local geochemical variations. Ibid., 57, 47-62.

Juteau, M., Michard, A. and Albarede, F.(1986): The Pb-Sr-Nd isotope geochemistry of some recent circum-Mediterranean granites. Contrib. Mineral. Petrol., 92, 331-340.

Kagami, H., Okano, O., Sudo, H. and Honma, H. (1982): Isotopic analysis of Rb and Sr using a full-automatic thermal ionization mass spectrometer. Papers of the Inst. of Thermal Spring Res., Okayama Univ., 52, 51-70 (in Japanese with English abstract).

Kagami, H., Iwata, M., Sano, S. and Honma, H. (1987), Sr and Nd isotopic compositions and Rb, Sr, Sm and Nd concentrations of standard samples. Tech. Rep. ISEI., Okayama Univ., Ser. B, 4, 1-16.

Kanayama, K. and Hiroi, Y.(1979): Geology of the Mt. Hodatsu area in the Hida metamorphic terrain, Central Japan. J. Japan. Assoc. Min. Petr. Econ. Geol., 74, 36-43 (in Japanese with English abstract).

Kano, T.(1974): Plutonic rocks of the Hida metamorphic region. Bull. Geol. Geograph. Research Toyama Prefecture, 6, 155-186 (in Japanese with English abstract).

Kano, T.(1980): Geological study of northern-half of western part of Hida metamorphic region, Central Japan. J. Geol. Soc. Japan, 86, 687-704 (in Japanese with English abstract).

Kano, T.(1981): Migmatite structure of the Hida metamorphic region, central Japan. Ibid., 87, 315-328 (in Japanese with English abstract).

Kano, T.(1990): Intrusive relation of the Okumayama Granitic Mass (Shimonomoto type) into the Iori Granitic Mass (Funatsu type) in the Hayatsukigawa area; Re-examination of the subdivision for early Mesozoic granites (Funatsu Granites) in the Hida region. J. Geol. Soc. Japan, 96, 379-388 (in Japanese with English abstract).

Kano, T., Shibata, K. and Terayama, S.(1989): K-Ar age of hornblende from a dioritic rock in the Tochibora ore deposit of the Kamioka mine, in the Hida metamorphic region, central Japan. Mining Geol., 39, 283-288 (in Japanese with English abstract).

Kaseno, Y., Ishida, S., Nakanishi, N.and Ichikawa, W.(1965): Geology of Noto Peninsula, Japan. in "Scientific Reports of Noto Peninsula, Japan." published by the Ishikawa Prefectural Government, p.1-93, and geological map (1:75,000) (in Japanese).

Katoh, Y.(1989): Tectonic development of the Unazuki Belt in the Unazuki district, Japan. Master's Thesis, Hiroshima Univ.

Katoh, Y., Hayasaka, Y., Hara, I., Tanaka, S. and Kagami, H.(1989): Structural analysis of the Hida belt in the Unazuki district, Hida Mountains. Abst. 96th Meeting Geol. Soc. Japan, 584 (in Japanese).

Kawano, M. and Nozawa, T.(1968): Petrochemistry of granitic rocks in Hayatsukigawa area, Hida Mountains. Bull. Geol. Surv. Japan, 19, 641-651.

Kawano, Y. and Ueda, Y.(1966): K-A dating on the igneous rocks in Japan (V) - Granitic rocks in southwestern Japan -. J. Japan. Assoc. Min. Petr. Econ. Geol., 56, 191-211 (in Japanese with English abstract).

Kistler, R.W. and Peterman, Z.E.(1973): Variations in Sr, Rb, K, Na, and initial $^{87}Sr/^{86}Sr$ in Mesozoic granitic rocks and intruded wall rocks in central California. Geol. Soc. Am. Bull., 84, 3489-3512.

Kobayashi, H., Watanabe, T. and Iizumi, S.(1981): A full-automatic analysis of silicate rocks by X-ray fluorescence methode. Mem. Fac. Sci., Shimane Univ., 15, 115-124 (in Japanese with English abstract).

Kojima, S.(1988): Mesozoic terranes in East Asia and the Mino terrane. Abst. 42th Meetig Assoc. Geol. Col. Japan, 65-70 (in Japanese).

Komatsu, M. and Suwa, K.(1986): The structure and tectonics of pre-Jurassic serpentinite melange and overlying Hida nappe in central Japan. International Symposium on Pre-Jurassic East Asia. IGCP Project 224. Rep. and Abst., 97-103.

Konishi, K.(1954): Note on the Moscovian (?) deposits at Itoshiro-mura, Fukui, Japan. J. Geol. Soc. Japan, 60, 7-17 (in Japanese with English abstract).

Kostyuk, E.A. and Sobolev, V.S.(1969): Paragenetic type of calciferous amphiboles of metamorphic rocks. Lithos, 2, 67-82.

Krogh, T.E.(1973): A low-contamination method for hydrothermal decomposition of zircon and extraction of U and Pb for isotopic age determinations. Geochim. Cosmochim. Acta, 37, 485-494.

Kuno, H.(1969): Andesite in Time and Space: Oregon Dept. Geology Mineral Industries, Bull., 65, 13-20.

Kuno, H., Baadsgaard, H., Goldich, S. and Shinobara, K.(1960): Potassium-argon dating of the Hida metamorphic complex. Japanese J. Geol. Geograph. 31, 273-278.

Leak, B.E.(1968): A catalog of analyzed calciferous and subcalciferous amphiboles together with their nomenclature and associated minerals. Geol. Soc. Amer. Spec. Paper, no.98, 210p.

Leak, B.E.(1971): On aluminous and edenitic hornblendes. Mineral. Mag., 38, 389-407.

Le Maitre, R.W.(1981): GENMIX - A generalized petrological mixing model program. Comput. Geosci., 7, 229-247.

Lee, D.S.(1980): Igneous activity and geotectonic interpretation in the Ogcheon geosynclinal zone, Korea —especially referred to ophiolite determination. Yosei Nonchong, 17, 109-137.

Lee, S.M.(1981): Geology and metallic mineralization associated with Mesozoic granitic magmatism in South Korea. Mining Geol., 31, 235-244.

Leterrier, J., Maury, R.C., Thonon, P., Girard, D. and Marchal, M.(1982): Clinopyroxene composition as a method of identification of the magmatic affinities of paleo-volcanic series. Earth Planet. Sci. Lett., 59, 139-154.

Lewis, J.D. and Spooner, C.M.(1973): K/Rb ratios in Precambrian granulite terranes. Geochim. Cosmochim. Acta, 37, 1111-1118.

Liew, T.C. and McCulloch, M.T.(1985): Genesis of granitoid batholiths of Peninsular Malaysia and implications for models of crustal evolution: Evidence from a Nd-Sr isotopic and U-Pb zircon study. Ibid., 49, 587-600.

Lin, J.I., Fuller, M. and Zhang, W.Y.(1985): Preliminary Phanerozoic polar wander paths for the North and South China blocks. Nature, 313, 444-449.

Lugmair, G.W. and Marti, K.(1977): Lunar initial $^{143}Nd/^{144}Nd$: differential evolution of the lunar crust and mantle. Earth Planet. Sci. Lett., 39, 349-357.

Maeda, S.(1961): The Tetori Group along the Asuwa River in Fukui Prefecture. J. Geography, 721, 15-19 (in Japanese with English abstract).

Maruyama, S., Liou, J.G. and Seno, T.(1989): Mesozoic and Cenozoic evolution of Asia. In; The Evolution of the Pacific Ocean Margins (Ed. Z. Ben Avraham), Oxford Monograph on Geology and Geophysics, 8, 75-99.

Mattinson, J.M.(1978): Age, origin and thermal histories of some plutonic rocks from the Salinian Block of California. Contrib. Mineral. Petrol., 67, 233-245.

McCarthy, T.S. and Cawthorn, R.G.(1980): Changes in initial $^{87}Sr/^{86}Sr$ ratio during protracted fractionation in igneous complexes. J. Petrol., 21, 245-264.

McCulloch, M.T. and Perfit, M.R.(1981): $^{143}Nd/^{144}Nd$, $^{87}Sr/^{86}Sr$ and trace element constraints on the petrogenesis of Aleutian island arc magmas. Earth Planet. Sci. Lett., 56, 167-179.

McCulloch, M.T. and Chappell, B.W.(1982): Nd isotopic characteristics of S- and I-type granites. Ibid., 58, 51-64.

McCulloch, M.T., Bradshaw, J.Y. and Taylor, S.R. (1987): Sm-Nd and Rb-Sr isotopic and geochemical systematics in Phanerozoic granulites from Fiordland, Southwest New Zealand. Contrib. Mineral. Petrol., 97, 183-195.

McCulloch, M.T. and Wasserburg, G.L.(1978): Sm-Nd and Rb-Sr chronology of continental crust formation. Science, 200, 1003-1011.

McLennan, S.M. and Taylor, S.R.(1982): Geochemical constraints on the growth of the continental crust. J. Geol., 90, 347-361.

McNutt, R.H., Crocket, J.H., Clark, A.H., Caclles, J.C., Farrar, E., Haynes, S.J. and Zentilli, M. (1975): Initial $^{87}Sr/^{86}Sr$ ratios of plutonic and volcanic rocks of the central Andes between latitudes 26° and 29° south. Earth Planet. Sci. Lett., 27, 305-313.

Michael, P.J.(1984): Chemical differentiation of the Cordillera Paine granite (south Chile) by in situ fractional crystallization. Contrib. Mineral. Petrol., 87, 179-195.

Mitchell, A.H. and Reading, H.G.(1969): Continental margins, geosynclines and ocean floor spreading. J. Geol., 77, 629-646.

Miyashiro, A.(1974): Volcanic rock series in island arcs and active continental margins. Am. J. Sci., 274, 321-355.

Morris, J.D. and Hart, S.R.(1983): Isotopic and incompatible element constraints on the genesis of island arc volcanics from Cold Bay and Amak Island, Aleutians, and implications for mantle structure. Geochim. Cosmochim. Acta, 47, 2015-2030.

MMAJ.(1973): A report of the comprehensive survey in the Nagatoro district of 1972, Ministry of International Trade Industry, 13p.(in Japanese).

Mullen, E.D.(1983): $MnO/TiO_2/P_2O_5$: a minor element discriminant for basaltic rocks of oceanic environments and its implications for petrogenesis. Earth Planet. Sci. Lett., 62, 53-62.

Nakazawa, K., Kang, M.Y. and Tokuoka, T.(1982): The Ogcheon geosynclinal belt and the Hida metamorphic belt. Mem. Geol. Soc. Japan, 21, 91-101 (in Japanese with English abstract).

Nance, W.B. and Taylor, S.R.(1976): Rare earth element patterns and crustal evolution - 1. Australian post-Archean sedimentary rocks. Geochim. Cosmochim. Acta, 40, 1539-1551.

Nelson, B.K. and DePaolo, D.J.(1985): Rapid production of continental crust 1.7 to 1.9 b.y. ago: Nd isotopic evidence from the basement of the North American mid-continent. Geo. Soc. Am. Bull., 96, 746-754.

Niko, S. Suzuki, M. and Okimura, Y.(1984): Carboniferous acidic volcanic rocks from the Ichinotani formation in Fukuji area, Hida Marginal Belt. Abst. 91th Meeting Geol. Soc. Japan, 226 (in Japanese).

Nishimura, Y.(1989): "Sangun metamorphic rocks": Terrane problem. In Ichikawa, K., ed.: Pre-Cretaceous Terranes of Japan.

Nohda, S. and Wasserburg, G.J.(1981): Nd and Sr isotopic study of volcanic rocks from Japan. Earth Planet. Sci. Lett., 52, 264-276.

Nohda, S., Tatsumi, Y., Otofuji, Y., Matsuda, T. and Ishizaka, K.(1988): Asthenospheric injection and back-arc opening: isotopic evidence from northeast Japan. Chem. Geol., 68, 317-327.

Nozawa, T.(1977): Hida belt. in Tanaka, K. and Nozawa, T. ed., Geology and mineral resourses of Japan, 293-299.

Nozawa, T.(1979): Some problems on Funatsu granitic rocks. Memorial Vol. Prof. H. KANO "The basement of the Japanese Islands", 107-117 (in Japanese with English abstract).

Nozawa, T., Kawata, K. and Kawai, M.(1975): Geology of the Hida-Furukawa District. Quadrangle Series, Scale 1: 50,000, Geol. Surv. Japan, 79p (in Japanese with English abstract, 9p.).

Nozawa, T., Asami, M., Ito, M., Hiroi, Y., Hoshino M., Inazuki, T., Kanayama, K., Kano, T., Sohma, T. and Murakami, N.(1979): Contact phenomena of Funatsu granitic rocks in Hongo area, Hida Mountains. Mem. Geol. Soc. Japan, 17, 135-148 (in Japanese with English abstract).

Nozawa, T., Sakamoto, T., Kano, T. and Inazuki, T. (1981): Geology of the Shirokimine District. Quadrangle Series, Scale 1:50,000, Geol. Surv. Japan, 85p (in Japanese with English abstract, 10p.)

Ohmoto, H.(1964): K-Ar ages of hornblendes of the Hida gneiss complex in central Japan. Proc. Japan Acad., 40, 36-41.

Ohtsubo, T.(1985): Intrusive Mechanism of some plutonic rocks, in the Utsubo-Kagasawa area, Okuhida Plateau. Master's Thesis, Akita Univ. (in Japanese with English abstract).

Ohtsubo, T., Maruyama, T. and Kano, H.(1985): Form and emplacement of the Utsubo plutonic complex, Hida Mountainland. Magma, 73,87-91(in Japanese).

Okui, A.(1985): Polymetamorphism in the Hida metamorphic rocks of upper Katakai river area, Toyama Prefecture, central Japan, with special reference to the effect of intrusion of the Funatsu granitic rocks. J. Japan. Assoc. Min.

Petr. Econ. Geol., 80, 382-397 (in Japanese with English abstract).
O'Nions, R.K., Hamilton, P.J. and Evensen, N.M. (1977): Variations in $^{143}Nd/^{144}Nd$ and $^{87}Sr/^{86}Sr$ ratios in oceanic basalts. Earth Planet. Sci. Lett., 39, 13-22.
Otofuji, Y. and Masuda, T.(1983): Paleomagnetic evidence for the clockwise rotation of Southwest Japan. Ibid., 62, 349-359.
Patchett, P.J. and Arndt, N.T.(1986): Nd isotopes and tectonics of 1.9-1.7 Ga crustal genesis. Ibid., 78, 329-338.
Pearce, J.A., Harris, N.B.W. and Tindle, A.G. (1984): Trace element discrimination diagrams for the tectonic interpretation of granitic rocks. J. Petrol., 25, 956-983.
Petro, W., Vogel. T.A. and Wilband, J.T.(1979): Major-element chemistry of plutonic rock suites from compressional and extensional plate boundaries. Chem. Geol, 26, 217-235.
Philpotts, J.A. and Schnetzler, C.C.(1970): Phenocryst-matrix partition coefficients for K, Rb, Sr and Ba, with applications to anorthosite and basalt genesis. Geochim. Cosmochim. Acta, 34, 307-322.
Pitcher, W.S.(1983): Granite type and tectonic environment. in Hsü, K.J.,ed., Mountain building processes: London, Academic Press, p. 19-40.
Popp, P.K., Gilbert, M.C. and Craig, J.R.(1977): Stability of Fe-Mg amphiboles with respect to oxygen fugacity. Amer. Mineral., 62, 1-12.
Ren Jishun, Jiang Chunfa, Zhang Zhengkung and Qin Deyu (1987): Geotectonic evolution of China: Beijing, Science Press, and Berlin, Springer-Verlag, 203 p.
Robert, J.L.(1976): Titanium solubility in synthetic phlogopite solid solutions. Chem. Geol., 17, 213-227.
Robinson, P., Spear, F.S., Schumacher, J.C., Laird, J., Klein, C., Evans, B.W. and Doolan, B.L.(1982): Phase relations of metamorphic amphiboles: natural occurrence and theory. In: Veblen, D.R., & Ribbe, P.H. (eds.) Amphiboles: Petrology and experimental phase Relations. Rev. in Mineralogy, 9b. Mineral. Soc. Am.,1-227.
Rogers, N.W. and Hawkesworth, C.J.(1982): Proterozoic age and cumulate origin from granulite xenoliths, Lesotho. Nature, 299, 409-413.
Ruiz, J., Patchett, P.J. and Arculus, R.J.(1988): Nd-Sr isotope composition of lower crustal xenoliths —Evidence for the origin of mid-tertiary felsic volcanics in Mexico. Contrib. Mineral. Petrol., 99, 36-43.
Rutter, M.J. and Wyllie, P.J.(1988): Melting of vapour-absent tonalite at 10 kbar to simulate dehydration-melting in the deep crust. Nature, 331, 159-160.
Sato, S., Shirahase, T. and Shibata, H.(1967): Older granite based on the Rb-Sr dating in the Hida Massif in Japan. J. Geol. Soc. Japan, 73, 857 (in Japanese).
Schnetzler, C.C. and Philpotts, J.A.(1970): Partition coefficients of rare earth elements between igneous matrix material and rock-forming mineral phenocrysts, II. Geochim. Cosmochim. Acta, 34, 331-340.
Shibata, K. and Ishihara, S.(1979): Rb-Sr whole-rock and K-Ar mineral ages of granitic rocks in Japan. Geochem. J., 13, 113-119.
Shibata, K. and Ito, N.(1978): Isotopic ages of schist from the Asahidake-Shiroumadake area, Hida mountains. J. Japan. Assoc. Min. Petr. Econ. Geol., 73, 1-4.
Shibata, K. and Nishimura, Y.(1989): Isotopic ages of the Sangun crystalline schists, Southwest Japan. Mem. Geol. Soc. Japan, 33, 317-341 (in Japanese with English abstract).
Shibata, K. and Nozawa, T.(1966): K-Ar ages of Hida metamorphic rocks, Amo-Tsunokawa area and Oki area, Japan. Bull. Geol. Surv. Japan, 17, 20-26.
Shibata, K. and Nozawa, T.(1968): K-Ar age of Omi schist, Hida Mountains, Japan. Ibid., 19, 243-246.
Shibata, K. and Nozawa, T.(1978): K-Ar ages of hornblendes from the Hida metamorphic belt. J. Japan. Assoc. Min. Petr. Econ. Geol., 73, 137-141 (in Japanese with English abstract).
Shibata, K. and Nozawa, T.(1984): Isotopic ages of the Funatsu Granitic Rocks. Ibid., 79, 289-298 (in Japanese with English abstract).
Shibata, K. and Nozawa, T.(1986): Late Precambrian ages for granitic rocks intruding the Hida Metamorphic Rocks. Bull. Geol. Surv. Japan, 37, 43-51.
Shibata, K., Nozawa, T. and Wanless, R. K.(1970): Rb-Sr geochronology of the Hida metamorphic belt, Japan. Can. J. Earth Sci., 7, 1383-1401.
Shibata, K., Uchiumi, S. and Nakagawa, T.(1979): K-Ar age results-1, Bull. Geol. Surv. Japan, 30, 675-686 (in Japanese with English abstract).
Shibata, K., Nozawa, T. and Uchiumi, S.(1980): K-Ar ages on the Hida Marginal Belt. Hida Marginal Belt, 1, 110-112 (in Japanese).
Shibata, K., Uchiumi, S., Uto, K. and Nakagawa, T. (1984): K-Ar age results-2, new data from the Geological Survey of Japan. Bull. Geol. Surv. Japan, 35, 331-340 (in Japanese with English abstract).
Shibata, K., Ohtsubo, T. and Maruyama, T.(1988): A Rb-Sr whole-rock age of the Utsubo granitic complex, Hida mountains. Ibid., 39, 135-138 (in Japanese with English abstract).
Shibata, K., Kano, T. and Asano, M.(1989): Isotopic ages of the Gray granite from the upper Kubusu River area, Hida Mountains. J. Japan. Assoc. Min. Petr. Econ. Geol., 84, 243-251 (in Japanese with English abstract).
Simmons, E.C. and Hedge, C.E.(1978): Minor-element and Sr-Isotope Geochemistry of Tertiary stocks, Colorado Mineral Belt. Contrib. Mineral. Petrol., 67, 379-396.
Sohma, T.(1986): Metamorphic rocks in the Sokawa area, Gifu Prefecture. Abst. 93th Meeting Geol. Soc. Japan, 464 (in Japanese).
Sohma, T. and Doko, A.(1979): Chemical characteristics of igneous activity from geosynclinal to postorogenic stages in the Hida belt. Mem. Geol. Soc. Japan, 17, 149-164 (in Japanese with English abstract).
Sohma, T. and Akiyama, S.(1984): Geological structure and lithofacies in the central part of the Hida metamorphic belt. J. Geol. Soc. Japan, 90, 609-628 (in Japanese with English abstract).
Sohma, T., Minami, H., Maruyama, S. and Sasakura, Y.(1985): Geology of the Gamata area. Hida

Marginal Belt, Joetsu Belt, Ashio Belt 2, 169-174 (in Japanese).
Spear, F.S.(1981): An experimental study of hornblende stability and compositional variability in amphibolite. Amer. Jour. Sci., 281, 697-734.
Steiger, R.H. and Jäger, E.(1977): Subcommision on geochronology: Convection on the use of decay constants in geo- and cosmochronology. Earth Planet. Sci. Lett., 36, 359-362.
Suwa, K.(1966a): Radiometric age and mineralogy of muscovite from a granitic pegmatite transgressing the Hida Metamorphic Complex in the Upper Katakai River area, Toyama Prefecture, Central Japan. J. Geol. Soc. Japan, 72, 523-529.
Suwa, K.(1966b): Finding of conglomerate schist from the Upper Katakai River area, Toyama Prefecture, Central Japan. Ibid., 72, 585-591.
Suwa, K.(1979): Biotite schist and leptite from the Kitamata-dani and Kasa-dani of the upper Katakai-gawa area, Toyama Prefecture. Memorial Vol. Prof. H. KANO "The basement of the Japanese Islands", 15-27 (in Japanese).
Suzuki, M.(1975): On the petrochemical character of the pelitic gneiss from the southwestern part in the Hida Metamorphic Belt, Central Japan. J. Sci. Hiroshima Univ., C, 7, 3, 133-148.
Suzuki, M.(1977): Polymetamorphism in the Hida Metamorphic Belt, Central Japan. Ibid., 4, 217-296.
Suzuki, M., Nakazawa, S. and Osakabe, T.(1989): Tectonic development of the Hida Belt—with special reference to its metamorphic history and late Carboniferous to Triassic orogenies—. Mem. Geol. Soc. Japan, 33, 1-10 (in Japanese with English abstract).
Takahashi, M.(1983): Space-time distribution of late Mesozoic to early Cenozoic magmatism in east Asia and its tectonic implication. In Accretion Tectonics in the Circum-Pacific Regions (H. Hashimoto and S. Uyeda, eds.), 69-90. Terra Sci. Publ., Tokyo.
Tanaka, T. and Adachi, M.(1987): Slab ages of the Hida metamorphic rocks by Sm-Nd and Rb-Sr methods. Abst. Meeting Geochemical Soc. Japan, 77 (in Japanese).
Tanaka, S. and Maruyama, T.(1985a): Petrological study of the Funatsu granitic complex, in the Funatsu area in the Hida Mountains. Part 1 Petrography and inner structure. J. Japan. Assoc. Min. Petr. Econ. Geol., 80, 371-381 (in Japanese with English abstract).
Tanaka, S. and Maruyama, T.(1985b): Petrological study of the Funatsu granitic complex, in the Funatsu area in the Hida Mountains. Part 2 Chemical properties. Ibid., 80, 484-498 (in Japanese with English abstract).
Tanaka, S. and Ohtsubo, T.(1987): Trace element in the Funatsu Granitic Rocks —with special reference to high Sr contents in the Hayatsukigawa intrusion— . Earth Science (Chikyu-Kagaku), 41, 101-113 (in Japanese with English abstract).
Tanaka, S. and Kagami, H.(1987a): Regional variations of initial $^{87}Sr/^{86}Sr$ ratios in the Funatsu granitic rocks. Magma, 80, 10-14 (in Japanese).
Tanaka, S. and Kagami, H.(1987b): Rb-Sr isotopic ages of the granitic rocks in the Tsurugidake—Kekachiyama area, northern Japan Alps. J. Geol. Soc. Japan, 93, 929-932 (in Japanese).
Tanaka, S. and Kagami, H.(1989): A neodymium and strontium isotopic study of the early Mesozoic granitic rocks in the Hida Terrane, Central Japan. Structural development of the Japanese Islands, DELP publication, No.28, 13-18.
Tarney, J. and Windley, B.F.(1977): Chemistry, thermal gradients and evolution of the lower continental crust. J. Geol. Soc. London, 134, 153-172.
Taylor, H.P.(1980): The effects of assimilation of country rocks by magmas on $^{18}O/^{16}O$ and $^{87}Sr/^{86}Sr$ systematics in igneous rocks. Earth Planet. Sci. Lett., 47, 243-258.
Taylor, S.R. and McLennan, S.M.(1985): The continental crust: its composition and evolution. Oxford: Blackwell Scientific, 312p.
Tsukano, Z. and Miura, S.(1959): On the upper Cretaceous formation and related some problems in the western part of the Hida plateau, Japan. Mem. Fac. Lib. Art Fukui Univ., 9, 123-137 (in Japanese with English abstract).
Tuttle, O.F. and Bowen, N.L.(1958): Origin of granite in light of experimental studies in the system $NaAlSi_3O_8$-$KAlSi_3O_8$-SiO_2-H_2O, Geol. Soc. Am. Mem., 74, 153p.
Wasserburg, G.J., Jacobsen, S.B., DePaolo, D.J., McCulloch, M.T. and Wen, T.(1981): Precise determination of Sm/Nd ratios, Sm and Nd isotopic abundances in standard solutions. Geochim. Cosmochim. Acta, 45, 2311-2323.
Weaver, B.L. and Tarney, J.(1983): Elemental depletion in Archaean granulite-facies rocks. In Atherton, M.P. and Gribble, C.D. eds. Migmatites, melting and metamorphism, 250-263, Shiva Pub. Ltd.
White, A.J.R. and Chappell, B.W.(1977): Ultrametamorphism and granitoid genesis. Tectonophysics, 43, 7-22.
White, W.M. and Hofmann, A.W.(1982): Sr and Nd isotope geochemistry of oceanic basalts and mantle evolution. Nature, 296, 821-825.
White, W.M. and Patchett, J.(1984): Hf-Nd-Sr isotopes and incompatible element abundances in island arcs: implications for magma origins and crust-mantle evolution. Earth Planet. Sci. Lett., 67, 167-185.
White, W.M. Hofmann, A.W. and Puchelt, H.(1987): Isotope geochemistry of Pacific Mid-Ocean Ridge basalt. J. Geophys. Res., 92, 4881-4893.
Whitford, D.J., Nicolls, I.A. and Taylor, S.R. (1979): Spatial variations in the geochemistry of Quaternary lavas across the Sunda Arc in Java and Bali. Contr. Mineral. Petrol., 70, 341-356.
Whitford, D.J., White, W.M. and Jezek, P.A.(1981): Neodymium isotopic composition of Quaternary island arc lavas from Indonesia. Geochim. Cosmochim. Acta, 45, 989-995.
Whitney, J.A.(1988): The origin of granite: The role and source of water in the evolution of granitic magmas. Geol. Soc. Am. Bull., 100, 1886-1897.
Wickham, S.M.(1987): The segregation and emplacement of granitic magmas. J. Geo. Soc. London, 144, 281-297.
Won, C.K.(1987): Geology of Korea. In Lee, D.S., eds: Kyohaka-Sa Publishing Co., 313-326.

Wood, B.J. and Banno, S.(1973): Garnet-orthopyroxene and orthopyroxene-clinopyroxene relationships in simple and complex systems. Contrib. Mineral. Petrol., 42, 109-124.
Wyllie, P.J.(1977): Crustal anatexis: an experimental review. Tectonophysics, 43, 41-71.
Wyllie, P.J.(1983): Experimental and thermal constraints on the deep-seated parentage of some granitoid magmas in subduction zones. In Atherton, M.P and Gribble, C. D. eds., Migmatites, melting and metamorphism, 37-51, Shiva Pub. Ltd.
Yamada, N., Nozawa, T., Harayama, S., Takizawa, F. and Kato, H.(1989): 1:200,000 Geological Map Takayama.
Yamaguchi, M. and Yanagi, T.(1970): Geochronology of some metamorphic rocks in Japan. Eclogae Geol. Helv., 63, 371-388.
Yamamoto, Y.(1983): Reverse zoned garnets from pelitic gneisses in the Wada-gawa area, southeastern part of Toyama Prefecture, central Japan. J. Japan. Assoc. Min. Petr. Econ. Geol., 78, 313-323 (in Japanese with English abstract).
York, D.(1966): Least-squares fitting of a straight line. Can. J. Phys., 44, 1079-1086.
Zhang, Z.M., Liou, J.G. and Coleman, R.G.(1984): An outline of the plate tectonics of China. Geol. Soc. Am. Bull., 95, 295-312.

Shinobu TANAKA
Oyo Corporation, Hiroshima, 731-51, Japan.